

BIOMEDICAL

PHOTONICS

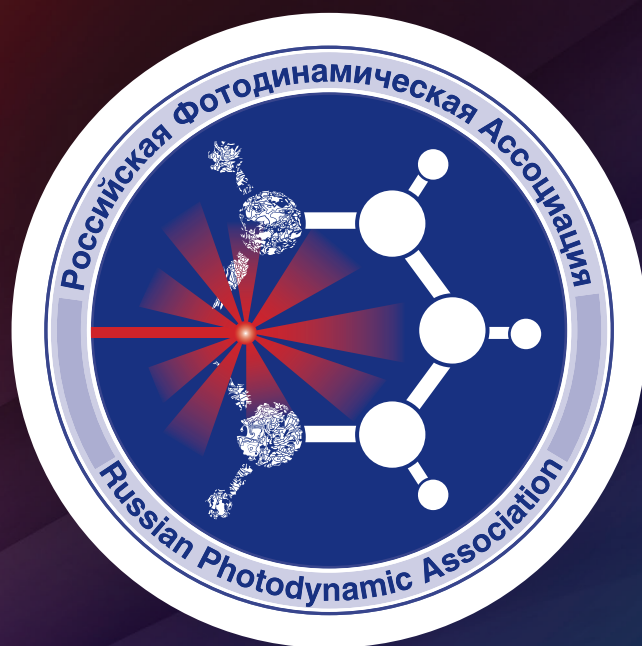
Volume 12, # 2, 2023

In the issue:

- Palliative surgical treatment using photodynamic therapy for biliary cancer complicated by obstructive jaundice
- Pulsed exposure mode of the 445 nm semiconductor laser in phonosurgery: an experimental study
- Videocapillaroscopic monitoring of microcirculation in rats during photodynamic therapy
- Experimental in vivo studies of the antitumor efficacy of photodynamic and radiodynamic therapy and their combinations
- Spectroscopic study of methylene blue photophysical properties in biological media
- Photodynamic therapy of acne

BMP

Российская Фотодинамическая Ассоциация



www.pdt-association.com

BIOMEDICAL PHOTONICS

FOUNDERS:

Russian Photodynamic Association
P.A. Herzen Moscow Cancer Research Institute

EDITOR-IN-CHIEF:

Filonenko E.V., Dr. Sci. (Med.), professor, head of the Centre of laser and photodynamic diagnosis and therapy of tumors in P.A. Herzen Moscow Cancer Research Institute (Moscow, Russia)

DEPUTY CHIEF EDITOR:

Grin M.A., Dr. Sci. (Chem.), professor, chief of department of Chemistry and technology of biological active substances named after Preobragenskiy N.A. in Moscow Technological University (Moscow, Russia)

Loschenov V.B., Dr. Sci. (Phys and Math), professor, chief of laboratory of laser biospectroscopy in the Natural Sciences Center of General Physics Institute of the Russian Academy of Sciences (Moscow, Russia)

EDITORIAL BOARD:

Kaprin A.D., Academician of the Russian Academy of Sciences, Dr. Sci. (Med.), professor, general director of National Medical Research Radiological Centre of the Ministry of Health of the Russian Federation (Moscow, Russia)

Romanko Yu.S., Dr. Sci. (Med.), professor of the department of Oncology, radiotherapy and plastic surgery named after L.L. Lyovshina in I.M. Sechenov First Moscow State Medical University (Moscow, Russia)

Stranadko E.Ph., Dr. Sci. (Med.), professor, chief of department of laser oncology and photodynamic therapy of State Research and Clinical Center of Laser Medicine named by O.K. Skobelcin of FMBA of Russia (Moscow, Russia)

Blondel V., PhD, professor at University of Lorraine, joint-Head of the Health-Biology-Signal Department (SBS) (Nancy, France)

Bolotina L., PhD, professor of Research Center for Automatic Control of Nancy (Nancy, France)

Douplik A., PhD, professor in Ryerson University (Toronto, Canada)

Steiner R., PhD, professor, the honorary director of Institute of Laser Technologies in Medicine and Metrology at Ulm University (Ulm, Germany)

BIOMEDICAL PHOTONICS –

research and practice, peer-reviewed, multidisciplinary journal.

The journal is issued 4 times per year.

The circulation – 1000 copies., on a quarterly basis.

The journal is included into the List of peer-reviewed science press of the State Commission for Academic Degrees and Titles of Russian Federation

The journal is indexed in the international abstract and citation database – Scopus.

The publisher «Agentstvo MORE».
Moscow, Khokhlovskiy lane., 9

Editorial staff:

Chief of the editorial staff Ivanova-Radkevich V.I.

Science editor professor Mamontov A.S.

Literary editor Moiseeva R.N.

Translators Kalyagina N.A.

Computer design Kreneva E.I.

Desktop publishing Shalimova N.M.

The Address of Editorial Office:

Russia, Moscow, 2nd Botkinskiy proezd, 3

Tel. 8 (495) 945–86–60

www: PDT-journal.com

E-mail: PDT-journal@mail.ru

Corresponding to:

125284, Moscow, p/o box 13

Registration certificate ПИ № ФС 77–51995, issued on 29.11.2012 by the Federal Service for Supervision of Communications, Information Technology, and Mass Media of Russia

The subscription index

of «Rospechat» agency – 70249

The editorial staff is not responsible for the content of promotional material. Articles represent the authors' point of view, which may be not consistent with view of the journal's editorial board. Editorial Board admits for publication only the articles prepared in strict accordance with guidelines for authors. Whole or partial presentation of the material published in the Journal is acceptable only with written permission of the Editorial board.

BIOMEDICAL PHOTONICS

BIOMEDICAL PHOTONICS –

научно-практический, рецензируемый,
мультидисциплинарный журнал.
Выходит 4 раза в год.
Тираж – 1000 экз., ежеквартально.

Входит в Перечень ведущих рецензируемых
научных журналов ВАК РФ.

Индексируется в международной
реферативной базе данных Scopus.

Издательство «Агентство МОРЕ».
Москва, Хохловский пер., д. 9

Редакция:

Зав. редакцией	Иванова-Радкевич В.И.
Научный редактор	проф. Мамонтов А.С.
Литературный редактор	Моисеева Р.Н.
Переводчики	Калягина Н.А.
Компьютерный дизайн	Кренева Е.И.
Компьютерная верстка	Шалимова Н.М.

Адрес редакции:

Россия, Москва, 2-й Боткинский пр., д. 3
Тел. 8 (495) 945–86–60
www: PDT-journal.com
E-mail: PDT-journal@mail.ru

Адрес для корреспонденции:

125284, Москва, а/я 13

Свидетельство о регистрации ПИ
№ ФС 77–51995, выдано 29.11.2012 г.
Федеральной службой по надзору в сфере
связи, информационных технологий
и массовых коммуникаций (Роскомнадзор)

Индекс по каталогу агентства

«Роспечать» – 70249

Редакция не несет ответственности за содержа-
ние рекламных материалов.

В статьях представлена точка зрения авторов,
которая может не совпадать с мнением редак-
ции журнала.

К публикации принимаются только статьи, под-
готовленные в соответствии с правилами для
авторов, размещенными на сайте журнала.

Полное или частичное воспроизведение матери-
алов, опубликованных в журнале, допускается
только с письменного разрешения редакции.

УЧРЕДИТЕЛИ:

Российская Фотодинамическая Ассоциация
Московский научно-исследовательский онкологический институт
им. П.А. Герцена

ГЛАВНЫЙ РЕДАКТОР:

Филоненко Е.В., доктор медицинских наук, профессор, руководитель
Центра лазерной и фотодинамической диагностики и терапии опухолей
Московского научно-исследовательского онкологического института
им. П.А. Герцена (Москва, Россия)

ЗАМ. ГЛАВНОГО РЕДАКТОРА:

Грин М.А., доктор химических наук, профессор, заведующий
кафедрой химии и технологии биологически активных соединений
им. Н.А. Преображенского Московского технологического университета
(Москва, Россия)

Лощенов В.Б., доктор физико-математических наук, профессор,
заведующий лабораторией лазерной биоспектроскопии в Центре
естественно-научных исследований Института общей физики
им. А.М. Прохорова РАН (Москва, Россия)

РЕДАКЦИОННАЯ КОЛЛЕГИЯ:

Каприн А.Д., академик РАН, доктор медицинских наук, профессор,
генеральный директор Национального медицинского исследовательского
центра радиологии Минздрава России (Москва, Россия)

Романко Ю.С., доктор медицинских наук, профессор кафедры онкологии,
радиотерапии и пластической хирургии им. Л.Л. Лёвшина Первого Москов-
ского государственного медицинского университета имени И.М. Сеченова
(Москва, Россия)

Странадко Е.Ф., доктор медицинских наук, профессор, руководитель отделен-
ия лазерной онкологии и фотодинамической терапии ФГБУ «Государствен-
ный научный центр лазерной медицины им. О.К.Скобелкина ФМБА России»

Blondel V., профессор Университета Лотарингии, руководитель отделения
Здравоохранение-Биология-Сигналы (SBS) (Нанси, Франция)

Bolotine L., профессор научно-исследовательского центра автоматки
и управления Нанси (Нанси, Франция)

Douplik A., профессор Университета Райерсона (Торонто, Канада)

Steiner R., профессор, почетный директор Института лазерных технологий
в медицине и измерительной технике Университета Ульма (Ульм, Германия)

ORIGINAL ARTICLES

Palliative surgical treatment using photodynamic therapy for biliary cancer complicated by obstructive jaundice

Tseimakh A.E., Mitshenko A.N., Kurtukov V.A., Shoykhet Ia.N.

4

Pulsed exposure mode of the 445 nm semiconductor laser in phonosurgery: an experimental study

Ryabova M.A., Mitrofanova L.B., Ulupov M.Y., Stepanova V.A., Sterkhova K.A.

11

Videocapillaroscopic monitoring of microcirculation in rats during photodynamic therapy

Guryleva A.V., Machikhin A.S., Grishacheva T.G., Petrishchev N.N.

16

Experimental in vivo studies of the antitumor efficacy of photodynamic and radiodynamic therapy and their combinations

Tzerkovsky D.A., Kozlovsky D.A., Mazurenko A.N., Adamenko N.D., Borichevsky F.F.

24

Spectroscopic study of methylene blue photophysical properties in biological media

Pominova D.V., Ryabova A.V., Romanishkin I.D., Markova I.V., Akhlustina E. V., Skobeltsin A.S.

34

REVIEWS OF LITERATURE

Photodynamic therapy of acne

Filonenko E.V., Ivanova-Radkevich V.I.

48

ОРИГИНАЛЬНЫЕ СТАТЬИ

Паллиативное хирургическое лечение с применением фотодинамической терапии больных со злокачественными новообразованиями желчевыводящей системы, осложненными обструктивной желтухой

А.Е. Цеймах, А.Н. Мищенко, В.А. Куртуков, Я.Н. Шойхет

4

Импульсный режим воздействия полупроводникового лазера с длиной волны 445 нм в фонохирургии: экспериментальное исследование

М.А. Рябова, Л.Б. Митрофанова, М.Ю. Улулов, В.А. Степанова, К.А. Стерхова

11

Применение видеокапилляроскопии для мониторинга микроциркуляции в коже при фотодинамической терапии

А.В. Гурылева, А.С. Мачихин., Т.Г. Гришачева, Н.Н. Петрищев

16

Экспериментальные исследования in vivo противоопухолевой эффективности фотодинамической и радиодинамической терапии, а также их сочетания

Д.А. Церковский, Д.И. Козловский, А.Н. Мазуренко, Н.Д. Адаменко, Ф.Ф. Боричевский

24

Спектроскопическое исследование фотофизических свойств метиленового синего в биологических средах

Д.В. Поминова, А.В. Рябова, И.Д. Романишкин, И.В. Маркова, Е.В. Ахлюстина, А.С. Скобельцин

34

ОБЗОРЫ ЛИТЕРАТУРЫ

Фотодинамическая терапия при акне

Е.В. Филоненко, В.И. Иванова-Радкевич

48

PALLIATIVE SURGICAL TREATMENT USING PHOTODYNAMIC THERAPY FOR BILIARY CANCER COMPLICATED BY OBSTRUCTIVE JAUNDICE

Tseimakh A.E.¹, Mitshenko A.N.², Kurtukov V.A.², Shoykhet Ia.N.¹

¹Altai State Medical University, Barnaul, Russia

²State hospital №5, Barnaul, Russia

Abstract

The article presents the results of a study of survival, markers of hemostasis, proteolysis, and tumor invasion after complex palliative treatment of patients with histologically verified malignant tumors of the bile ducts complicated by obstructive jaundice in two comparable groups of patients. The aim of the study was to evaluate the effectiveness of palliative surgical treatment using photodynamic therapy in patients with malignant tumors of the biliary system complicated by obstructive jaundice. In 10 patients of the main group, palliative surgical treatment was performed using photodynamic therapy; in 20 patients of the comparison group, palliative surgical treatment was performed without photodynamic therapy. In patients of the main group, a statistically significant increase in life expectancy by 104 days ($p=0.033$) was observed compared to the comparison group. At the same time, a statistically significant effect of tumor necrosis factor α , a marker of tumor invasion, on survival ($p=0.012$) and a decrease in its level after photodynamic therapy by 15 pg/ml ($p=0.041$) was revealed. Thus, palliative treatment using photodynamic therapy of malignant tumors of the bile ducts, complicated by obstructive jaundice, can increase the survival rate of patients by reducing tumor invasion.

Key words: biliary cancer; photodynamic therapy; survival.

Contacts: Tseimakh A.E., e-mail: alevtsei@rambler.ru

For citations: Tseimakh A.E., Mitshenko A.N., Kurtukov V.A., Shoykhet Ia.N. Palliative surgical treatment using photodynamic therapy for biliary cancer complicated by obstructive jaundice, *Biomedical Photonics*, 2023, vol. 12, no. 2, pp. 4–10. doi: 10.24931/2413-9432-2023-12-2-4-10.

ПАЛЛИАТИВНОЕ ХИРУРГИЧЕСКОЕ ЛЕЧЕНИЕ С ПРИМЕНЕНИЕМ ФОТОДИНАМИЧЕСКОЙ ТЕРАПИИ БОЛЬНЫХ СО ЗЛОКАЧЕСТВЕННЫМИ НОВООБРАЗОВАНИЯМИ ЖЕЛЧЕВЫВОДЯЩЕЙ СИСТЕМЫ, ОСЛОЖНЕННЫМИ ОБСТРУКТИВНОЙ ЖЕЛТУХОЙ

А.Е. Цеймах¹, А.Н. Мищенко², В.А. Куртуков², Я.Н. Шойхет¹

¹Алтайский государственный медицинский университет, Барнаул, Россия

²Городская больница №5, Барнаул, Россия

Резюме

В работе представлены результаты исследования выживаемости, маркеров гемостаза, протеолиза и опухолевой инвазии после комплексного паллиативного лечения больных с гистологически верифицированными злокачественными новообразованиями желчевыводящих протоков, осложненными обструктивной желтухой в двух сопоставимых группах больных. Целью исследования было оценить эффективность паллиативного хирургического лечения с применением фотодинамической терапии (ФДТ) у больных злокачественными новообразованиями желчевыводящей системы, осложненными обструктивной желтухой. У 10 пациентов основной группы проводилось паллиативное хирургическое лечение с применением ФДТ, у 20 пациентов группы сравнения проводилось паллиативное хирургическое лечение без применения ФДТ. У пациентов основной группы наблюдалось статистически значимое увеличение продолжительности жизни по сравнению с группой сравнения на 104 дня ($p=0,033$). При этом выявлено статистически значимое влияние маркера опухолевой инвазии – фактора некроза опухоли α на выживаемость ($p=0,012$) и уменьшение его уровня после ФДТ с $43,53 \pm 33,99$ пг/мл до $28,33 \pm 26,12$ пг/мл ($p=0,041$). Таким образом, паллиативное лечение с применением ФДТ злокачественных новообразований желчевыводящих протоков, осложненных обструктивной желтухой, позволяет увеличить выживаемость пациентов за счет уменьшения опухолевой инвазии.

Ключевые слова: злокачественные новообразования желчевыводящей системы, фотодинамическая терапия, выживаемость.

Контакты: Цеймах А.Е., e-mail: alevtsei@rambler.ru.

Для цитирования: Цеймах А.Е., Мищенко А.Н., Куртуков В.А., Шойхет Я.Н. Паллиативное хирургическое лечение с применением фотодинамической терапии больных со злокачественными новообразованиями желчевыводящей системы, осложненными обструктивной желтухой // Biomedical Photonics. – 2023. – Т. 12, № 2. – С. 4–10. doi: 10.24931/2413-9432-2023-12-2-4-10.

Introduction

Biliary tract cancer is a rare oncological pathology, which includes distal and proximal cholangiocarcinoma, and gallbladder cancer [1, 2, 3]. The structure of morbidity and mortality in biliary cancer is assessed together with hepatocellular cancer [1]. The prevalence of cancer of the biliary tract together with hepatocellular cancer is 6.7 per 100,000 population. Malignant neoplasms of the bile ducts have one of the highest rates of overall mortality (35.2%) and mortality in the first year after diagnosis (66.8%) [1–5].

Despite the development of methods of radiation and chemotherapy, the main method of treatment of biliary cancer remains surgical. However, at the time of diagnosis, 57.3% of patients already have an advanced stage IV of the underlying disease, and 80.3% of patients have an advanced or locally advanced process [1, 2]. Thus, more than 80% of patients can only undergo palliative treatment, the main component of which is the elimination of life-threatening complications of the underlying disease, such as obstructive jaundice and cholangitis [4–6].

One of the methods of palliative treatment that complements surgical treatment is photodynamic therapy (PDT). PDT is a method of treating malignant neoplasms, in which the tumor is irradiated with light of a certain wavelength, which transfers the molecules of a special substance (a photosensitizer) selectively accumulated in the tumor tissue, into an excited state in the presence of oxygen. The resulting reactive oxygen species lead tumor cells to death by apoptosis, necrosis, and autophagy. Studies of the effectiveness of PDT in cancer of the biliary tract conducted in previous years gave encouraging results, indicating the promise of this method in the palliative treatment of this category of patients, which increases the survival of patients to an average of 8 months when local PDT is performed with hematoporphyrin derivatives [8–13].

The aim of the study was to evaluate the effectiveness of palliative surgical treatment using PDT in patients with malignant neoplasms of the biliary system complicated by obstructive jaundice.

Materials and Methods

An open non-randomized comparative survival study included 30 patients with histologically verified

bile duct adenocarcinoma complicated by obstructive jaundice, who underwent complex treatment at the regional hepatological center of the City Hospital No. 5, Barnaul (Barnaul, Russia) from 2016 to 2020. The patients were divided into two groups. The inclusion criteria for the study were age over 18 years, histologically verified diagnosis of a malignant neoplasm of the bile ducts, and signed informed consent for surgical treatment during hospitalization. The exclusion criteria were mortality during the hospital stay and the presence of blood cancer. The main group included 10 patients who underwent palliative surgical treatment with PDT. The comparison group included 20 patients who underwent palliative surgical treatment without PDT. The distribution of patients into groups was carried out without the use of randomization. Patients who signed a consent to PDT due to the presence of contraindications to the use of alternative methods of treatment were included in the main group. Patients who refused PDT were included in the comparison group. The design of the study was approved by the Local Ethics Committee of the Altai State Medical University of the Ministry of Health of the Russian Federation (extract from protocol No. 11 dated November 27, 2017). Comparative characteristics of groups by sex, age, routine laboratory parameters of inflammation, bilirubinemia, and liver enzymes are presented in Table. 1. The groups were comparable in terms of the main characteristics.

Comparative characteristics of the groups according to the localization of the malignant neoplasm are presented in Table. 2. No statistically significant differences were found.

Palliative surgical treatment included surgical treatment of life-threatening complications, primarily of obstructive jaundice: percutaneous transhepatic mono- and bilobar drainage of the bile ducts, and bile duct stenting under ultrasound and X-ray control. Symptomatic conservative treatment included infusion, detoxification, analgesic, hepatoprotective, and antibacterial therapy [4, 5].

All patients of the main group underwent PDT according to the following algorithm: fluorescence diagnosis on a laser electron-spectrum device "Biospec" (New Surgical Technologies, Russia), local and systemic PDT on a programmed two-wavelength laser device "LAMI-Helios (LLC New Surgical technologies",

Таблица 1

Характеристика пациентов, включенных в исследование

Table 1
Characteristics of patients included in the study

Показатель Value	Основная группа Main group	Группа сравнения Comparison group	p
	M±SD	M±SD	
Возраст, лет Age, years	61,3±16,9	69,8±9,4	0,168
Число женщин Number of women	2	5	0,879
Число мужчин Number of men	8	15	0,879
Лейкоциты, *10 ⁹ /л Leukocytes, *10 ⁹ /L	8,87±3,16	9,71±2,16	0,487
Тромбоциты, *10 ⁹ /л Thrombocytes, *10 ⁹ /L	285,33±164,42	258,67±43,15	0,649
Общий билирубин, мкмоль/л Common bilirubin, mcmol/L	197,32±173,09	115,00±56,19	0,210
АСТ, Ед/л AST, U/L	96,83±63,07	53,17±29,51	0,097
АЛТ, Ед/л ALT, U/L	98,99±73,51	58,22±41,79	0,206

Примечание: p – статистическая значимость различий между основной группой и группой сравнения.

Note: p – statistical significance of differences between the main group and the comparison group.

Russia) according to TU 9444-001-53807582-2010. Photoditazine based on chlorin e6 (LLC VETA-GRAND, Russia) was used as a photosensitizer. Systemic PDT was performed through peripheral access to the cubital vein with monochromatic light with a wavelength of 662-665 nm with a light dose of 1200-1400 J/cm² with a power of 0.7 W and a radiation power density of 0.22 W/cm² using an apparatus for intravenous blood irradiation during intravenous administration of a photosensitizer at a dose of 1-1.4 mg/kg of body weight. Local contact PDT was carried out by irradiation with monochromatic light with a wavelength of 662 nm at a light dose of 220 J/cm² with a programmed specialized two-wavelength laser apparatus with a power of 0.7 W and a radiation power density of 0.22 W/cm² after 5 hours from the end of systemic PDT [6]. Access for PDT was carried out by

percutaneous transhepatic external drainage of the bile ducts under ultrasound control. Then a conductor was inserted through the lumen of the common bile duct and brought down into the duodenum. The major duodenal papilla was cannulated along the retracted guidewire and endoscopic papillosphincterotomy was performed on the guidewire, after which endoscopic balloon dilatation of the lumen of the intramural part of the choledochus was performed along the guidewire and the introduction of the DPOC guiding catheter with its fixation. Then, a transnasal gastroscope was inserted through the DPOC catheter into the lumen of the choledochus. The balloon was inflated in the area of the bifurcation of the lobar ducts. Then, transluminal PDT was performed under video endoscopic visual control. The purpose of local PDT was to normalize the outflow through the extrahepatic bile ducts by reducing the volume of tumor tissue in the lumen of the bile ducts with the appearance of both fluoroscopically and visually free lumen (priority application notification and registration No. 2023105379).

Complications of surgical treatment were assessed using the Clavien-Dindo scale [14].

Determination of plasma fibrinogen concentration according to Clauss (1957) was carried out using a set of reagents from the Technology-Standard company (Russia).

To determine the concentration of tissue plasminogen activator (t-PA), tissue plasminogen activator inhibitor-1 (PAI-1), tissue factor (TF), tissue factor pathway inhibitor (TFPI), and tumor necrosis factor-alpha (TNF-α) in serum standard kits for enzyme immunoassay TECHNOZYM manufactured by Technoclone Herstellung von Diagnostika und Arzneimitteln GmbH (Austria) were used. Optical density was measured using a universal automatic photometer for microplates Elx808 from BioTec Instruments, Inc. (USA).

Statistical analysis was performed using the SigmaPlot 14.0 statistical software package (registration number 775400014). When testing normality using the Shapiro-Wilk test, it was revealed that all the studied indicators, except for gender and age, had a distribution that did not correspond to the Gaussian distribution in both groups. For the analysis of independent samples, the nonparametric Mann-Whitney test was used, and for paired samples, the Wilcoxon test was used. To compare unrelated groups with a normal distribution, the Student's parametric test was used, and for relative values – Fisher's z-test. The method of Kaplan-Meier curves was used to assess the overall life expectancy, and the log-rank test was used for a comparative analysis of survival. To assess the influence of factors on the prognosis of the disease, multiple linear regression analysis was used. The critical level of significance of the study results was taken as p < 0.05.

Таблица 2

Сравнительная характеристика больных по локализации и распространенности новообразования

Table 2

Comparative characteristics of patients by localization and prevalence of tumor

Локализация злокачественного новообразования Localisation of malignant tumor	Основная группа Main group		Группа сравнения Comparison group		p
	абс. abs.	%	абс. abs.	%	
Дистальная холангиокарцинома, в том числе Distal cholangiocarcinoma including	2	20,00	9	45,00	0,348
стадия IIIa по классификации TNM (8 редакция) stage IIIa according to the TNM classification (8th edition)	1	10,00	7	35,00	0,307
стадия IV по классификации TNM (8 редакция) stage IV according to TNM classification (8 edition)	1	10,00	2	10,00	0,519
Проксимальная холангиокарцинома, в том числе Proximal cholangiocarcinoma including	5	50,00	6	30,00	0,503
тип II по классификации Bismuth-Corlette Bismuth-Corlette type II	2	20,00	1	5,00	0,519
тип IIIa/IIIb по классификации Bismuth-Corlette Bismuth-Corlette type IIIa/IIIb	2	20,00	5	25,00	0,879
тип IV по классификации Bismuth-Corlette Bismuth-Corlette type IV	1	10,00	0	0,00	
стадия IIIa по классификации TNM (8 редакция) stage IIIa according to the TNM classification (8th edition)	2	20,00	5	25,00	0,879
стадия IV по классификации TNM (8 редакция) stage IV according to TNM classification (8 edition)	3	30,00	1	5,00	0,184
Аденокарцинома большого дуоденального сосочка, в том числе Adenocarcinoma of big duodenal ampulla including	3	30,00	3	15,00	0,628
стадия IIIa по классификации TNM (8 редакция) stage IIIa according to the TNM classification (8th edition)	2	20,00	2	10,00	0,849
стадия IV по классификации TNM (8 редакция) stage IV according to TNM classification (8 edition)	1	10,00	1	5,00	0,796
Желчный пузырь Gallbladder	0	0,00	2	10,00	0,796
стадия IV по классификации TNM (8 редакция) stage IV according to TNM classification (8 edition)	0	0,00	2	10,00	0,796

Примечание: p – статистическая значимость различий между основной группой и группой сравнения.

Note: p – statistical significance of differences between the main group and the comparison group.

Results and Discussion

In 1 patient (10.0%) of the main group, postoperative acute hemorrhagic anemia was observed after percutaneous transhepatic monobar drainage of the bile ducts. Complications after PDT were not observed.

In 2 patients (10.0%) of the comparison group, prolapse of percutaneous transhepatic drainage with the development of bile peritonitis was detected, in 1 patient (5.0%) of the comparison group, postoperative acute hemorrhagic anemia was observed after percutaneous transhepatic monobar drainage of the bile ducts. In a comparative analysis, the groups were comparable both in terms of the total number of postoperative complications ($p=0.519$) and in Clavien-Dindo stratification: 1 (10.0%)

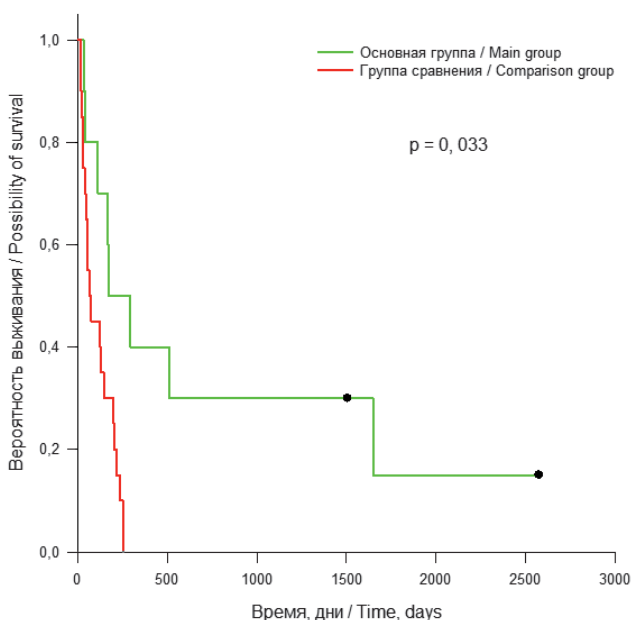
grade IIIa complications in the main group and 3 (15.0%) in the comparison group ($p=0.849$) [7].

When assessing life expectancy in parallel compared groups (Table 3), a statistically significantly higher median survival was found in the main group compared to the comparison group ($p = 0.033$) (Fig. 1).

At present, there are still few studies on palliative PDT for malignant neoplasms of the bile ducts, and the results of studies vary significantly [8-13]. In the studies of Haider et al. [8] the median survival of patients who underwent PDT was 14 months (9 patients with distal cholangiocarcinoma, local PDT with a photosensitizer based on a hematoporphyrin derivative at a dose of 2 mg/kg with monochromatic light irradiation with a

Таблица 3
Сравнительный анализ выживаемости больных**Table 3**
Comparative analysis of survival of patients

Группа Group	Медиана выживания, дни Median survival, days Me (Q1; Q3)	95% доверительный интервал 95% confidence interval	p
Основная Main	170 (1648;113)	-25,235-365,235	0,033
Сравнения Comparison	66 (200;29)	33,13-98,87	

**Рис. 1.** Общая выживаемость пациентов основной группы и группы сравнения.**Fig. 1.** Overall survival of patients in the main group and comparison group.

wavelength of 630 nm with a light dose of 180 J/cm²). At the same time, in a meta-analysis by Moole et al. [11] based on 9 studies of the effectiveness of local PDT with hematoporphyrin derivatives a median survival rate of 7.6 months was obtained in patients with unresectable cholangiocarcinoma after PDT. On the other hand, a study by Pereira et al. [12] conducted a comparative analysis between the group that received palliative choledochal stenting and chemotherapy and the group that received combined treatment consisting of PDT and chemotherapy. After reaching a median survival of 8.4 months, patients who did not undergo PDT lived longer (46 patients with distal and proximal cholangiocarcinoma, gallbladder cancer, local PDT with a hematoporphyrin derivative at a dose of 2 mg/kg with monochromatic light irradiation with a wavelength of 630-635 nm with a light dose of 186 J/cm²). A meta-analysis by Maswikiti

et al. [13] based on 7 studies of the combined use of PDT with hematoporphyrin derivatives and chemotherapy provide other data that patients who received combined PDT and chemotherapy lived twice as long as patients who received these treatments separately. Significant differences in the results of studies are due to the high dependence of PDT results on the light dose, power, and control of the laser delivery to the tumor tissue. At the same time, the issue of the possibility of improving long-term outcomes in patients with unresectable cholangiocarcinoma, including through PDT, which is a safe method of treatment according to the world literature and our data, remains relevant.

The analysis of indicators of inflammation, hemostasis, and proteolysis in dynamics was carried out. There was a statistically significant decrease in TNF- α after PDT from 43.53 \pm 33.99 pg/ml to 28.33 \pm 26.12 pg/ml ($p = 0.041$) (Fig. 2).

TNF- α is known as a significant factor in neovascularization, which is the main component of tumor invasion during carcinogenesis due to stimulation of cyclooxygenase-2 (COX-2) production [14, 15]. Many studies have shown a direct proportional relationship between the concentration of TNF- α and the growth rate of a malignant neoplasm, leading to a decrease in overall life expectancy [14, 15].

We confirmed the literature data in the course of multiple linear regression analysis of factors affecting survival in patients with biliary cancer. A statistically significant inversely proportional effect on survival of TNF- α concentration before treatment was obtained (Table 4).

Changes in the hemostasis system in cancer patients are one of the leading problems of modern oncology, while thrombotic complications are one of the leading causes of death in cancer patients [15].

The results obtained confirm the data of previous studies. PDT is a safe method of choice for palliative surgical treatment of patients with biliary cancer. This is especially relevant for patients with advanced stage IV of the disease, in whom PDT can significantly increase life expectancy in the absence of side effects from therapy.

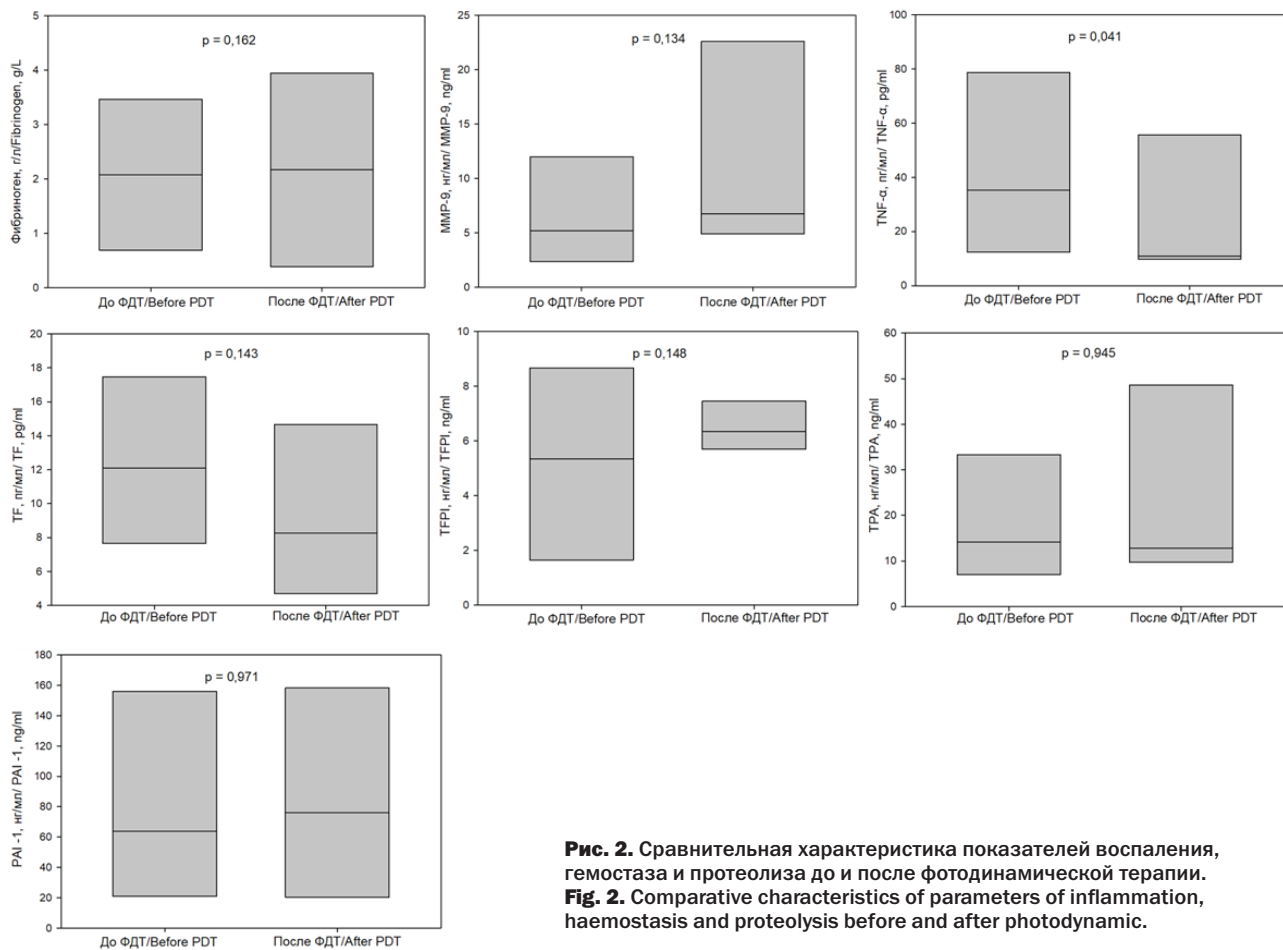


Таблица 4

Модель множественного линейного регрессионного анализа для оценки влияния значения TNF-α, TPA, PAI-1, общего билирубина до лечения на медиану выживаемости у пациентов основной группы

Table 4

Model of multiple linear regression analysis to assess the effect of TNF-α, TPA, PAI-1 and total bilirubin before treatment on the median survival in patients of the main group

Показатель Value	$\beta \pm \sigma$	p
Константа Constant	2003,485±393,260	<0,001
TNF-α	-17,074±5,659	0,012
TPA	-3,940±3,436	0,276
PAI-1	-3,525±2,721	0,222
Общий билирубин Common bilirubin	-1,260±1,021	0,243

Медиана выживаемости = 2003,485 – (17,074 * Показатель TNF- α) – (3,940 * Показатель TPA) – (3,525 * Показатель PAI-1) – (1,260 * Показатель общего билирубина)

Survival median = 2003,485 – (17,074 * Value of TNF- α) – (3,940 * Value of TPA) – (3,525 * Value of PAI-1) – (1,260 * Value of common bilirubin)

R = 0,777; R² = 0,603; F = 4,185; p = 0,027

Conclusion

Thus, complex palliative treatment using PDT of malignant neoplasms of the bile ducts can increase the

life expectancy of patients, while not having significant side effects on the patient. PDT may be recommended for the palliative treatment of biliary cancer.

REFERENCES

1. Status of oncological care for the population of Russia in 2020 / ed. A.D. Kaprin, V.V. Starinskogo, G.V. Petrova – M.: MSIOI named after. P.A. Herzen, branch of the FSBI «NMICR» of the Russian Ministry of Health, 2021, p. 239.
2. Zhang X. et al. Comparison of current guidelines and consensus on the management of patients with cholangiocarcinoma: 2022 update. *Intractable Rare Dis Res*, 2022, vol. 11(4), pp. 161-172.
3. Russian Oncology Association. Biliary cancer. Clinical guidelines. 2020. 51 p. Accessed March 23, 2023 (In Russian) https://oncology-association.ru/wp-content/uploads/2020/09/biliary_rak.pdf
4. Zerem E., Imširović B., Kunosić S. et al. Percutaneous biliary drainage for obstructive jaundice in patients with inoperable, malignant biliary obstruction. *Clin Exp Hepatol*, 2022, vol. 8(1), pp. 70-77.
5. Shah R., John S. Cholestatic Jaundice. In: *StatPearls [Internet]. Treasure Island (FL): StatPearls Publishing*, 2022, PMID: 29489239.
6. Tseimakh A.E. et al. Method for complex mini-invasive treatment of obstructive jaundice, cholangitis, intrahepatic abscesses of tumor genesis using local and systemic photodynamic therapy. Patent RF, no. 2704474, 2019. (In Russian)
7. Dindo D., Demartines N., Clavien P.A. Classification of surgical complications: a new proposal with evaluation in a cohort of 6336 patients and results of a survey. *Annals of Surgery*, 2004, vol. 240(2), pp. 205-213.
8. Haider H., Chapman C.G., Siddiqui U.D. Maximizing survival in hilar cholangiocarcinoma patients using multi-modality therapy: photodynamic therapy (pdt) with stenting, chemotherapy, and radiation. *Gastrointestinal Endoscopy*, 2020, vol. 91(6), pp. 1-5. doi: 10.1016/j.gie.2020.03.2226
9. Lu Y. et al. Efficacy and safety of photodynamic therapy for unresectable cholangiocarcinoma: A meta-analysis. *Clinics and research in hepatology and gastroenterology*, 2015, vol. 39(6), pp. 718-724. doi: 10.1016/j.clinre.2014.10.015.
10. Li Z. et al. Long-Term Results of ERCP- or PTCS-Directed Photodynamic Therapy for Unresectable Hilar Cholangiocarcinoma. *Surg Endosc*, 2021, vol. 35(10), p. 5655-5664. doi: 10.1007/s00464-020-08095-1
11. Moole H. et al. Success of Photodynamic Therapy in Palliating Patients With Nonresectable Cholangiocarcinoma: A Systematic Review and Meta-Analysis. *World J Gastroenterol*, 2017, vol. 23(7), pp. 1278-88. doi: 10.3748/wjg.v23.i7.1278
12. Pereira S.P. et al. PHOTOSTENT-02: Porfimer Sodium Photodynamic Therapy Plus Stenting Versus Stenting Alone in Patients With Locally Advanced or Metastatic Biliary Tract Cancer. *ESMO Open*, 2018, vol. 3(5), p. e000379. doi: 10.1136/esmoopen-2018-000379
13. Maswikiti E.P., Chen H. Photodynamic therapy combined with systemic chemotherapy for unresectable extrahepatic cholangiocarcinoma: A systematic review and meta-analysis. *Photodiagnosis Photodyn Ther*, 2023, vol 2 (41), p.103318. doi: 10.1016/j.pdpdt.2023.103318.
14. Момот А.П., Цывкина Л.П., Тараненко И.А. Современные методы распознавания состояния тромботической готовности. *Москва: Издательство «Знание-М»*, 2022, p. 146.
15. Streiff M.B. et al. Cancer-Associated Venous Thromboembolic Disease, Version 2.2021 NCCN Clinical Practice Guidelines in Oncology. *Journal of the National Comprehensive Cancer Network*, 2021, vol. 19(10), pp. 1181-1201.

ЛИТЕРАТУРА

1. Состояние онкологической помощи населению России в 2020 году / под ред. А.Д. Каприна, В. В. Старинского, Г. В. Петровой – М.: МНИОИ им. П.А. Герцена – филиал ФГБУ «НМИЦ» Минздрава России. – 2021. – С. 239.
2. Zhang X. et al. Comparison of current guidelines and consensus on the management of patients with cholangiocarcinoma: 2022 update // *Intractable Rare Dis Res*. – 2022. – Vol. 11(4). – P. 161-172.
3. Общероссийский национальный союз «Ассоциация онкологов России». Рак желчевыводящей системы. Клинические рекомендации. – 2020. – С. 51. Ссылка активна на 23.03.2023. https://oncology-association.ru/wp-content/uploads/2020/09/biliary_rak.pdf
4. Zerem E., Imširović B., Kunosić S. et al. Percutaneous biliary drainage for obstructive jaundice in patients with inoperable, malignant biliary obstruction // *Clin Exp Hepatol*. – 2022. – №8(1). – P. 70-77.
5. Shah R., John S. Cholestatic Jaundice // In: *StatPearls [Internet]. Treasure Island (FL): StatPearls Publishing*. – 2022. – PMID: 29489239.
6. Цеймах А.Е., Лазарев А.Ф., Куртуков В.А. и соавт. Способ комплексного мини-инвазивного лечения механической желтухи, холангита, внутрипеченочных абсцессов опухолевого генеза с применением локальной и системной фотодинамической терапии. – Патент РФ №2704474. – 2019. [Tseimakh A.E. et al. Method for complex mini-invasive treatment of obstructive jaundice, cholangitis, intrahepatic abscesses of tumor genesis using local and systemic photodynamic therapy. Patent RF, no. 2704474. – 2019. (In Russian)]
7. Dindo D., Demartines N., Clavien P.A. Classification of surgical complications: a new proposal with evaluation in a cohort of 6336 patients and results of a survey // *Annals of Surgery*. – 2004. – Vol. 240(2). – P. 205-213.
8. Haider H., Chapman C.G., Siddiqui U.D. Maximizing survival in hilar cholangiocarcinoma patients using multi-modality therapy: photodynamic therapy (pdt) with stenting, chemotherapy, and radiation // *Gastrointestinal Endoscopy*. – 2020. – Vol. 91(6). – P. 1-5. doi: 10.1016/j.gie.2020.03.2226
9. Lu Y. et al. Efficacy and safety of photodynamic therapy for unresectable cholangiocarcinoma: A meta-analysis // *Clinics and research in hepatology and gastroenterology*. – 2015. – Vol. 39(6). – P. 718-724. doi: 10.1016/j.clinre.2014.10.015.
10. Li Z. et al. Long-Term Results of ERCP- or PTCS-Directed Photodynamic Therapy for Unresectable Hilar Cholangiocarcinoma // *Surg Endosc*. – 2021. – Vol. 35(10). – P. 5655-64. doi: 10.1007/s00464-020-08095-1
11. Moole H. et al. Success of Photodynamic Therapy in Palliating Patients With Nonresectable Cholangiocarcinoma: A Systematic Review and Meta-Analysis // *World J Gastroenterol*. – 2017. – Vol. 23(7). – P. 1278-88. doi: 10.3748/wjg.v23.i7.1278
12. Pereira S.P. et al. PHOTOSTENT-02: Porfimer Sodium Photodynamic Therapy Plus Stenting Versus Stenting Alone in Patients With Locally Advanced or Metastatic Biliary Tract Cancer // *ESMO Open*. – 2018. – Vol. 3(5). – P. e000379. doi: 10.1136/esmoopen-2018-000379
13. Maswikiti E.P., Chen H. Photodynamic therapy combined with systemic chemotherapy for unresectable extrahepatic cholangiocarcinoma: A systematic review and meta-analysis // *Photodiagnosis Photodyn Ther*. – 2023. – Vol. 2 (41). – P. 103318. doi: 10.1016/j.pdpdt.2023.103318.
14. А. П. Момот, Л. П. Цывкина, И. А. Тараненко Современные методы распознавания состояния тромботической готовности // *Москва: Издательство «Знание-М»*. – 2022. – С. 146.
15. Streiff M.B. et al. Cancer-Associated Venous Thromboembolic Disease, Version 2.2021 NCCN Clinical Practice Guidelines in Oncology // *Journal of the National Comprehensive Cancer Network*. – 2021. – Vol. 19(10). – P. 1181-1201.

PULSED EXPOSURE MODE OF THE 445 NM SEMICONDUCTOR LASER IN PHONOSURGERY: AN EXPERIMENTAL STUDY

Ryabova M.A.¹, Mitrofanova L.B.², Ulupov M.Y.¹, Stepanova V.A.¹, Sterkhova K.A.²

¹Pavlov First Saint Petersburg State Medical University, Saint-Petersburg, Russia

²Almazov National Medical Research Centre, Russia, Saint-Petersburg, Russia

Abstract

The study presents the results of an experimental study devoted to the choice of the most optimal mode of pulsed contact laser exposure of semiconductor laser with a wavelength of 445 nm in phonosurgery, which implies maximum preservation of anatomically and functionally significant structures of the larynx combined with a radical approach to the pathological process. From the standpoint of the mucoundular theory of voice formation, wave-like oscillations of the vocal folds are possible due to the mobility of the cover layer of the vocal fold (epithelium, superficial layer of the lamina propria) relative to its body (deep layer of the lamina propria, vocal muscle). Thus, any injury at the level of the integumentary layer is associated with the risk of excessive scarring and loss of the ability to wave-like sliding. Pig vocal folds, according to a number of authors, have a structure similar to human ones in terms of both histological structure and acoustic parameters, which justifies the rationality of their use as an experimental model. In a series of experiments using a 445 nm laser, contact pulsed impacts on a biological model were carried out with pulse durations of 10, 20, 50, and 100 ms, followed by evaluation of the following parameters based on the data of histological sections: the depth and width of the ablation crater, the width of the zone of lateral thermal damage. Thus, the most optimal for phonosurgical interventions modes of pulsed laser exposures with a wavelength of 445 nm are described.

Key words: phonosurgery, laser 445 nm, dysphonia, laser surgery, laryngology.

Contacts: Stepanova V.A., e-mail: valerija.stepanova15@gmail.com

For citations: Ryabova M.A., Mitrofanova L.B., Ulupov M.Y., Stepanova V.A., Sterkhova K.A. Pulsed exposure mode of the 445 nm semiconductor laser in phonosurgery: an experimental study, *Biomedical Photonics*, 2023, vol. 12, no. 2, pp. 11–15. doi: 10.24931/2413-9432-2023-12-2-11-15.

ИМПУЛЬСНЫЙ РЕЖИМ ВОЗДЕЙСТВИЯ ПОЛУПРОВОДНИКОВОГО ЛАЗЕРА С ДЛИНОЙ ВОЛНЫ 445 НМ В ФОНОХИРУРГИИ: ЭКСПЕРИМЕНТАЛЬНОЕ ИССЛЕДОВАНИЕ

М.А. Рябова¹, Л.Б. Митрофанов², М.Ю. Улулов¹, В.А. Степанова¹, К.А. Стерхова²

¹ФГБОУ ВО «Первый Санкт-Петербургский государственный медицинский университет им. акад. И.П. Павлова» Минздрава России, Санкт-Петербург, Россия

²ФГБУ «Национальный медицинский исследовательский центр им. В.А. Алмазова» Минздрава России, Санкт-Петербург, Россия

Резюме

В работе представлены результаты экспериментального исследования, посвященного выбору наиболее оптимального режима импульсного контактного лазерного воздействия полупроводникового лазера с длиной волны 445 нм в хирургии голосовых складок (фонохирургии). Эндоларингеальная фонохирургия подразумевает собой максимальную сохранность анатомически и функционально значимых структур гортани в сочетании с радикальностью в отношении патологического процесса. С позиции мукоундулярной теории голосообразования волнообразные колебания голосовых складок возможны за счет подвижности покровного слоя голосовой складки (эпителий, поверхностный слой собственной пластинки) относительно ее тела (глубокий слой собственной пластинки, голосовая мышца). Таким образом, любая травматизация на уровне покровного слоя сопряжена с риском его избыточного рубцевания и потерей способности к волнообразному скольжению. Голосовые складки свиньи, по данным ряда авторов, имеют схожее строение с человеческими как по гистологическому строению (толщина слоев, соотношение коллагеновых и эластических волокон), так и по акустическим параметрам, что обосновывает рациональность их использования в качестве экспериментальной модели. В серии экспериментов с использованием лазера 445 нм проведены контактные импульсные воздействия на биологическую модель с длительностью импульсов 10, 20, 50 и 100 мс с последующей оценкой по данным гистологических срезов следующих параметров:

глубина и ширина кратера абляции, ширина зоны бокового термического повреждения. Таким образом, описаны наиболее оптимальные для фонохирургических вмешательств режимы импульсных воздействий лазера с длиной волны 445 нм.

Ключевые слова: фонохирургия, лазер 445 нм, дисфония, лазерная хирургия, ларингология.

Контакты: Степанова В.А., e-mail: valerii.stepanova15@gmail.com

Для цитирования: Рябова М.А., Митрофанова Л.Б., Улулов М.Ю., Степанова В.А., Стерхова К.А. Импульсный режим воздействия полупроводникового лазера с длиной волны 445 нм в фонохирургии: экспериментальное исследование // Biomedical Photonics. – 2023. – Т. 12, № 2. – С. 11–15. doi: 10.24931/2413-9432-2023-12-2-11-15.

Introduction

Benign neoplasms of the larynx are the most common pathology of the larynx, leading to persistent dysphonia, which leads to a decrease in the quality of life and often a loss in the productivity of professional activity. Treatment of this pathology is possible only with the use of surgical techniques.

Endolaryngeal phonosurgery implies the maximum preservation of anatomically and functionally significant structures of the larynx, combined with a radical approach to the pathological process. The maximum preservation of structures involves, first of all, the integumentary layer of the vocal fold. From the standpoint of the biomechanics of the vibrational oscillations necessary for the emergence of a voice, the structure of the vocal folds is divided into the so-called “integumentary layer” and “body”. The mucous membrane (the epithelium and the surface layer of the lamina propria) is the “integumentary layer” and represents a single morphofunctional unit capable of self-sustaining oscillations relative to the “body”, which is formed by a deep layer of the lamina propria lying on the vocal muscle, while the middle layer of the lamina propria is designated as “transition zone”. Later, some different divisions were proposed, the differences in which mainly relate to the position of the intermediate layer of the lamina propria, although in any case, the main idea is that the “cover” and “body” have different biomechanics [1]. The surface layer of the lamina propria contains the least amount of fibrillar proteins (collagen and elastin), which determines its high mobility. Thus, any trauma at this level and stimulation of fibroblast activity can lead to excessive scarring and limitation of mobility of the vocal fold integumentary layer.

In phonosurgery for benign lesions of the vocal folds, it should always be taken into account that surgical tissue incision, excision, or ablation may themselves cause excessive tissue scarring as a consequence of its healing [2]. Thus, the surgeon is always faced with the task of minimizing trauma to the tissues of the vocal folds during surgery, which confirms the validity of the search and introduction into practice of new, more gentle, methods of phonosurgical interventions [3].

Materials and methods

In the experimental part of the study, an assessment was made of the impact of 445 nm semiconductor laser

radiation on a biological tissue model. The *ex vivo* vocal folds of pigs (*Sus scrofa domestica*) were used as a biological model, and were collected within 2 hours after the humane death of animals in the slaughterhouse and then stored at a temperature of 2°C to avoid biological tissue degradation until the experiment.

For laser irradiation, an IPG Photonics laser system (Russia) with a wavelength of 445 nm was used. A reusable non-sterile fiber instrument IPG Surgical Fiber Reusable (Russia) with a core diameter of 400 μm was used as an optical fiber.

The experiment was carried out after preliminary natural warming of the biological tissue to room temperature. During the experiment, a semiconductor laser with a wavelength of 445 nm was used in a pulsed mode by applying individual point laser effects in the contact mode at a maximum power of 13 W with individual pulse durations of 10, 20, 50, and 100 ms. For each pulse mode, 10 separate laser exposures were performed along the medial edge of one vocal fold. Thus, 5 swine larynxes were used in the experiment: 4 of which were for the experimental part, and 1 – as a control.

After irradiation was completed, the biological tissue samples were dissected (Fig. 1), then the material was fixed in 10% buffered neutral formalin solution for 48 hours (the ratio of the fixative and the studied samples was 10:1). Afterwards the biological material was cut into plates 5 mm thick and fit into histological cassettes. Next, the sections were decalcified in an acid solution (the ratio of the decalcifier and the samples under study was 50:1) and standard alcohol wiring was embedded in paraffin according to the generally accepted method [4]. Then, sections were made from the blocks with a thickness of 2 μm on a Leica DM1000 light microtome (Germany), followed by their staining with hematoxylin and eosin according to the standard method. Then, histological sections were digitized using an Aperio AT2 scanning microscope (Germany). Morphometry was performed using an Aperio ImageScope 12.4.6.5003 image analyzer. Due to the high power density in the zone of contact between the fiber and the tissue surface, a tissue destruction (ablation) site (crater) is formed, the diameter and depth of which were measured in the experiment, as a result of which ranges of damage values were obtained for each pulse duration. The area of laser exposure was considered to be an optically void area in which evaporation of normal histological structures occurred and interruption



Рис. 1. Макроскопические препараты голосовых складок свиной после лазерного воздействия (а – 10 мс, б – 20 мс, с – 50 мс, д – 100 мс).

Fig. 1. Macroscopic preparations of the pig vocal folds after laser exposure (a – 10 ms, b – 20 ms, c – 50 ms, d – 100 ms).

of normal stratified squamous nonkeratinized epithelium with the formation of a specific ablation crater was objectively noted, as well as tissue adjacent to the crater (lamina propria, vocalis muscle) with signs of thermal damage in the form of a violation of the nuclear structure and disorientation of the course of elastic and collagen fibers.

Statistical processing of the results was carried out on the Jupyter Notebook platform using Python 3.9 with correlation calculation using Spearman's (r) coefficient.

Results and discussion

The gold standards of phonosurgery are interventions using cold microinstruments and CO₂ laser. Speaking about classical "cold" phonomicrosurgery, despite the active introduction of minimally invasive techniques (microflap, mini-microflap), it is worth noting that for many benign lesions of the vocal folds, the volume of surgery is calculated in micrometers, which makes it difficult for the surgeon to calculate the accuracy of his actions using microsurgical scissors, scalpel, and other instruments. Thus, the trauma of the tissue of the vocal folds associated with the "cold" intervention is potentially more pronounced due to the large size of the instruments compared to the necessary sizes in the micron range for radicalization in relation to the pathological process.

As mentioned above, with regard to the most gentle restoration of the vibrational oscillations of the vocal fold during phonosurgery, it is important to perform intervention within the epithelium and the surface layer of the lamina propria, which will subsequently avoid exces-

sive scarring and impaired mobility of the cover layer of the fold relative to its body. According to a number of publications, the surface layer makes up about 30–40% of the entire depth of the lamina propria, the thickness of which, in turn, is 1 mm on average [5, 6, 7]. The depth of the epithelium of the true vocal fold, in this case, is about 80–100 μm [8] and, thus, the depth of the cover layer of the vocal fold is on average 400–500 μm, within which phonosurgical intervention is allowed to avoid binding of the scar tissue to the body of the vocal fold and mobility restrictions.

Several researchers believe that in pigs it can be distinguished a tendency to a similar three-layered structure of the lamina propria with a similar ratio of collagen and elastic fibers throughout the entire depth of the lamina propria. The thickness of the mucous membrane of the vocal folds of pigs is on average 0.9 mm [9]. According to the acoustic analysis of the natural phonation of animals, it was found that the range of phonation frequencies in pigs is the closest to that in humans [10,11].

Despite the anatomical and histological advantage of porcine vocal fold models and the rationality of their use as a scientific model for testing surgical techniques (due to their easy availability in the slaughterhouse, without the need to sacrifice animals for research purposes), there are currently a small number of publications in which this model is evaluated from the point of view of laser exposure, which is used in human vocal fold phonosurgery.

In none of the articles, we found a histological assessment to analyze point laser effects on biological tissue using laser radiation with a wavelength of 445 nm on the vocal folds of laboratory biological models, which determines the relevance of our experimental work.

When performing point pulsed laser actions using a laser with a wavelength of 445 nm, an increase in the pulse duration leads to an increase in the depth of the ablation crater and an increase in the thickness of the lateral thermal damage zone (Fig. 2), while there was no significant increase in the width of the ablation crater (Fig. 3).

The data of the statistical analysis of the measurements are presented in Table. 1.

The Spearman correlation coefficient for the relationship between the pulse duration and the depth of the ablation crater was 0.81, for the thickness of the lateral thermal damage zone it was 0.74, and for the width of the ablation crater – 0.45 ($p < 0.05$). It follows from the presented data that there is a relationship between the pulse duration and each of the estimated parameters and it is statistically significant. At the same time, this relationship is less typical for the width of the ablation crater, which can be explained by the physical properties of laser radiation, when, in the contact mode of exposure, radiation absorption mainly occurs deep into the biological tissue.

The presented histological sections clearly demonstrate an increase in the depth and width of the zone of

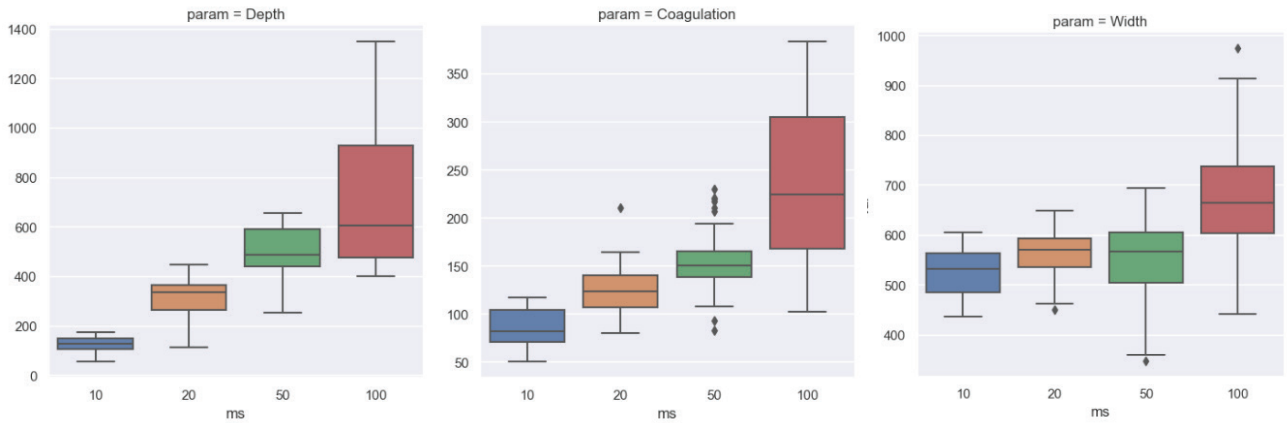


Рис. 2. Зависимость глубины кратера абляции в мкм (слева, ось y) и толщины зоны бокового термического повреждения в мкм (справа, ось y) от длительности импульса лазерного воздействия в мс (ось x).

Fig. 2. Dependence of the ablation crater depth in μm (left, y-axis) and the thickness of the lateral thermal damage zone in μm (right, y-axis) on the laser exposure pulse duration in ms (x-axis).

Рис. 3. Зависимость ширины кратера абляции в мкм (ось y) от длительности импульса лазерного воздействия мс (ось x).

Fig. 3. Dependence of the ablation crater width in μm (y-axis) on the laser exposure pulse duration in ms (x-axis).

Таблица 1

Зависимость глубины, ширины кратера абляции и зоны бокового термического повреждения от длительности импульсного лазерного воздействия с длиной волны 445 нм.

Table 1

Dependence of the depth, width of the ablation crater and the zone of lateral thermal damage on the duration of pulsed laser exposure with wavelength of 445 nm.

		Глубина кратера абляции, мкм The depth of the ablation crater, μm	Зона бокового термического повреждения, мкм The lateral thermal damage zone, μm	Ширина кратера абляции, мкм The width of the ablation crater, μm
10 мс 10 ms	Среднее значение (стандартное отклонение) Mean value (standard deviation)	124,8 (32,9)	85,2 (20,0)	526,6 (55,2)
	Мин; макс min; max	104; 148	71; 104	485; 563
20 мс 20 ms	Среднее значение (стандартное отклонение) Mean value (standard deviation)	312,5 (83,8)	126,8 (27,8)	564,0 (51,7)
	Мин; макс min; max	262; 365	107; 140	536; 593
50 мс 50 ms	Среднее значение (стандартное отклонение) Mean value (standard deviation)	498,6 (93,7)	152,4 (30,6)	548,7 (90,1)
	Мин; макс min; max	440; 592	138; 165	504; 604
100 мс 100 ms	Среднее значение (стандартное отклонение) Mean value (standard deviation)	730,3 (313,9)	235,7 (82,6)	673,4 (115,7)
	Мин; макс min; max	475; 926	168; 304	602; 737

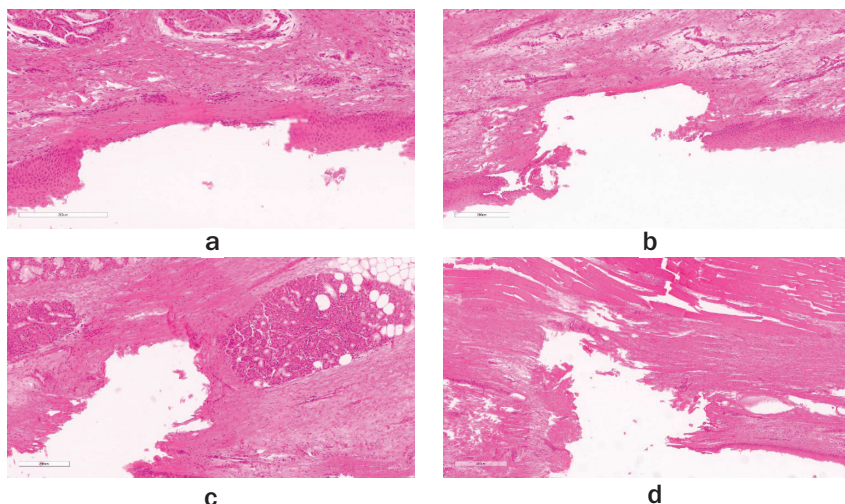


Рис 4. Микрофотографии гистологических срезов голосовых складок свиней после нанесенных лазерных воздействий, окраска гематоксилином и эозином: а – длительность импульса 10 мс, масштаб 200 мкм; ареактивный (без воспалительного инфильтрата) язвенный дефект с некрозом всех слоев плоскоклеточного эпителия; б – длительность импульса 20 мс, масштаб 200 мкм; очаговый некроз ¼ собственной пластинки слизистой оболочки; с – длительность импульса 50 мс, масштаб 200 мкм; очаговый некроз голосовой складки с распространением на 2/3 глубины собственной пластинки слизистой оболочки; д – длительность импульса 100 мс, масштаб 400 мкм; увеличение очага некроза за счет вовлечения большей площади эпителия и некроза 1/3 мышечных волокон голосовой складки.

Fig. 4. Micrographs of histological sections of the vocal folds of pigs after laser exposure, stained with hematoxylin and eosin: а – pulse duration 10 ms, scale 200 μ m; areactive (without inflammatory infiltrate) ulcerative defect with necrosis of all layers of the squamous epithelium; б – pulse duration 20 ms, scale 200 μ m; focal necrosis of the lamina propria and ¼ of the muscle fibers of the vocal fold; с – pulse duration 50 ms, scale 200 μ m; focal necrosis of the vocal fold extending to 2/3 of the depth of the mucosal lamina propria; д – pulse duration 100 ms, scale 400 μ m; an increase in the focus of necrosis due to the involvement of a larger area of the epithelium and necrosis of 1/3 of the muscle fibers of the vocal fold.

lateral thermal damage (Fig. 4, a-d). At the same time, it is noticeable that with a pulse duration of 100 ms, the damage zone overcomes all layers of the lamina propria and most of the muscle fibers of the vocal fold.

Conclusion

Thus, the pulse duration during phonosurgical interventions should be chosen directly by the surgeon, depending on the pathological formation of the vocal fold. In our opinion, the most optimal modes of laser exposure are radiation with a single pulse duration of 10 ms and 20 ms, which, with a high probability, will effectively remove epithelial or subepithelial formations within the surface layer of the lamina propria of the vocal fold. In cases of mass lesions on a wide base, a mode with a single pulse duration of 50 ms can be recommended, while a pulse duration of 100 ms should be avoided during phonosurgical intervention, given the high probability of laser radiation penetrating the entire thickness of the vocal fold proper.

REFERENCES

1. Hirano M. Vocal mechanisms in singing: Laryngological and phoniatric aspects. *Journal of Voice*, 1988, vol. 2(1), pp. 51-69.
2. Allen J. Cause of Vocal Fold Scar. *Curr Opin Otolaryngol Head Neck Surg*, 2010, vol.18, pp. 475-480.
3. Karpishchenko S.A., Ryabova M.A., Ulupov M.Yu. Laser surgery in otorhinolaryngology at the present stage. *Consilium medicum*, 2014, vol. 16(11), pp. 73-76.
4. Sarkisov, D.S. Microscopic technique / D. S. Sarkisov, Yu.L. Perov. – M.: Medicine, 1996, p. 544.
5. Nick J.I. Hamilton. The life-cycle and restoration of the human vocal fold. *Laryngoscope Investig Otolaryngol*, 2023, vol. 8(1), pp. 168-176.
6. Woodson G. Developing a Porcine Model for Study of Vocal Fold Scar. *Journal of Voice*, 2012, vol. 26(6), pp. 706-710.
7. Laszlo Peter Ujvary et al. Experimental model for controlled endoscopic subepithelial vocal fold injury in rats. *Acta Cir Bras*, 2022, vol. 37(1), p. e370106.
8. Kaiser M.L. et al. Laryngeal epithelial thickness: a comparison between optical coherence tomography and histology. *Clinical Otolaryngology*, 2009, vol. 34(5), pp. 460-466.
9. Alipour F., Finnegan E.M. & Jaiswal S. Phonatory Characteristics of the Excised Human Larynx in Comparison to Other Species. *Journal of Voice*, 2013, vol. 27(4), pp. 441-447.
10. Schlegel P. et al. Objective Assessment of Porcine Voice Acoustics for Laryngeal Surgical Modeling. *Appl Sci (Basel)*, 2021, vol. 11(10), p. 4489.
11. Connor M.P. et al. Effect of Vocal Fold Injection of Cidofovir and Bevacizumab in a Porcine Model. *JAMA Otolaryngology-Head & Neck Surgery*, 2014, vol. 140(2), p. 155.

ЛИТЕРАТУРА

1. Hirano M. Vocal mechanisms in singing: Laryngological and phoniatric aspects // *Journal of Voice*. – 1988. – Vol. 2(1). – P. 51-69.
2. Allen J. Cause of Vocal Fold Scar // *Curr Opin Otolaryngol Head Neck Surg*. – 2010. – Vol.18. – P. 475-480
3. Карпищенко С.А., Рябова М.А., Улупов М.Ю. Лазерная хирургия в оториноларингологии на современном этапе // *Consilium medicum*. – 2014. – Т. 16, №11. – С. 73-76.
4. Саркисов, Д. С. Микроскопическая техника / Д. С. Саркисов, Ю. Л. Перов. – М.: Медицина. – 1996. – С. 544.
5. Nick J I Hamilton. The life-cycle and restoration of the human vocal fold // *Laryngoscope Investig Otolaryngol*. – 2023. – Vol. 8(1). – P. 168-176.
6. Woodson G. Developing a Porcine Model for Study of Vocal Fold Scar // *Journal of Voice*. – 2012. – Vol. 26(6). – P.706-710.
7. Laszlo Peter Ujvary et al. Experimental model for controlled endoscopic subepithelial vocal fold injury in rats // *Acta Cir Bras*. – 2022. – Vol. 37(1). – P. e370106.
8. Kaiser M.L. et al. Laryngeal epithelial thickness: a comparison between optical coherence tomography and histology // *Clinical Otolaryngology*. – 2009. – Vol. 34(5). – P. 460-466.
9. Alipour F., Finnegan E.M. & Jaiswal S. Phonatory Characteristics of the Excised Human Larynx in Comparison to Other Species // *Journal of Voice*. – 2013. – Vol. 27(4). – P.441-447.
10. Schlegel P. et al. Objective Assessment of Porcine Voice Acoustics for Laryngeal Surgical Modeling // *Appl Sci (Basel)*. – 2021. – Vol. 11(10). – P. 4489.
11. Connor M. P. et al. Effect of Vocal Fold Injection of Cidofovir and Bevacizumab in a Porcine Model // *JAMA Otolaryngology-Head & Neck Surgery*. – 2014. – Vol. 140(2). – P.155.

VIDEOCAPILLAROSCOPIC MONITORING OF MICROCIRCULATION IN RATS DURING PHOTODYNAMIC THERAPY

Guryleva A.V.¹, Machikhin A.S.¹, Grishacheva T.G.², Petrishchev N.N.²

¹Scientific and Technological Center for Unique Instrumentation of the Russian Academy of Sciences, Moscow, Russia

²First St. Petersburg State Medical University named after Academician I.P. Pavlova, St. Petersburg, Russia

Abstract

The proposed approach to microcirculation assessment is non-invasive, informative, and can be implemented during photoactivation, and thus is perspective both for research tasks and clinical practice. The functional principles of the vasculature response to photodynamic exposure, identified using this technique, also foster the efficiency and safety of photodynamic therapy. The developed setup allows simultaneous photodynamic exposure and studying the microcirculation parameters by videocapillaroscopy and photoplethysmography techniques. Photodynamic action is carried out by 662 nm laser radiation with a power density of 15 mW/cm² in continuous and pulsed modes. The imaging system of the setup consists of a large working distance microscope, an optical filter, and a monochrome camera. The illumination system is based on LED with a central wavelength of 532 nm. The acquired images were processed in order to obtain morphometric and hemodynamic microcirculation data in the inspected skin area. To compare the proposed approach with existing methods, we measured blood flow parameters by a laser Doppler flowmeter. We tested the developed setup on rats injected with a photosensitizer and obtained active vessel maps, photoplethysmograms, and skin vessel density values before, during, and after photoactivation in both generation modes. The proposed approach allows to reveal differences in the microcirculation response to photodynamic effects of low power densities in different modes, in particular, the discrepancy between the time from the start of exposure to the cessation of blood flow and the start of the recovery period.

Key words: photodynamic therapy, microcirculation, photoplethysmography, videocapillaroscopy, laser Doppler flowmetry.

Contacts: Grishacheva T.G., e-mail: tgrishacheva@gmail.com

For citation: Guryleva A.V., Machikhin A.S., Grishacheva T.G., Petrishchev N.N. Videocapillaroscopic monitoring of microcirculation in rats during photodynamic therapy, *Biomedical Photonics*, 2023, vol. 12, no. 2, pp. 16–23. doi: 10.24931/2413–9432–2023–12-2-16–23.

ПРИМЕНЕНИЕ ВИДЕОКАПИЛЛЯРОСКОПИИ ДЛЯ МОНИТОРИНГА МИКРОЦИРКУЛЯЦИИ В КОЖЕ ПРИ ФОТОДИНАМИЧЕСКОЙ ТЕРАПИИ

А.В. Гурылева¹, А.С. Мачихин¹, Т.Г. Гришачева², Н.Н. Петрищев²

¹Научно-технологический центр уникального приборостроения Российской академии наук, Москва, Россия

²Первый Санкт-Петербургский государственный медицинский университет имени академика И.П. Павлова» Министерства здравоохранения Российской Федерации, Санкт-Петербург, Россия

Резюме

Предложено аппаратно-программное и методическое обеспечение для оценки микроциркуляции, которое отличается неинвазивностью, информативностью, а главное, возможностью проводить исследование в ходе фотоактивации, и может стать дополнением к существующим диагностическим методам как в исследовательских задачах, так и в клинической практике. Выявленные с помощью разработанного подхода функциональные принципы реакции сосудистой сети на фотодинамическое воздействие представляются полезными для повышения эффективности и безопасности фотодинамической терапии. Разработка и апробация методов видеокapилляроскопии и фотоплетизмографии для изучения ранних изменений микроциркуляции при фотодинамической активации. Разработанная установка позволяет одновременно проводить фотодинамическое воздействие и исследование параметров микроцир-

куляции методами видеокапилляроскопии и фотоплетизмографии. Фотодинамическое воздействие осуществляется через 3 ч после внутривенного введения фотосенсибилизатора на основе хлорина е6 (5 мг/кг) лазерным излучением с длиной волны 662 нм и плотностью мощности 15 мВт/см² в непрерывном и импульсном режимах. Визуализирующая система установки состоит из микроскопа с большим рабочим расстоянием, цифровой высокоскоростной камеры и оптического фильтра, отсекающего отраженное от исследуемой поверхности излучение фотоактивации. Осветительная система представлена диодным источником излучения с центральной длиной волны 532 нм. Зарегистрированные установкой изображения исследуемого участка кожи обрабатываются в разработанном авторами программном обеспечении для получения морфометрических и гемодинамических данных о микроциркуляции. Для сравнения предложенного подхода с существующими методами параметры кровотока регистрировали также лазерным доплеровским флоуметром. В ходе апробации разработанной установки на инъецированных фотосенсибилизатором крысах получены наборы карт действующих сосудов, фотоплетизмограмм и значений плотности сосудов кожи до, во время и после фотоактивации в двух режимах генерации. Проведен совместный анализ данных видеокапилляроскопии, фотоплетизмографии и лазерной доплеровской флоуметрии. Показано, что предложенный подход позволяет выявить различия в механизмах реакции микроциркуляции на фотодинамическое воздействие с малой плотностью мощности в различных режимах, в частности, несовпадение времени от начала экспозиции до остановки кровотока и начала восстановительного периода.

Ключевые слова: фотодинамическая терапия, микроциркуляция, фотоплетизмография, видеокапилляроскопия, лазерная доплеровская флоуметрия

Контакты: Гришачева Т.Г., e-mail: tgrishacheva@gmail.com

Ссылка для цитирования: Гурьева А.В., Мачихин А.С., Гришачева Т.Г., Петрищев Н.Н. Применение видеокапилляроскопии для мониторинга микроциркуляции в коже при фотодинамической терапии // Biomedical Photonics. – 2023. – Т. 12, № 2. – С. 16–23. doi: 10.24931/2413–9432–2023–12–2–16–23.

Introduction

Photodynamic therapy (PDT) is a treatment method based on a combination of a light-sensitive pharmacological drug, a photosensitizer (PS), and exposure to electromagnetic radiation of a certain wavelength. PS photoactivation initiates photochemical reactions, which are accompanied by the formation of reactive oxygen species (ROS), which have a cytotoxic effect on the cells of the treated tissues. PDT is used to treat a number of dermatological skin diseases, including acne, psoriasis, dermatosis, and some forms of skin cancer, such as basal cell and squamous cell carcinomas [1, 2]. The effect of PDT on microcirculation (MC) in the skin is of great importance for achieving a therapeutic effect.

The study of MC in the upper layers of the skin during photoactivation (PA) provides information on its functional response to PA, which is necessary to increase its effectiveness and safety of treatment, as well as to study the mechanisms of PDT action. Among the existing methods for studying MC in the skin to identify the features of the vascular response in tumor damage after PA, the most common method is laser Doppler flowmetry (LDF). It provides registration of changes in tissue perfusion integrally from a certain area of the skin based on the Doppler effect [3–5].

Laser spectroscopy is also used to analyze MC and study the mechanisms of photodynamic action. It is based on the use of spectral analysis of radiation reflected from the skin to determine in real time the content of oxygenated hemoglobin and deoxygenated hemoglobin in capillaries, which is one of the key indicators of the effectiveness of PDT [6]. There are known methods for assessing blood flow dynamics using fluorescent contrast agents,

including with the use of confocal microscopy [7, 8], which makes it possible to visualize *in vivo* the vascular network with high resolution and evaluate responses to PDT both at the level of vascular endothelial cells and at the level of a separate vessel. Optical coherence tomography makes it possible to visualize the capillary network and assess vascular occlusion after PDT both in the tumor and in surrounding healthy tissues [9].

Although most of the existing methods for diagnosing MC during PDT are non-invasive and can provide *in vivo* measurements, they do not allow monitoring directly during PA. In addition, the methods have a number of disadvantages, such as dependence on the orientation of the sensors and the experience of the operator, the need to use coloring agents, as well as the complexity and high cost of the equipment.

One of the promising methods for *in vivo* assessment of the morphological and functional characteristics of the capillary bed of the skin is video capillaroscopy (VCS) [10,11]. It is based on the registration of a sequence of skin images and their subsequent spatial-frequency analysis. The result of videocapillaroscopic studies is a map of active vessels with active blood flow, as well as hemodynamic characteristics, including a map of the speed of erythrocyte movement. VCS is featured in that it does not require the use of tinting agents, provides a spatial distribution of the studied parameters, is simple and accessible in technical implementation, and also provides comprehensive information on the morphometric and hemodynamic parameters of the microvasculature. In a number of studies, VCS is used to evaluate the PDT efficiency and determine the optimal photosensitizer doses and radiation parameters [12].

The equipment for VCS makes it possible to quantify tissue perfusion by recording and analyzing photoplethysmograms (PPGs). The amount of radiation reflected from the skin changes along with the optical density of the studied tissues, which in turn depends on the blood supply [13]. PPG is a temporal periodic signal proportional to the intensity of radiation reflected from the skin, which characterizes tissue perfusion and is used to assess MC in solving many biomedical problems [14–16].

An important property of the VCS methods and photoplethysmography is the non-contact measurements, which are important for monitoring during PA. However, to the best of our knowledge, no description of the implementation of such a study has been provided so far. In this paper, we consider the possibility of using VCS and photoplethysmography to study early changes in MC during PA, depending on the regime of laser radiation generation.

Materials and methods

Experimental animals

The study was conducted on the basis of the Pavlov First Saint Petersburg State Medical University of the Ministry of Health of Russia. The work was performed on male Wistar rats weighing 250 ± 25 g, obtained from the "Rappolovo" Laboratory Animals Nursery of the National Research Centre "Kurchatov Institute" in accordance with the EU directive (The European Council Directive (86/609 /EEC)) on the observance of ethical principles in work with laboratory animals. The animals were kept on unlimited intake of food (standard diet for laboratory rats K-120 (Informkorm, Russia)) and water at a standard twelve-hour regimen (12 h in light, 12 h in dark). The temperature was maintained within 22–25°C, and the relative humidity was 50–70%. The duration of the quarantine (acclimatization period) for all animals was at least 14 days.

Before the start of the experiment, the animals were anesthetized by intravenous administration of Zoletil 100 (VIRBAC, France) and Xyla (De Adelaar B.V., Netherlands) in equal volumes at a dose of 0.5 ml/kg. Then the rat was

placed on a thermostated table TCAT-2 (Physitemp, USA) with constant maintenance of rectal temperature within 37–37.5°C. The skin of the back was cleaned of coat mechanically. The rats were divided into 2 groups. For the first group, PA was performed in a continuous generation mode, and for the second, in a pulsed generation mode. Intact rats were used as controls. The study of MC in the skin was carried out 3 hours after the administration of a photosensitizer based on chlorin e6, radachlorin (RADA-PHARMA, Russia), at a dose of 5 mg/kg into the tail vein.

Equipment

To assess the MC during PDT, a setup containing a PDT laser source and a video conferencing system has been developed and tested (Fig. 1). The VCS system includes a LED source with a center wavelength of 520 nm and a bandwidth of 30 nm (LED), a microscope (M) with a long working distance and x1.5 magnification, a monochrome camera (C) (Allied Vision Procolica GT2000, Germany) with a resolution of 2048×1088 pixels, a pixel size of $5.5 \times 5.5 \mu\text{m}$, a frame rate of up to 54 Hz, a GigE interface, and a 12-bit ADC and a computer (PC). The selected irradiation wavelength allows for increasing the contrast of capillaries against the background of surrounding tissues. The microscope and camera provide high resolution, magnification, and frame-rate imaging of the rat skin. To provide a sharp image throughout the entire field of view, the region under study was covered with a thin glass plate (GP). To obtain images under the same conditions before, during, and after PDT, an optical filter (F) was placed in front of the microscope to cut off radiation in the spectral range above 570 nm. An optical fiber (OF) with a microlens that transmits PA laser radiation from an ALOD laser device (L) (Alkom Medica, Russia) with a wavelength of 662 nm and a power density of $15 \text{ mW}/\text{cm}^2$ was fixed in a position that provides the diameter of the laser spot of 3 cm on the tissue under study.

Blood flow was measured using both the VSC and LDF (Transonic Systems Inc., BLF21). The power of the LDF diode radiation source with a wavelength of 780 nm

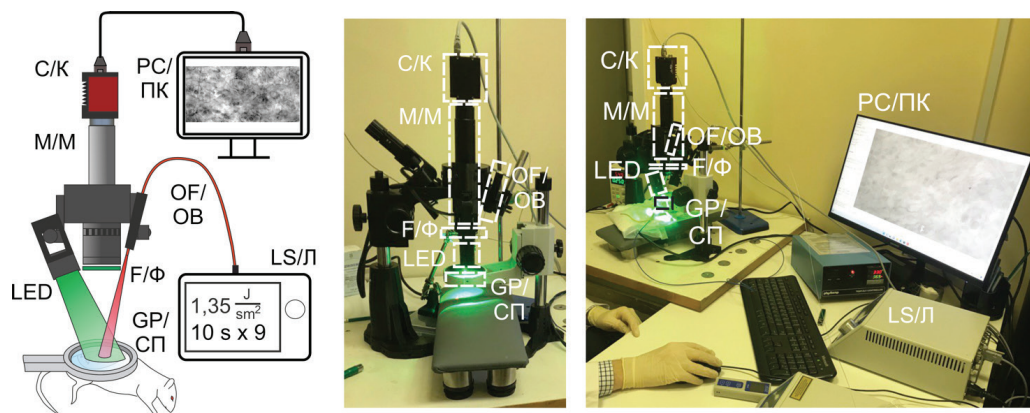


Рис. 1. Схема установки (К – камера, М – микроскоп, ПК – персональный компьютер, ОБ – оптическое волокно, Л – лазерный аппарат, Ф – оптический фильтр, СП – стеклянная пластина).
Fig. 1. Assembled setup (C – Camera, M – Microscope, PC – personal computer, OF – optical fiber, LS – laser, F – optical filter, GP – glass plate).

did not exceed 2 mW. The flowmeter allowed to register tissue perfusion from 0 to 100 ml/min per 100 g of tissue. The results were evaluated in perfusion units (pf. un.). The volume of the zone studied with the help of a laser sensor did not exceed 1 mm³, and the depth of probing microhemodynamics was up to 1 mm.

Experiment Protocol

The scheme of the experiment is shown in Fig. 2. The MC parameters were estimated for two PA modes. The exposure in the continuous mode was 1.5 min, the exposure in the pulsed mode was 3 min, while the pulse duration and the interval between pulses were 10 s. The energy density in both groups was 1.35 J/cm².

Video capillaroscopic examination was performed 1.5 min before, during, and 20 min after PA. Before and after PA, image sequences of 1000 12-bit frames were recorded at a frame rate of 43 Hz. For a detailed analysis of changes in the MC during the exposure, shooting was

carried out at the same frame rate, but for a time equal to the duration of the PDT time pulse, i.e., 10 s.

The fixation of blood flow parameters during PA using LDF was not performed due to the contact nature of the method; therefore, the data were recorded before and after PA. To reduce the effect of interference, the information was read three times for 1 min and the smallest value was recorded. The MC index (IM) was recorded before PA for 1 min and immediately after turning off the laser radiation for 20 min. To exclude the effect of LDF radiation on MC in the skin of PS-introduced rats, the measurements on intact rats have been performed without PS as an IM control.

Digital data processing algorithm for VCS

The image sequences obtained by the VCS method were processed using the algorithm implemented in MATLAB and described in detail in [17]. The main stages of the algorithm are shown in Fig. 3. The pre-processing

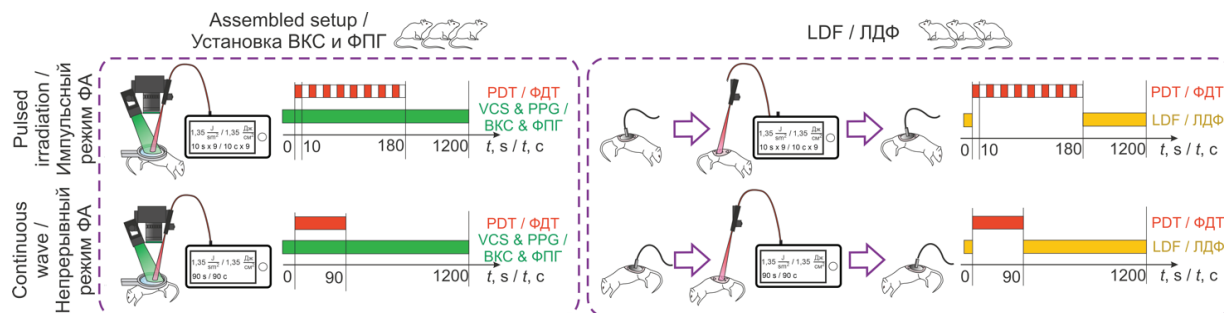


Рис. 2. Протокол эксперимента (ВКС – видеокапилляроскопия, ФПГ – фотоплетизмография, ЛДФ – лазерная Допплеровская флоуметрия, ФДТ – фотодинамическая терапия, ФА – фотоактивация).
Fig. 2. Experimental design (VCS – videocapillaroscopy, PPG – photoplethysmography, PDT – photodynamic therapy, LDF – laser Doppler flowmetry).

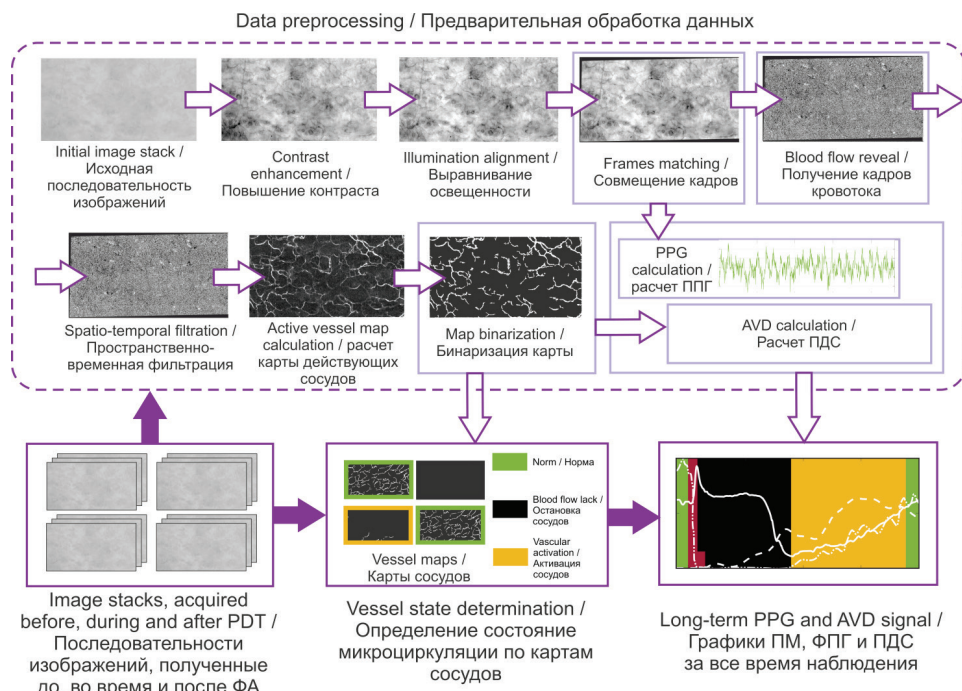


Рис. 3. Алгоритм цифровой обработки данных видеокapилляроскопии и фотоплетизмограмм (ППГ – фотоплетизмография, ПДС – плотность действующих сосудов, ПМ – показатель микроциркуляции, ФА – фотоактивация).
Fig. 3. Data processing pipeline (PPG – photoplethysmography, AVD – active vessel density, PDT – photodynamic therapy).

data is used to improve images, in particular, to expand the dynamic range, eliminate illumination nonuniformity, compensate for sample displacement, etc.

Enhanced images consist of pixels related to vessels and their surrounding tissues. Within each sequence in the pixels related to the vessels, there is a periodic change in intensity associated with the movement of red blood cells. The intensities of the pixels of the tissues surrounding the vessels have practically unchanged values. With the help of spatial frequency analysis, vessel maps were calculated for each image sequence. For each such map, the density of active vessels measured as a percentage can be calculated as the ratio of pixels belonging to the active capillary network to the total number of image pixels. The time points associated with the onset of vascular shutdown, complete stopping of blood flow, and vascular activation were determined using a visual analysis of the resulting map, based on which the graph was further marked.

A decrease or increase in the optical density of the studied area, modulated by heart rate and blood supply, leads to a corresponding change in the intensity of image pixels from frame to frame. Averaging the pixel intensity of each image of all registered sequences makes it possible to obtain a set of points equal to the number of frames. Such points form a PPG that describes perfusion during the experiment and is measured in relative units (rel. un.). Further, the low-frequency component is removed from the PPG signal and only the amplitude of local periodic changes in the signal associated with the heart rhythm is analyzed. However, in the present work, for long-term perfusion analysis, the low-frequency component is also a useful signal. The PPG signal was subjected only to smoothing by the sliding window method to eliminate the noise component.

Results

Data on the state of MC in the skin during PDT using the developed VCS and LDF setups are shown in Fig. 4. Maps of vessels, PPG, curves of changes in vascular density, blood flow velocity, and MC (IM) are shown on one graph for two PA modes. The graphs are marked with colors following the state of the vessels based on the analysis of maps and vessel density.

According to LDF data, the IM in the skin before exposure ranged from 2.3 to 6.5 pf. un., and the average value was 4.7 ± 0.5 pf. un. Immediately after PA in the continuous mode of laser generation, a decrease in the IM to 0.4 ± 0.4 pf. un. was observed. During the first 7 minutes there was a gradual increase in IM and by 8 minutes this indicator was 3.7 ± 0.3 pf. un. During the subsequent registration of blood flow for 10 min, there was a significant increase in the IM in the skin up to 9.9 ± 0.7 pf. un. On the 20th min of registration, the IM was 7.2 ± 0.4 pf. un.

In the group of rats that were exposed to the pulse mode, immediately after PA, a decrease in IM to 0.6 ± 0.4 pf. un. was registered. By 4 min of observation of MCR in the skin, the IM was 4.7 ± 0.3 pf. un. Then there was an increase in IM to 14.5 ± 0.8 pf. un. By the end of the time of monitoring the blood flow, the IM was 7.4 ± 0.4 pf. un.

Before PA, the initial values of PPG and AVD were, respectively, from 0.4 to 0.8 rel. un. and from 7.1% to 11.9%. During laser exposure, a decrease in AVD and an increase in PPG amplitude were observed. The decrease in AVD in the group with continuous PA occurred on average by 39 s of laser exposure, which corresponds to 0.585 J/cm^2 . In the group with the pulsed generation, a decrease in the same values was recorded on average by 44 s, that is, when the energy density reached 0.33 J/cm^2 . At the same time, the complete absence of blood flow in the group of continuous irradiation was recorded on average for 96 s, that is, 6 s after the termination of laser exposure. In the pulse mode group, the complete absence of blood flow was registered at 128 s, which means during PA.

The recovery period, accompanied by the appearance of blood flow, in the group with a continuous mode of exposure began on average 8 minutes after the start of laser exposure, which coincided with the moment when the PPG values began to increase. Registration of restoration of blood flow in the pulsed mode occurred 4.7 minutes after the end of laser exposure, however, an increase in PPG values occurred later, on average, after 7.5 minutes.

Discussion

PDT has established itself as an effective method for the treatment of malignant neoplasms and a number of non-tumor diseases [18,19]. During PA, the energy of laser radiation is absorbed and transferred to the conjugated system of the PS molecule. The interaction of a photoactivated PS molecule with an oxygen molecule leads to the transfer of electronic excitation energy to the molecular oxygen of the medium, followed by its transfer to a more reactive state and the formation of ROS, causing lipid and protein peroxidation in cell membranes, causing their damage and death. In addition, in the mechanism of biological action in PDT, the violation of the MCR, as well as the local response to immune reactions, is important. The state of the MCR provides a certain content of oxygen necessary for the formation of its active forms in the PA zone, as well as the delivery of immune-competent cells.

One of the parameters influencing the result of photodynamic action is the mode of radiation generation. In practice, as a rule, a continuous mode of radiation generation is used, which consists in irradiating a skin area during the entire exposure time with

radiation with constant characteristics and leading to intense depletion of ROS as a result of photochemical reactions [20, 21]. The pulse mode, which is characterized by successive periods of turning the laser source on and off during exposure, makes it possible to reduce this effect [23, 24]. Evaluation of the influence of different regimens on MC remains relevant, allowing to increase the effectiveness of therapy. In the work, a multiparametric analysis of MC blood flow was carried out by various methods.

The reflectivity of the skin is largely determined by the filling of tissue with blood and its oxygenation. With an increase in blood supply and oxygenation, there is an increase in absorption and a decrease in the reflectivity of the tissue. An increase in PPG corresponds to a greater amount of radiation incident on the sensor of the video camera and hence reflected from the surface under study. A rise in the PPG value in the first minutes of PA (Fig. 4, red zone) may indicate a decrease in the amount of blood in the measured area of the skin, together with the degree of its oxygenation. The dose of laser PA was insignificant, therefore, for some time after the end of PA, the mechanism of autoregulation was triggered. The decrease in the value of PPG during the period of complete cessation of blood flow (Fig. 4, black zone) is due to the activation of regulatory mechanisms and changes in MC in the deeper layers of the skin, causing a rush of oxygenated blood to the site of

exposure. An increase in the IM values recorded by LDF corresponds to the same processes. The result of regulatory processes after the termination of PA is the restoration of blood flow in the vessels accessible for visualization by VCS (Fig. 4, yellow zone) and the subsequent return to an equilibrium state with an increase in PPG and a decrease in IM to values close to the initial ones (Fig. 4, green zone).

In both continuous and pulsed modes, PA led to a stop in the movement of erythrocytes through the vessels, as well as to a change in the values of PPG, IM, and AVD, which returned to their original or close values 15 min after the beginning of PA. However, the nature of the response of rat skin microvessels to low doses of PA turned out to be different for the two regimens. In the group of animals subjected to PA in the pulsed mode, the beginning of the recovery period (Fig. 4, yellow zone), i.e., the return to the initial values of PPG, IM, and AVD, was observed earlier than in the group with continuous PA. Moreover, in the recovery period for the pulsed PA group, a local increase in IM by more than 3 times relative to the norm was observed, followed by a decrease to normal values.

The data obtained, showing the return of PPG and AVD to the initial values in the recovery period, correlate with the corresponding increase in IM obtained using LDF. At the same time, during the period of complete stoppage of blood flow in the superficial vessels

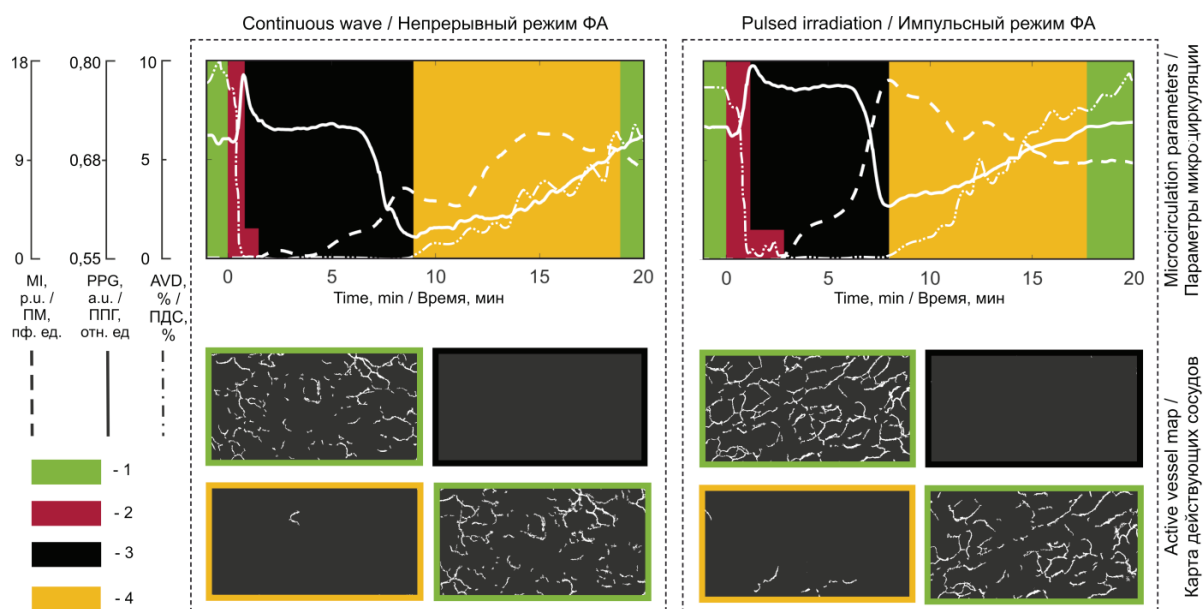


Рис. 4. Морфометрические и гемодинамические параметры микроциркуляции, полученные методами видеокапилляроскопии, фотоплетизмографии и лазерной доплеровской флоуметрии, для периодов соответствующих: 1 – нормальному состоянию сосудов относительно значений ФПГ, 2 – фотоактивации, 3 – остановке кровотока, 4 – восстановительному периоду (ПМ – показатель микроциркуляции, ППГ – фотоплетизмография, ПДС – плотность действующих сосудов, ФА – фотоактивация).
Fig. 4. Morphometric and hemodynamic microcirculation parameters acquired by means of videocapillaroscopy, photoplethysmography, and laser Doppler flowmetry: 1 – normal vessel functioning, 2 – photodynamic activation, 3 – cessation of blood flow, 4 – vascular activation (MI – microcirculation index, PPG – photoplethysmography, AVD – active vessel density).

and zero values of the AVD, the IM had non-zero values. Such differences may indicate the registration of MC parameters from different depths relative to the skin surface by different methods. Thus, with the help of LDF, blood flow parameters in the skin are examined at a depth of up to 1 mm, that is, in the capillaries and superficial arteriovenular plexus [20]. At the same time, VCS provides visualization of vessels lying at a depth of up to 0.5–1 mm [25, 26].

Conclusion

The results of this study showed the fundamental possibility of using the developed setup and method for monitoring skin MC during PDT, including directly during PA. The data obtained correlate with modern ideas about the mechanisms of the reaction of MC to PA and with the results obtained by methods common in practice [27, 28].

A methodical approach and its hardware-software implementation have been developed and tested, providing non-invasive obtaining of vascular maps, PPG, and AVD graphs before, after, and most importantly, during PA. A study of the mechanisms of skin reaction in different modes of generating photodynamic exposure at low doses of PA was performed using the proposed approach. For two modes of generation, the difference in time intervals between the beginning of PA, the stoppage of blood flow in the vessels, and the beginning of the recovery period, as well as in the duration of the latter, is shown. The described method of multiparametric assessment of the vasculature can serve as a valuable addition to the existing methods for the analysis of MC in research tasks and clinical practice.

The study was carried out within the State Assignment of the STC UI RAS (project FFNS-2022-0010).

REFERENCES

1. Dougherty T.J. et al. Photodynamic Therapy JNCI: Journal of the National Cancer Institute. *Oxford Academic*, 1998. Vol. 90(12), pp. 889-905.
2. Li X. et al. Clinical development and potential of photothermal and photodynamic therapies for cancer. *Nature Publishing Group*, 2020, Vol. 17(11), pp. 657-674.
3. Korbely M. et al. Nitric oxide production by tumour tissue: impact on the response to photodynamic therapy. *Br J Cancer. Nature Publishing Group*, 2000, Vol. 82(11), p. 1835.
4. Souza C.S. et al. Long-term follow-up of topical 5-aminolaevulinic acid photodynamic therapy diode laser single session for non-melanoma skin cancer. *Photodiagnosis Photodyn Ther*, 2009, Vol. 6 (3-4), pp. 207-213.
5. Chen D. et al. Intraoperative monitoring of blood perfusion in port wine stains by laser Doppler imaging during vascular targeted photodynamic therapy: A preliminary study. *Photodiagnosis Photodyn Ther. Elsevier*, 2016, Vol. 14, pp. 142-151.
6. Orlova A. et al. Diffuse Optical Spectroscopy Monitoring of Experimental Tumor Oxygenation after Red and Blue Light Photodynamic Therapy. *Photonics* 2022, Vol. 9, p. 19. *Multidisciplinary Digital Publishing Institute*, 2021. Vol. 9(1), p. 19.
7. Khurana M. et al. Intravital high-resolution optical imaging of individual vessel response to photodynamic treatment. *J Biomed Opt*, 2008, Vol. 13(4), p. 1.
8. Grishacheva T.G. et al. Digital Analysis of Colposcopic Images Before and After Photodynamic Therapy with Open Source Software ImageJ and Fluorescence diagnostics. *Optica Publishing Group*, 2020, p. JW3A.2.
9. Christou E.E. et al. Evaluation of the choriocapillaris after photodynamic therapy for chronic central serous chorioretinopathy. A review of optical coherence tomography angiography (OCT-A) studies. *Graefes Arch Clin Exp Ophthalmol. Graefes Arch Clin Exp Ophthalmol*, 2022, Vol. 260(6), pp. 1823-1835.
10. Gallucci F. et al. Indications and results of videocapillaroscopy in clinical practice. *Advances in medical sciences*, 2008, Vol. 53(2), pp. 149-157.
11. Machikhin A.S. et al. Exoscope-based videocapillaroscopy system for in vivo skin microcirculation imaging of various body areas. *Biomedical Optics Express*, 2021, Vol. 12(8), pp. 4627-4636. *Optica Publishing Group*, 2021, Vol. 12(8), pp. 4627-4636.
12. Da Silva F.A.M., Newman E.L. Dynamic capillaroscopy: a minimally invasive technique for assessing photodynamic effects in vivo. *Photochem Photobiol. John Wiley & Sons, Ltd*, 1993, Vol. 58(6), pp. 884-889.

ЛИТЕРАТУРА

1. Dougherty T.J. et al. Photodynamic Therapy JNCI: Journal of the National Cancer Institute // *Oxford Academic*. – 1998. – Vol. 90(12). – P. 889-905.
2. Li X. et al. Clinical development and potential of photothermal and photodynamic therapies for cancer // *Nature Publishing Group*. – 2020. – Vol. 17(11). – P. 657-674.
3. Korbely M. et al. Nitric oxide production by tumour tissue: impact on the response to photodynamic therapy // *Br J Cancer. Nature Publishing Group*. – 2000. – Vol. 82(11). – P. 1835.
4. Souza C.S. et al. Long-term follow-up of topical 5-aminolaevulinic acid photodynamic therapy diode laser single session for non-melanoma skin cancer // *Photodiagnosis Photodyn Ther*. – 2009. – Vol. 6 (3-4). – P. 207-213.
5. Chen D. et al. Intraoperative monitoring of blood perfusion in port wine stains by laser Doppler imaging during vascular targeted photodynamic therapy: A preliminary study // *Photodiagnosis Photodyn Ther. Elsevier*. – 2016. – Vol. 14. – P.142-151.
6. Orlova A. et al. Diffuse Optical Spectroscopy Monitoring of Experimental Tumor Oxygenation after Red and Blue Light Photodynamic Therapy // *Multidisciplinary Digital Publishing Institute*. – 2021. – Vol. 9(1). – P. 19.
7. Khurana M. et al. Intravital high-resolution optical imaging of individual vessel response to photodynamic treatment // *J Biomed Opt. J Biomed Opt*. – 2008. – Vol. 13(4). – P. 1.
8. Grishacheva T.G. et al. Digital Analysis of Colposcopic Images Before and After Photodynamic Therapy with Open Source Software ImageJ and Fluorescence diagnostics // *Optica Publishing Group*. – 2020. – P. JW3A.2.
9. Christou E.E. et al. Evaluation of the choriocapillaris after photodynamic therapy for chronic central serous chorioretinopathy. A review of optical coherence tomography angiography (OCT-A) studies // *Graefes Arch Clin Exp Ophthalmol. Graefes Arch Clin Exp Ophthalmol*. – 2022. – Vol. 260(6). – P. 1823-1835.
10. Gallucci F. et al. Indications and results of videocapillaroscopy in clinical practice // *Advances in medical sciences*. – 2008. – Vol. 53(2). – P. 149-157.
11. Machikhin A.S. et al. Exoscope-based videocapillaroscopy system for in vivo skin microcirculation imaging of various body areas. *Optica Publishing Group*. – 2021. – Vol. 12(8). – P. 4627-4636.
12. Da Silva F.A.M., Newman E.L. Dynamic capillaroscopy: a minimally invasive technique for assessing photodynamic effects in vivo // *Photochem Photobiol. John Wiley & Sons, Ltd*. – 1993. – P. Vol. 58(6). – P. 884-889.

13. Kamshilin A.A. et al. A new look at the essence of the imaging photoplethysmography. *Scientific Reports. Nature Publishing Group*, 2015. Vol. 5(1), pp. 1-9.
14. Kumar M. et al. PulseCam: a camera-based, motion-robust and highly sensitive blood perfusion imaging modality. *Scientific Reports*, 2020, Vol. 10(1), Nature Publishing Group, 2020. Vol. 10(1), pp. 1-17.
15. Park J. et al. Photoplethysmogram Analysis and Applications: An Integrative Review. *Front Physiol. Frontiers Media S.A.*, 2022, Vol. 12, p. 2511.
16. Allen J. Photoplethysmography and its application in clinical physiological measurement. *Physiol Meas*, 2007. Vol. 28(3).
17. Guryleva A.V. et al. Feasibility of videocapillaroscopy for characterization of microvascular patterns in skin lesions. *Proceedings of SPIE – The International Society for Optical Engineering*, 2022, Vol. 12147.
18. Dolmans D.E.J.G.J., Fukumura D., Jain R.K. Photodynamic therapy for cancer. *Nature Reviews Cancer*, 2003, Vol. 3(5). *Nature Publishing Group*, 2003, Vol. 3(5), pp. 380-387.
19. Gunaydin G., Gedik M.E., Ayan S. Photodynamic Therapy—Current Limitations and Novel Approaches. *Front Chem. Frontiers Media S.A.*, 2021. Vol. 9. P. 400.
20. Foster T., et al. Oxygen consumption and diffusion effects in photodynamic therapy. *Radiat. Res*, 1991, Vol. 126, pp. 296-303.
21. Henderson B., et al. Oseroff, Photofrin photodynamic therapy can significantly deplete or preserve oxygenation in human basal cell carcinomas during treatment, depending on fluence rate. *Cancer Res*, 2000, Vol. 60, pp. 525-529.
22. Klimenko V.V., et al. Pulse mode of laser photodynamic treatment induced cell apoptosis. *Photodiagnosis Photodyn Ther*, 2016, Vol. 13, pp. 101-107.
23. Wilson B.C., Patterson M.S. The physics, biophysics and technology of photodynamic therapy. *Phys Med Biol*, 2008, Vol. 53(9), pp. 61-109.
24. Abbot N.C. et al. Laser Doppler Perfusion Imaging of Skin Blood Flow Using Red and Near-Infrared Sources. *Journal of Investigative Dermatology Elsevier*, 1996, Vol. 107(6), pp. 882-886.
25. Moço A., Verkruyse W. Pulse oximetry based on photoplethysmography imaging with red and green light: Calibratability and challenges. *J Clin Monit Comput. Springer Science and Business Media B.V.*, 2021, Vol. 35(1), pp. 123-133.
26. Han S. et al. Design of Multi-Wavelength Optical Sensor Module for Depth-Dependent Photoplethysmography. *Multidisciplinary Digital Publishing Institute*, 2019. Vol. 19(24), p. 5441.
27. Volkov M. V et al. Evaluation of blood microcirculation parameters by combined use of laser. *Doppler flowmetry and videocapillaroscopy methods*, 2017.
28. Dremmin V. et al. Dynamic evaluation of blood flow microcirculation by combined use of the laser Doppler flowmetry and high-speed videocapillaroscopy methods. *J Biophotonics*, 2019, Vol. 12(6).
13. Kamshilin A.A. et al. A new look at the essence of the imaging photoplethysmography. *Scientific Reports. Nature Publishing Group*. – 2015. – Vol. 5(1). – P. 1-9.
14. Kumar M. et al. PulseCam: a camera-based, motion-robust and highly sensitive blood perfusion imaging modality // *Nature Publishing Group*. – 2020. – Vol. 10(1). – P. 1-17.
15. Park J. et al. Photoplethysmogram Analysis and Applications: An Integrative Review // *Front Physiol. Frontiers Media S.A.* – 2022. – Vol. 12. – P. 2511.
16. Allen J. Photoplethysmography and its application in clinical physiological measurement // *Physiol Meas. Physiol Meas.* – 2007. – Vol. 28(3). – C. R1
17. Guryleva A.V. et al. Feasibility of videocapillaroscopy for characterization of microvascular patterns in skin lesions // *Proceedings of SPIE – The International Society for Optical Engineering*. – 2022. – Vol. 12147.
18. Dolmans D.E.J.G.J., Fukumura D., Jain R.K. Photodynamic therapy for cancer // *Nature Publishing Group*. – 2003. – Vol. 3(5). – P. 380-387.
19. Gunaydin G., Gedik M.E., Ayan S. Photodynamic Therapy—Current Limitations and Novel Approaches // *Front Chem. Frontiers Media S.A.* – 2021. – Vol. 9. – P. 400.
20. Foster T., et al. Oxygen consumption and diffusion effects in photodynamic therapy // *Radiat. Res.* – 1991. – Vol. 126. – P. 296-303.
21. Henderson B., et al. Oseroff, Photofrin photodynamic therapy can significantly deplete or preserve oxygenation in human basal cell carcinomas during treatment, depending on fluence rate // *Cancer Res.* – 2000. – Vol. 60. – P. 525-529.
22. Klimenko V.V., et al. Pulse mode of laser photodynamic treatment induced cell apoptosis // *Photodiagnosis Photodyn Ther.* – 2016. – Vol. 13. – P. 101-107.
23. Wilson B.C., Patterson M.S. The physics, biophysics and technology of photodynamic therapy // *Phys Med Biol.* – 2008. – Vol. 53(9). – P. 61-109.
24. Abbot N.C. et al. Laser Doppler Perfusion Imaging of Skin Blood Flow Using Red and Near-Infrared Sources // *Journal of Investigative Dermatology Elsevier*. – 1996. – Vol. 107(6). – P. 882-886.
25. Moço A., Verkruyse W. Pulse oximetry based on photoplethysmography imaging with red and green light: Calibratability and challenges. *J Clin Monit Comput // Springer Science and Business Media B.V.* – 2021. – Vol. 35(1). – P. 123-133.
26. Han S. et al. Design of Multi-Wavelength Optical Sensor Module for Depth-Dependent Photoplethysmography // *Multidisciplinary Digital Publishing Institute*. – 2019. – Vol. 19(24). – P. 5441.
27. Volkov M. V et al. Evaluation of blood microcirculation parameters by combined use of laser // *Doppler flowmetry and videocapillaroscopy methods*. – 2017.
28. Dremmin V. et al. Dynamic evaluation of blood flow microcirculation by combined use of the laser Doppler flowmetry and high-speed videocapillaroscopy methods // *Journal of biophotonics*. – 2019. – T. 12. – №. 6. – C. e201800317.

EXPERIMENTAL IN VIVO STUDIES OF THE ANTITUMOR EFFICACY OF PHOTODYNAMIC AND RADIODYNAMIC THERAPY AND THEIR COMBINATIONS

Tzerkovsky D.A.¹, Kozlovsky D.A.¹, Mazurenko A.N.¹, Adamenko N.D.², Borichevsky F.F.³

¹N.N. Alexandrov National Cancer Center of Belarus, Lesnoy, Republic of Belarus

²Vitebsk State University named after P.M. Masherov, Vitebsk, Republic of Belarus

³Minsk Regional Clinical Hospital, Lesnoy, Republic of Belarus

Abstract

The authors studied the antitumor efficacy of photodynamic therapy (PDT) in combination with radiodynamic therapy (RDT) in an *in vivo* experiment. The study was approved by the Ethics Committee of the N.N. Alexandrov National Cancer Center of Belarus (protocol dated February 25, 2022, № 180). The work was performed on 26 white non-linear rats weighing 200 ± 50 g. Pliss lymphosarcoma (PLS) was used as a tumor model, which was transplanted subcutaneously. Photosensitizer (PS) «Photolon» (RUE «Belmedpreparaty», Belarus) was administered intravenously at a dose of 2.5 mg/kg of body weight. The RDT session was performed by the contact method (CRT) once 2.5–3 times after the end of the infusion of the PS on the «microSelectron-HDR V3 Digital apparatus» (Elekta, Sweden) using γ -radiation (^{192}Ir) in a single focal dose 6 Gy. A PDT session was performed once immediately after exposure to ionizing radiation using a «PDT diode laser» (LTD Imaf Axicon, Belarus, $\lambda=660\pm 5$ nm) at an exposure dose of 100 J/cm^2 with a power density of 0.2 W/cm^2 and a power of 0.353 watts. All rats were divided into 4 groups of 6–7 animals each: intact control (IC), PS + PDT, PS + CRT, PS + CRT + PDT. The criteria for evaluating antitumor efficacy were: the average volume of tumors (V_{av} , cm^3), the coefficient of absolute growth of tumors (K, in RU), the coefficient of tumor growth inhibition (TGI, %), the frequency of complete tumor regressions (CR, %), the proportion of cured rats (%), an increase in the average duration of dead rats (%). Differences were considered statistically significant at $p < 0.05$. On the 18th day of the experiment, V_{av} in groups was $63.25 \pm 2.76 \text{ cm}^3$; $29.03 \pm 6.06 \text{ cm}^3$ ($p=0.0002$); $22.18 \pm 5.94 \text{ cm}^3$ ($p < 0.0001$); $11.76 \pm 3.29 \text{ cm}^3$ ($p=0.0000$), respectively. Coefficients K – 4516.86 RU; 2638.09 RU; 2024.45 RU; 979.00 RU. TGI coefficients – 54.10% (PS + PDT); 64.93% (PS + CRT); 81.41% (PS + CRT + PDT). An increase in the average duration of dead rats indicator – 48.57% (PS + PDT); 60.00% (PS + CRT); 97.71% (PS + CRT + PDT). On the 60th and 90th days of the experiment, the frequency of PR and the proportion of cured rats were the same and amounted to 0%; 16.7%; 14.3%, and 28.6%, respectively. The results obtained indicate the prospects and relevance of further research in this scientific direction.

Key words: experimental research, rats, transplanted tumors, photodynamic therapy, radiodynamic therapy, photosensitizer.

Contacts: Tzerkovsky D.A., e-mail: tzerkovsky@mail.ru

For citations: Tzerkovsky D.A., Kozlovsky D.A., Mazurenko A.N., Adamenko N.D., Borichevsky F.F. Experimental *in vivo* studies of the antitumor efficacy of photodynamic and radiodynamic therapy and their combinations, *Biomedical Photonics*, 2023, vol. 12, no. 2, pp. 24–33. doi: 10.24931/2413-9432-2023-12-2-24-33.

ЭКСПЕРИМЕНТАЛЬНЫЕ ИССЛЕДОВАНИЯ IN VIVO ПРОТИВООПУХОЛЕВОЙ ЭФФЕКТИВНОСТИ ФОТОДИНАМИЧЕСКОЙ И РАДИОДИНАМИЧЕСКОЙ ТЕРАПИИ, А ТАКЖЕ ИХ СОЧЕТАНИЯ

Д.А. Церковский¹, Д.И. Козловский¹, А.Н. Мазуренко¹, Н.Д. Адаменко², Ф.Ф. Боричевский³

¹Республиканский научно-практический центр онкологии и медицинской радиологии им. Н.Н. Александрова, аг. Лесной, Республика Беларусь

²Витебский государственный университет им. П.М. Машерова, г. Витебск, Республика Беларусь

³Минская областная клиническая больница, аг. Лесной, Республика Беларусь

Резюме

В рамках пилотного исследования авторами изучена противоопухолевая эффективность фотодинамической терапии (ФДТ) в комбинации с радиодинамической терапией (РДТ) в эксперименте *in vivo* на подкожно перевитой опухолевой модели лимфосаркомы Плисса

(ЛСП) у крыс. Фотосенсибилизатор (ФС) на основе хлорина е6 вводили внутривенно в дозе 2,5 мг/кг массы тела. Сеанс РДТ проводили на установке для контактной лучевой терапии (КЛТ) однократно через 2,5–3 ч после окончания введения ФС с использованием γ -излучения (^{192}Ir) в разовой очаговой дозе 6 Гр. Сеанс ФДТ осуществляли однократно непосредственно после воздействия ионизирующим излучением с помощью полупроводникового лазера «PDT diode laser» (ООО «Imaf Axicon», Беларусь, $\lambda=660\pm 5$ нм) со световой дозой 100 Дж/см² с плотностью мощности 0,2 Вт/см² и мощностью 0,353 Вт. Все крысы были разделены на 4 группы по 6–7 особей в каждой: интактный контроль (ИК), ФС + ФДТ, ФС + КЛТ, ФС + КЛТ + ФДТ. Критерии оценки противоопухолевой эффективности: средний объем опухолей (V_{cp} , см³), коэффициент абсолютного прироста опухолей (К, в относительных единицах (ОЕ), показатель торможения роста опухолей (ТРО, %), частота полной регрессии опухоли (ПР, %), доля излеченных крыс (%), показатель увеличения продолжительности жизни (УПЖ, %). Различия считались статистически значимыми при уровне значимости $p < 0,05$. На 18-е сутки эксперимента V_{cp} в группах составил $63,25\pm 2,76$ см³; $29,03\pm 6,06$ см³ ($p=0,0002$); $22,18\pm 5,94$ см³ ($p < 0,0001$); $11,76\pm 3,29$ см³ ($p=0,0000$), соответственно. Коэффициенты К – 4516,86 ОЕ; 2638,09 ОЕ; 2024,45 ОЕ; 979,00 ОЕ. Показатель ТРО – 54,10% (ФС + ФДТ); 64,93% (ФС + КЛТ); 81,41% (ФС + КЛТ + ФДТ). Показатель УПЖ – 48,57% (ФС + ФДТ); 60,00% (ФС + КЛТ); 97,71% (ФС + КЛТ + ФДТ). На 60-е и 90-е сутки эксперимента частота ПР и доля излеченных крыс были одинаковыми и составили в группах 0%; 16,7%; 14,3% и 28,6%, соответственно. Полученные результаты свидетельствуют о перспективности и актуальности дальнейших исследований в данном научном направлении.

Ключевые слова: экспериментальное исследование, крысы, перевивные опухоли, фотодинамическая терапия, радиодинамическая терапия, фотосенсибилизатор.

Контакты: Церковский Д.А., tzerkovsky@mail.ru

Для цитирования: Церковский Д.А., Козловский Д.И., Мазуренко А.Н., Адаменко Н.Д., Боричевский Ф.Ф. Экспериментальные исследования *in vivo* противоопухолевой эффективности фотодинамической и радиодинамической терапии, а также их сочетания // Biomedical Photonics. – 2023. – Т. 12, № 2. – С. 24–33. doi: 10.24931/2413-9432-2023-12-2-24-33.

Introduction

Photodynamic therapy (PDT) is a method for the treatment of precancerous diseases and malignant neoplasms, the effectiveness of which has been proven and confirmed by the results of numerous preclinical studies on cell cultures and laboratory animals with transplanted tumors, as well as clinical studies, i.a. multicenter randomized studies including a significant number of patients with various nosological forms of oncological pathology [1, 2]. PDT is based on the use of special drugs – photosensitizers (PS), the activation of which in pathologically altered tissues is realized by exposure to laser radiation with a certain wavelength [3, 4, 5]. However, in recent years, scientific projects have actively explored the possibility of using other physical factors, such as ultrasound (“sonodynamic therapy”), hyperthermia (“thermodynamic therapy”), electric fields (“electrodynamical therapy”), and ionizing radiation (“radiodynamic therapy”) as ways to launch complex physicochemical reactions at the molecular and cellular levels, leading to the transition of PS molecules from the ground state to an excited state, similar to PDT, followed by the destruction of tumor cells, in particular, and tumor death, in general [6, 7, 8].

In order to increase the antitumor efficacy of PDT, it is advisable to use the method in combination with traditional approaches in the treatment of malignant neoplasms, in particular, with radiation therapy (RT) [9, 10]. The combined use of PDT and RDT makes it possible to use subtherapeutic modes of laser and ionizing radiation. Such modes lead to an increase in the effect of each of the therapeutic methods due to a synergistic effect with a significant reduction in the risk of several adverse

reactions that occur when high doses of these physical factors are used, primarily, of RT.

Materials and methods

Laboratory animals

The pilot study was performed on 26 white nonlinear outbred male rats obtained from the vivarium of N. N. Alexandrov National Cancer Centre of Belarus, with a body weight of 200 ± 50 g, aged 2.5–3 months. The duration of quarantine before inclusion in the experiment was 14 days. The rats were kept under standard conditions of food and drink rations *ad libitum*, with 12-hour illumination, at a temperature of 20–22°C and a humidity of 50–60% in individual cages, 6–7 individuals in each. The conditions for keeping rats in the laboratory, as well as indicators of humidity, temperature, and illumination in the room, corresponded to the current sanitary rules for the arrangement, equipment, and maintenance of vivariums (Sanitary rules and regulations 2.1.2.12-18-2006 “Arrangement, equipment and maintenance of experimental biological clinics (vivariums); Decree of the Chief State Sanitary Doctor of the Republic of Belarus, dated October 31, 2006 No. 131) and Interstate standards: State Standard 33216-2014 (“Guidelines for keeping and caring for laboratory animals. Rules for keeping and caring for laboratory rodents and rabbits” and State Standard 33215-2014 “Guidelines for the maintenance and care of laboratory animals. Rules for the equipment of premises and organization of procedures”, approved by the Resolution of the Interstate Council for Standardization, Metrology and Certification, a protocol of December 22, 2014, No. 73-P).

Tumor strain

Pliss lymphosarcoma (PLS) obtained as a cell culture (Russian Collection of Cell Cultures, Institute of Cytology RAS, St. Petersburg, Russian Federation) was used as a tumor strain.

Tumor model

PLS cell culture was inoculated subcutaneously in rats and maintained by passivation *in vivo*. Subcutaneous inoculation of the experimental study included the introduction under the skin of the left inguinal region of 0.5 ml of a suspension of tumor cells in 20% Hanks solution, obtained after taking and homogenizing tumor pieces from a donor rat. PLS is one of the rapidly growing tumors with a short latent period. In this regard, rats with PLS were included in the experiment on the 6th day after transplantation, when the diameter of the tumor node, on average, was 3–5 mm.

Ethical aspects

Experimental studies were carried out in accordance with international legislation and the regulatory legal acts in force in the Republic of Belarus for conducting experimental studies with laboratory animals, namely:

1. European Convention for the Protection of Vertebrate Animals used for Experimental or Other Scientific Purposes (Strasbourg, France, of 18.03.1986), as amended in accordance with the provisions of the Protocol (ETS No. 170 of 02.12.2005).

2. Directive 2010/63/EU of the European Parliament and the European Union on the protection of animals used for scientific purposes (dated 22.09.2010).

3. Technical Code of Common Practice No 125-2008 "Good Laboratory Practice" (GLP) (Decree of the Ministry of Health of the Republic of Belarus No. 56 dated March 28, 2008).

The nature of the studies performed was consistent with the principles of "3Rs" developed by W.M. Russell and R.L. Berch (1959), namely:

- 1) "Reduction" – reduction in the number of laboratory animals used in the experiment.

- 2) "Refinement" – improvement of the methodology of the experiment through the use of painkillers and non-traumatic methods.

- 3) "Replacement" – replacement (transition from animal research to methods that do not use living beings).

Before irradiation, rats were anesthetized (neuroleptanalgesia: 0.005% fentanyl solution + 0.25% droperidol solution, in a ratio of 2:1, 0.2 ml per 100 g of body weight, intramuscularly). After the end of the observation period, the rats were sacrificed using generally accepted methods of euthanasia (*aether pro narcosi*) in compliance with the humane methods of handling laboratory animals.

The study was approved by the Ethics Committee of N. N. Alexandrov National Cancer Centre of Belarus (extract from the protocol dated February 25, 2022 No. 180).

Photo- and radiosensitizer

As a drug, an injectable form of PS based on chlorin e6 photolon (RUE "Belmedpreparaty", Minsk, Republic of Belarus, registration number 16/11/886 dated November 08, 2016, 100 mg) was used. Before use, PS powder was diluted with 0.9 % sodium chloride solution and administered once by intravenous infusion into the tail vein of a rat in a darkened room at a dose of 2.5 mg/kg.

Radiodynamic therapy

The irradiation of inoculated tumors was carried out by the contact method (contact radiation therapy, CRT) using a microSelectron-HDR V3 Digital apparatus (Elekta, Sweden) using γ -radiation (^{192}Ir). The source had a high activity (at the beginning of the experiments it was 5.2 Ci), which determined the high dose rate and short duration of irradiation sessions required for rats in a state of drug sleep. To conduct CRT on the area of the inoculated tumor, a Leipzig applicator was used, which was fixed on the surface of the tumor with soft rubber holders. Irradiation was performed once at a single focal dose (SFD) of 6 Gy, which is equivalent to 10.8 Gy at $\alpha/\beta = 3$, 2.5–3 hours after the end of the infusion. The time of the irradiation session was calculated using the Oncentra Brachy v4.5.2 planning system (Elekta, Sweden) on an empty series of images using the TG-43 algorithm without taking into account the reflection and scattering of radiation inside the applicator. The CRT technique was used with normalization to a point located at a distance of 5 mm from the therapeutic surface of the applicator, in accordance with the size of the target and the recommendations of GEC-ESTRO ACROP and others. The used method of irradiation made it possible to apply the planned SFD to transplanted tumors in rats without over-irradiation of normal tissues surrounding the tumor.

Photodynamic therapy

PDT sessions were performed once right after exposure to ionizing radiation (IRT) using a PDT diode laser (LTD Imaf Axicon, Minsk, Republic of Belarus) with a wavelength of 660 ± 5 nm. Irradiation of grafted tumors was started 2.5–3 hours after the end of PS infusion with a light dose of 100 J/cm^2 with a power density of 0.2 W/cm^2 and a power of 0.353 W. The duration of exposure was 8 minutes.

Study design

All exposures were performed on the 6th day after PLS inoculation when the diameter of the tumor node was at least 3–5 mm. All rats, 26 individuals (males), included in the study, were randomly distributed into 4 groups of 6–7 individuals in each. Rats with transplanted

tumors, which were not injected with PS and did not undergo any irradiation, acted as controls (intact control, IC) (Table 1).

Таблица 1
 Дизайн экспериментального исследования
Table 1
 Experimental study design

Наименование группы Study groups	Число крыс в группе, n Number of rats in the group, n
ИК Intact control	6
ФС 2,5 мг/кг + КЛТ РОД 6 Гр PS 2.5 mg/kg + CRT SFD 6 Gy	7
ФС 2,5 мг/кг + ФДТ 100 Дж/см ² 0,2 Вт/см ² PS 2.5 mg/kg + PDT 100 J/cm ² 0.2 W/cm ²	6
ФС 2,5 мг/кг + КЛТ РОД 6 Гр+ ФДТ 100 Дж/см ² 0,2 Вт/см ² PS 2.5 mg/kg + CRT SFD 6 Gy + PDT 100 J/cm ² 0.2 W/cm ²	7

* ФС – фотосенсибилизатор; КЛТ – контактная лучевая терапия; РОД – разовая очаговая доза; ФДТ – фотодинамическая терапия.
 * PS – photosensitizer; CRT – contact radiotherapy; SFD – single focal dose; PDT – photodynamic therapy.

Criteria for evaluating antitumor efficacy

The antitumor efficacy of the interventions was assessed according to the indicators generally accepted in experimental oncology, which characterize the dynamics of changes in the average tumor volume (V_{av} , cm³), as well as the change in the coefficient of absolute tumor growth (K) and the index of tumor growth inhibition (TGI, %). The growth dynamics of transplanted tumors was recorded starting from the 6th day after transplantation of the PLS tumor strain for 2 weeks with an interval of 2–3 days.

Tumor volume was calculated using the following formula (1):

$$V = \frac{1}{6} \pi \times d_1 \times d_2 \times d_3$$

where

$d_{1,2,3}$ – three mutually perpendicular tumor diameters (in cm);

$\pi/6 = 0.52$ – a constant value;

V – the volume of the tumor (in cm³).

The coefficient of absolute tumor growth (K) was calculated by the following formula (2):

$$K = \frac{V_t - V_0}{V_0}$$

where

V_0 – the initial volume of the tumor (before exposure);

V_t – the tumor volume for a certain period of observation.

The value of the index $K > 0$ (V at the corresponding period of observation exceeded its initial value) was regarded as continued tumor growth; $-1 < K < 0$ (V at the corresponding observation period was less than its initial value) was regarded as inhibition of tumor growth; and $K = -1$ – as complete tumor regression.

The coefficient of tumor growth inhibition (TGI) was calculated by the following formula (3):

$$TGI\% = \frac{V_{control} - V_{experience}}{V_{control}} * 100\%$$

where

$V_{control}$ – the average volume of the tumor in the control group (in cm³);

$V_{experience}$ – the average volume of the tumor in the main group (in cm³).

The minimally significant criterion demonstrating the effectiveness of the treatment of transplanted tumors was considered $TGI > 50\%$.

The frequency of complete tumor regressions (CR) was assessed 60 days after the end of exposure by the absence of visual and palpatory signs of tumor growth.

The proportion of cured rats in the groups was determined 90 days after the end of exposure by the absence of visual and palpatory signs of tumor growth.

Quantitative criteria for assessing the inhibitory effect on grafted tumors in rats were as follows (Table 2) [11]:

The evaluation of the antitumor effect by increasing the lifespan was carried out at the end of the experiment and the death of all rats. The average life expectancy (ALE, days) in the groups was determined and the indicators of life expectancy increase (LEI, %) were calculated using the formula (4):

$$LEI\% = \frac{ALE_{experiment} - ALE_{control}}{ALE_{control}} * 100\%$$

where

LEI – an indicator of the increase in the life expectancy of dead rats (in%);

$ALE_{experiment}$ – the average life expectancy of dead rats in the experimental groups (per day);

$ALE_{control}$ – the average life expectancy of dead rats in the control group (per day).

Statistical processing of the obtained data

Statistical processing of the results (V_{av} , K, and TGI) was performed using Excel, Origin Pro (version 7.0), and

Таблица 2

Критерии оценки противоопухолевой эффективности по коэффициенту торможения роста опухоли и частоте полных регрессий

Table 2

Criteria for evaluating antitumor efficacy in terms of the coefficient of tumor growth inhibition and the frequency of complete regressions

Критерии противоопухолевой эффективности Criteria of antitumor efficacy	Значения эффективности Values efficiency
TPO < 20% TGI < 20%	0
TPO < 20–50% TGI < 20–50%	±
TPO < 51–80%/ TGI < 51–80%	+
TPO < 81–90% TGI < 81–90%	++
TPO < 91–100% + < 50% ПР/ TGI < 91–100% + CR < 50%	+++
TPO > 91–100% + > 50% ПР/ TGI > 91–100% + CR > 50%	++++

* ТРО – коэффициент торможения роста опухоли; ПР – полная регрессия.

* TGI – tumor growth inhibition; CR – complete regression.

Statistica (version 10.0) software packages. Data are presented as $M \pm m$ (mean \pm error of the mean). To assess the significance of differences, the Mann-Whitney U test was used. Overall survival was assessed using the non-parametric Kaplan-Meier method. The date of tumor inoculation was taken as point 0, the death of a rat was considered an event, and the end of observation was the death of all rats in the experimental group. Comparative data analysis was performed using a nonparametric log-rank test. Differences were considered statistically significant at $p < 0.05$.

Results

The inoculation of the tumor strain was 100% (26 out of 26 rats had visual and palpatory signs of tumor growth at the time of the start of therapeutic interventions, on the 6th day after inoculation).

Adverse reactions and complications associated with intravenous administration of PS, as well as PDT and CRT sessions, were not registered.

In the experiment, the antitumor efficacy of the method of combined therapy of transplantable tumors was evaluated, including systemic (intravenous) administration of a PS based on chlorin e6, followed by a single exposure to ionizing radiation in the SFD of 6 Gy

and laser radiation with a light dose of 100 J/cm² with a power density of 0.2 W/cm² in comparison with each of the components of the method (PS + CRT, PS + PDT) and IC.

As can be seen from Table 3, during the entire period of evaluation of indicators characterizing the change in the growth dynamics of transplanted tumors (from 6 to 18 days after therapeutic exposure), its statistically significant inhibition was noted both in the combination therapy group and in the groups of rats that were treated in monomodes (PS + PDT and PS + CRT), compared with the IC group ($p < 0.05$).

On the 18th day of the experiment, V_{av} in the combination therapy group was statistically significantly less: 5.38 times compared with IC ($p = 0.00001$), 2.47 times compared with PS + PDT ($p = 0.025$), and tended to decrease compared with the PS + CRT group (1.89 times; $p = 0.15$).

Antitumor effectiveness of impacts on a semi-quantitative scale of assessment [11] is presented in Table 4.

Table 5 presents data on the survival rates of dead rats in this series of experiments. The results obtained testify to the high antitumor efficacy of the developed method of combined therapy: a statistically significant LEI was achieved in comparison with IC and a tendency to optimize the studied parameters was noted in comparison with each of the components of the method ($p = 0.12$ – PS + PDT and $p = 0.24$ – PS + CRT).

Thus, the developed method of combined therapy, which includes intravenous administration of a PS based on chlorin e6 at a dose of 2.5 mg/kg of body weight, followed, after 2.5–3 hours, by a single session of CRT in the SFD of 6 Gy and PDT with a light dose of 100 J/cm² with a power density of 0.2 W/cm² demonstrated high antitumor efficacy. On the 18th day after the session of treatment of animals, the coefficient K was 979.00 RU; the value of TGI, compared with the IC was 81.41%. On the 60th and 90th days, the CR and cure rates were 28.6% and 28.6%, respectively. ALE and LEI indicators were 34.60 ± 3.75 days and 97.71%, respectively. The effectiveness of the impact on a semi-quantitative scale of assessment was “+++”.

Discussion

As already mentioned, in recent years, the possibility of using such physical factors as ultrasound, hyperthermia, electric fields, etc., as trigger mechanisms for the activation of the PS molecule in pathologically altered cells and tissues has been actively studied [6, 7, 8]. One of the most relevant areas of scientific research in experimental and clinical oncology is radiodynamic therapy (RDT) – a method of treating malignant neoplasms based on the combined use of PS and their derivatives and ionizing radiation with certain param-

eters. PS traditionally used for PDT may have radiosensitizing properties, and in this case, they can be considered as radiosensitizing agents that increase the anti-tumor efficacy of RT. It is well known that tumor physiology is characterized by low oxygen tension (hypoxia, anoxia), low glucose and high lactate levels, interstitial hypertension, and extracellular acidosis. The vascu-

lar network of the tumor is characterized by the pronounced proliferation of endotheliocytes, which leads to the development of structural defects and functional failure of microcapillaries, as a result of which the intratumoral blood flow becomes chaotic with the presence of areas of insufficient vascularization. Hypoxic tumor cells have an increased resistance to ionizing radiation

Таблица 3
 Данные о динамике роста перевивных опухолей в эксперименте на крысах с ЛСП

Table 3
 Data on the growth dynamics of transplanted tumors in an experiment on rats with LSP

Наименование группы Groups	Сутки после перевивки Days after tumors transplantation					
	ИССЛЕДУЕМЫЕ КРИТЕРИИ: Средний объем, в см ³ (M±m) Коэффициент абсолютного прироста опухолей (К), в ОЕ Коэффициент торможения роста опухолей (ТРО), в % Уровень значимости различий по отношению к интактному контролю RESEARCH CRITERIA: Vav., cm ³ (M±m) Coefficient of absolute tumor growth (K), relative units (RU) Coefficient of tumor growth inhibition (TGI), % P vs. intact control					
	6	9	11	13	15	18
ИК IC	0,014±0,001	1,23±0,19	10,29±0,71	19,85±0,65	47,19±0,74	63,25±2,76
	-	86,86	734,00	1416,86	3369,71	4516,86
	-	-	-	-	-	-
	-	-	-	-	-	-
ФС + КЛТ PS + CRT	0,011±0,002	0,33±0,13	1,46±0,51	3,88±1,15	15,92±4,58	22,18±5,94
	-	29,00	131,73	351,73	1446,27	2024,45
	-	73,17	85,81	80,45	66,26	64,93
	>0,05	0,0018	0,00000	0,00000	0,00001	0,00002
ФС + ФДТ PS + PDT	0,011±0,002	0,62±0,20	3,02±0,62	7,76±2,01	22,69±5,43	29,03±6,06
	-	55,36	273,55	704,45	2061,73	2638,09
	-	49,59	70,65	60,91	51,92	54,10
	>0,05	0,046	0,000002	0,00007	0,0005	0,0002
ФС + КЛТ + ФДТ PS + CRT + PDT	0,012±0,001	0,17±0,03	1,15±0,46	3,88±1,13	11,14±3,42	11,76±3,29
	-	13,17	94,83	322,33	927,33	979,00
	-	86,18	88,82	80,45	76,39	81,41
	>0,05	0,00008	0,00000	0,00000	0,00000	0,00000

* ФС – фотосенсибилизатор; КЛТ – контактная лучевая терапия; ИК – интактный контроль; ФДТ – фотодинамическая терапия.
 * PS – photosensitizer; CRT – contact radiotherapy; IC – intact control; PDT – photodynamic therapy.

and require the use of high doses of radiation, leveling this effect, which, as a result, can lead to the development of radiation reactions and damage to normal tissues surrounding the tumor. The key to preventing this situation is the use of radiosensitizers that modify the antitumor efficacy of RT (in particular, PS) or a combination of RT with other therapeutic options (for example, PDT) using reduced doses of radiation [8, 9, 10, 12].

When interpreting the main mechanisms underlying tumor cell damage with the combined use of PS and ionizing radiation, the authors conclude that the key link in the realization of the antitumor effect of RDT is free radical oxidation, which develops as a result of exposure to radiation on the water in the cell with subsequent transfer of PS molecules from the ground state to the excited state and the formation of a significant amount of free radi-

Таблица 4

Критерии оценки противоопухолевой эффективности по коэффициенту торможения роста опухоли и частоте полных регрессий

Table 4

Criteria for evaluating antitumor efficacy in terms of the coefficient of tumor growth inhibition and the frequency of complete regressions

Наименование группы Groups	Критерии оценки эффективности Criteria for evaluating effectiveness		
	Показатель торможения роста опухолей (ТРО, %) Tumor growth inhibition coefficient TGI, %	Частота полных регрессий, % Frequency of complete regressions, %	Эффективность Efficacy
ИК IC	–	0,0	0
ФС + ФДТ PS + PDT	54,10	16,7	+++
ФС + КЛТ PS + CRT	64,93	14,3	+++
ФС + КЛТ + ФДТ PS + CRT + PDT	81,41	28,6	+++

* ФС – фотосенсибилизатор; КЛТ – контактная лучевая терапия; ИК – интактный контроль; ФДТ – фотодинамическая терапия.

* PS – photosensitizer; CRT – contact radiotherapy; IC – intact control; PDT – photodynamic therapy.

Таблица 5

Показатели выживаемости крыс после комбинированного лечения

Table 5

Survival rates of rats after combined treatment

Наименование группы Groups	Критерии оценки эффективности Criteria for evaluating effectiveness		
	Средняя продолжительность жизни, сут Average life expectancy, days	Увеличение средней продолжительности жизни, % Increase in average life expectancy, %	p относительно ИК p vs. IC
ИК IC	17,50±2,16	–	–
ФС + ФДТ PS + PDT	26,00±3,48	48,57	0,058
ФС + КЛТ PS + CRT	28,00±3,86	60,00	0,034
ФС + КЛТ + ФДТ PS + CRT + PDT	34,60±3,75	97,71	0,0017

* ФС – фотосенсибилизатор; КЛТ – контактная лучевая терапия; ИК – интактный контроль; ФДТ – фотодинамическая терапия.

* PS – photosensitizer; CRT – contact radiotherapy; IC – intact control; PDT – photodynamic therapy.

icals (reactive oxygen species – ROS) [13, 14]. Absorbing radiation, the PS molecule enters into a cascade of reactions, which leads to the formation of a hydroxyl radical, superoxide anion, and singlet oxygen in the cell, which are also accumulated due to the radiation radiolysis of water. Later, lethal damage to cellular components (cytoplasmic membranes, granular endoplasmic reticulum, mitochondria, DNA, etc.) occurs at the level of physicochemical processes. Possessing a high oxidative potential, ROS interact with membrane lipids of tumor cell organelles with the formation of oxidation products, destabilization, and subsequent destruction of the cell as a whole. The consequence of the above reactions to the combined effect is an oxidative stress syndrome that induces apoptosis [15].

In the available literature, there are few publications devoted to the study of the radiodynamic activity of PS based on protoporphyrin IX, hematoporphyrin and its derivatives in experiments *in vitro/in vivo* (gliomas c6 and U-373 MG, gliosarcoma 9L; squamous cell carcinoma of the human esophagus OE-21, adenocarcinoma human esophagus OE-33, human bladder carcinoma RT4, and colon adenocarcinoma HT-29) [13, 14, 16 17, 18]. The authors report a statistically significant reduction in the number of viable tumor cells and inhibition of the growth of grafted tumors in the combination therapy groups compared with RT alone.

Thus, American researchers (Panetta J.V. et al.) from the Fox Chase Cancer Center (USA) presented the results of the use of RDT with protoporphyrin IX in mice with an orthotopic model of human prostate carcinoma PC-3. 5-aminolevulinic acid (5-ALA), which causes the formation of endogenous PS protoporphyrin IX, was administered orally at a dose of 100 mg/kg 4 hours before the start of irradiation of subcutaneously transplanted tumors, which was carried out once at a dose of 4 Gy. The authors reported that after 7 and 14 days from the start of therapeutic interventions in the RDT group, the average tumor volume was $24\pm 9\%$ and $21\pm 8\%$ less compared to the RT group in monomode, respectively ($p < 0.05$) [19].

In their later study, D.M. Yang *et al.* (Fox Chase Cancer Center, USA) proved the presence of radiosensitizing properties in protoporphyrin IX in an experiment on C57BL/6 linear mice with a subcutaneously transplanted small cell lung cancer tumor KP1. 5-ALA was administered orally at a dose of 100 mg/kg 4 hours before the start of irradiation of subcutaneously transplanted tumors, which was carried out once in the SFD of 4 Gy. After 14 days from the start of treatment in the RDT group, inhibition of the growth of grafted tumors by 52.1%, 48.1% and 57.9% was registered compared with the groups of 5-ALA ($p < 0.001$), RT in monomode ($p < 0.001$) and intact control ($p < 0.001$), respectively [20].

Another study by Takahashi J. et al. (Health and Medical Research Institute, Japan) presents the results of RDT with protoporphyrin IX human glioblastomas U251MG

and U87MG in BALB/c nu/nu mice. 5-ALA was administered orally at doses of 60 and 120 mg/kg 4 h before the start of irradiation of subcutaneously transplanted tumors, which was carried out at SFD of 2 Gy 5 times a week for 6 weeks until a SFD of 60 Gy was reached. The authors report that the proposed method of irradiation had a pronounced inhibitory effect on the growth of both models of transplanted tumors during the entire observation period (42 and 70 days, respectively), causing the development of irreversible damage in the tumor tissue, registered according to a morphological study [12].

Y. Matsuyama et al. (Mie University Graduate School of Medicine, Japan) in their *in vivo* experiments studied the effect of ionizing radiation on the antitumor properties of a photosensitizing substance, acridine orange (AO). As objects of study, the authors used C3H/HeSlc and BALB/cSlc-nu/nu linear mice with transplanted tumors: LM8 mouse osteosarcoma, PC-3 human prostate cancer, and MDA-MB-231 human breast cancer. AO was injected subcutaneously along the perimeter of tumors at a dose of 1 $\mu\text{g}/\text{mL}$. Irradiation was performed once per SFD of 5 Gy. The authors reported that RDT with AO showed a pronounced cytostatic effect against all types of tumors. On the 14th day after the start of therapeutic effects, the average volume of LM8 tumors in the control group was 890 mm^3 , AO – 780 mm^3 , RT SFD of 5 Gy – 120 mm^3 and AO + RT SFD of 5 Gy – 42 mm^3 ($p < 0.05$); for MDA-MB-231 – 1060, 620, 1010 and 29 mm^3 ($p < 0.05$), and for PC-3 – 530, 200, 45 and 14 mm^3 ($p < 0.05$), respectively [21].

And finally, C. Dupin et al. (Bordeaux Institute of oncology, France) presented the experience of using the RDT method in an experiment on immunodeficient RAGy2C–/– mice with an orthotopic model of human glioblastoma P3. 5-ALA was used as a photosensitizing agent and was administered intraperitoneally at a dose of 100 mg/kg. Irradiation of transplanted tumors was carried out 3 times a week in the following modes: 3×2 Gy, 5×2 Gy, and 5×3 Gy; 2.55 Gy/min. Based on the analysis of the obtained results according to the criterion of survival, the optimal effect was fractionated irradiation in the mode of 5×3 Gy 3 times a week (73–83 days) vs. control (without exposure) (15–24 days), RT 3×2 Gy (41–47 days) and RT 5×3 Gy (48–62 days) ($p < 0.05$). In a comparative aspect, there was a tendency to optimize survival rates in the 5-ALA + RT 5×2 Gy group (53–67 days) to the RT 5×2 Gy group ($p = 0.24$) [22].

Several clinical trials have been initiated in large cohorts of patients to evaluate the safety and tolerability of RDT. Thus, the clinical trial “A Phase I Dose Finding Study Of Low-dose Radiation With Sensitization Using 5-aminolevulinic Acid In Advanced Malignancies”, which is based on the determination of optimal doses of RT and PS in patients with various nosological forms of malignant neoplasms (solid tumors of the head and neck, chest and abdominal cavities, small pelvis) was launched

by Fox Chase Cancer Center (USA) in July 2020. The study is planned to include 130 patients. As a PS, 5-ALA is used in 3 doses. Irradiation is carried out fractionally, the course of therapy is carried out once and is 21 days. In the future, patients are under dynamic observation for 56 days to assess the frequency and severity of adverse reactions, as well as preliminary data on the antitumor efficacy of the method [23].

A clinical trial "Phase I/II Dose Escalation Trial of Radiodynamic Therapy (RDT) With 5-Aminolevulinic Acid in Patients With First Recurrence of Glioblastoma" led by Prof. Stummer W. (University Hospital Münster, Germany) started in October 2022. It is planned to include 34 patients with a recurrent form of glioblastoma (the first recurrence after combined or complex treatment). 5-ALA is used as a PS. Irradiation will be fractionated, and the aim of the study will be to determine the maximum tolerated doses of PS and RT, as well as the optimal number of RDT sessions. Patient survival rates (overall 6-month survival, 6-month progression-free survival, etc.) will be studied as criteria for antitumor efficacy [24].

The analyzed data testify to the significant prospects of this direction in experimental oncology. The results obtained in experiments *in vitro/in vivo* allow to conclude that several PS have radiosensitizing properties, which creates prerequisites for optimizing and further improv-

ing the combined and complex therapy of patients with malignant neoplasms of various localizations.

Conclusion

PDT is a method of therapy for precancerous diseases and malignant neoplasms, demonstrating high antitumor efficacy against these diseases in experimental and clinical oncology [25, 26, 27]. Nevertheless, to optimize the use of PDT, it is advisable to use it in combination with a number of other methods of therapy. Pilot data obtained on the basis of an analysis of the immediate and long-term results of an experimental study on transplantable tumors in rats indicate a pronounced trend towards a higher antitumor effect of combined treatment, including the use of PS followed by RDT and PDT sessions with a single irradiation regimen compared to RDT and PDT in monomodes. No publications devoted to the study of the effectiveness of the combined use of PS of the chlorin series and these methods of therapy, demonstrating positive results, were found in the available literature sources, which allows to conclude that it is necessary and promising to develop deeper research in this direction.

This work was financially supported by the National Academy of Sciences of Belarus (grant no. 2021-61-284, task 3.05.3).

REFERENCES

1. Yanovsky R.L., Bartenstein D.W., Rogers G.S., Isakoff S.J., Chenet S.T. Photodynamic therapy for solid tumors: A review of the literature // *Photodermatol. Photoimmunol. Photomed.* – 2019. – Vol. 35. – P. 295-303. doi: 10.1111/phpp.12489.
2. Gunaydin G., Gedik M.E., Ayan S. Photodynamic therapy for the treatment and diagnosis of cancer – a review of the current clinical status // *Front. Chem.* 2021. – Vol. 9. – P. e686303. doi:10.3389/fchem.2021.686303.
3. Castano A.P., Mroz P., Hamblin M.R. Photodynamic therapy and anti-tumour immunity // *Nature Reviews Cancer.* – 2006. – Vol. 6(7). – P. 535-545. doi: 10.1038/nrc1894.
4. Agostinis P., Berg K., Cengel K.A., Foster T.H., Girotti A.W., Gollnick S.O., Hahn S.M., Hamblin M.R., Juzeniene A., Kessel D., Korbelik M., Moan J., Mroz P., Nowis D., Piette J., Wilson B.C., Golab J. Photodynamic therapy of cancer: an update // *CA-A Cancer J. Clin.* – 2011. – Vol. 61(4). – P. 250-281. doi: 10.3322/caac.20114.
5. Correia J.H., Rodrigues J.A., Pimenta S., Dong T., Yang Z. Photodynamic therapy review: principles, photosensitizers, applications, and future directions // *Pharmaceutics.* – 2021. – Vol. 13. – P. e1332. doi:10.3390/pharmaceutics13091332.
6. Yang M., Yang T., Mao C. Enhancement of photodynamic cancer therapy by physical and chemical factors // *Angew Chem Int Ed Engl.* – 2019. – Vol. 58(40). – P. 14066-14080. doi:10.1002/anie.201814098.
7. Hu H., Feng W., Qian X., Yu L., Chen Y., Li Y. Emerging nanomedicine-enabled/enhanced nanodynamic therapies beyond traditional photodynamics. // *Adv. Mater.* – 2021. – Vol. 33(12). – P. e2005062. doi: 10.1002/adma.202005062.
8. Rodrigues J.A., Correia J.H. Enhanced photodynamic therapy: a review of combined energy sources // *Cells.* – 2022. – Vol. 11(24). – P. 3995. doi: 10.3390/cells11243995.
9. Larue L., Mihoub A.B., Youssef Z., Colombeau L., Acherar S., André J.C., Arnoux P., Baros F., Vermandel M., Frochot C. Using X-rays in photodynamic therapy: an overview // *Photochem. Photobiol. Sci.* – 2018. – Vol. 17(11). – P. 1612-1650. doi: 10.1039/c8pp00112j.

ЛІТЕРАТУРА

1. Yanovsky R.L., Bartenstein D.W., Rogers G.S., Isakoff S.J., Chenet S.T. Photodynamic therapy for solid tumors: A review of the literature. *Photodermatol. Photoimmunol. Photomed.* 2019, vol. 35, pp. 295-303. doi: 10.1111/phpp.12489.
2. Gunaydin G., Gedik M.E., Ayan S. Photodynamic therapy for the treatment and diagnosis of cancer – a review of the current clinical status. *Front. Chem.* 2021, vol. 9, pp. e686303. doi:10.3389/fchem.2021.686303.
3. Castano A.P., Mroz P., Hamblin M.R. Photodynamic therapy and anti-tumour immunity. *Nature Reviews Cancer*, 2006, vol. 6(7), pp. 535-545. doi: 10.1038/nrc1894.
4. Agostinis P., Berg K., Cengel K.A., Foster T.H., Girotti A.W., Gollnick S.O., Hahn S.M., Hamblin M.R., Juzeniene A., Kessel D., Korbelik M., Moan J., Mroz P., Nowis D., Piette J., Wilson B.C., Golab J. Photodynamic therapy of cancer: an update. *CA-A Cancer J. Clin.* 2011, vol. 61(4), pp. 250-281. doi: 10.3322/caac.20114.
5. Correia J.H., Rodrigues J.A., Pimenta S., Dong T., Yang Z. Photodynamic therapy review: principles, photosensitizers, applications, and future directions. *Pharmaceutics*, 2021, vol. 13, p. e1332. doi:10.3390/pharmaceutics13091332.
6. Yang M., Yang T., Mao C. Enhancement of photodynamic cancer therapy by physical and chemical factors. *Angew Chem Int Ed Engl.* 2019, vol. 58(40), pp. 14066-14080. doi:10.1002/anie.201814098.
7. Hu H., Feng W., Qian X., Yu L., Chen Y., Li Y. Emerging nanomedicine-enabled/enhanced nanodynamic therapies beyond traditional photodynamics. *Adv. Mater.* 2021, vol. 33(12), p. e2005062. doi: 10.1002/adma.202005062.
8. Rodrigues J.A., Correia J.H. Enhanced photodynamic therapy: a review of combined energy sources. *Cells*, 2022, vol. 11(24), p. 3995. doi: 10.3390/cells11243995.
9. Larue L., Mihoub A.B., Youssef Z., Colombeau L., Acherar S., André J.C., Arnoux P., Baros F., Vermandel M., Frochot C. Using X-rays in photodynamic therapy: an overview. *Photochem. Photobiol. Sci.* 2018, vol. 17(11), pp. 1612-1650. doi: 10.1039/c8pp00112j.

10. He L., Yu X., Li W. Recent progress and trends in X-ray-induced photodynamic therapy with low radiation doses // *ACS Nano*, 2022, vol. 16(12), pp. 19691-19721. doi: 10.1021/acsnano.2c07286.
11. Руководство по экспериментальному (доклиническому) изучению новых фармакологических веществ / под общ. ред. чл.-корр. РАМН проф. Р. У. Хабриева. – 2 изд., перераб. и доп. – М.: ОАО «Издательство «Медицина». – 2005. – С. 647-649.
12. Takahashi J., Nagasawa S., Doi M., Takahashi M., Narita Y., Yamamoto J., Ikemoto M.J., Iwahashi H. In vivo study of the efficacy and safety of 5-aminolevulinic radiodynamic therapy for glioblastoma fractionated radiotherapy // *Int. J. Mol. Sci.* – 2021. – Vol. 22. – P. 1-15. doi:10.3390/ijms22189762.
13. Kulka U., Schaffer M., Siefert A. Photofrin as a radiosensitizer in an in vitro cell survival assay // *Biochem. Biophys. Res. Commun.* – 2003. – Vol. 311(1). – P. 98-103. doi: 10.1016/j.bbrc.2003.09.170.
14. Schaffer M., Kulka U., Ertl-Wagner B., Schaffer P.M., Friso E., Hell R., Jori G., Hofstetter A., Dühmke E. Effect of Photofrin II as a radiosensitizing agent in two different oesophageal carcinoma cell lines // *J. Porphyrins Phthalocyanines*. – 2005. – Vol. 9. – P. 470-475. doi:10.1142/S1088424605000587.
15. Benayoun L., Schaffer M., Bril R., Gingis-Velitski S., Segal E., Nevelsky A., Satchi-Fainaro R., Shaked Y. Porfimer-sodium (Photofrin II) in combination with ionizing radiation inhibits tumor-initiating cell proliferation and improves glioblastoma treatment efficacy // *Cancer Biol. Ther.* – 2013. – Vol. 14(1). – P. 64-74. doi: 10.4161/cbt.22630.
16. Schaffer M., Schaffer P.M., Corti L., Gardiman M., Sotti G., Hofstetter A., Jori G., Dühmke E. Photofrin as a specific radiosensitizing agent for tumors: studies in comparison to other porphyrins, in an experimental in vivo model // *J. Photochem. Photobiol. B: Biol.* – 2002. – Vol. 66. – P. 157-164. doi: 10.1016/s1011-1344(02)00237-3.
17. Rutkovskienė L., Plėšnienė L., Sendiulienė D., Stančius A., Liutkevičiūtė-Navickienė J. Sensitization of rat C6 glioma cells to ionizing radiation by porphyrins // *Acta Medica Lituan.* – 2011. – Vol. 18(2). – P. 56-62. doi:10.6001/actamedica.v18i2.1816.
18. Yamamoto J., Ogura S.I., Tanaka T., Kitagawa T., Nakano Y., Saito T., Takahashi M., Akiba D., Nishizawa S. Radiosensitizing effect of 5-aminolevulinic acid-induced protoporphyrin IX in glioma cells in vitro // *Oncology Rep.* – 2012. – Vol. 27. – P. 1748-1752. doi: 10.3892/or.2012.1699.
19. Panetta J.V., Cvetkovic D., Chen X., Chen L., Charlie Ma C.M. Radiodynamic therapy using 15-MV radiation combined with 5-aminolevulinic acid and carbamide peroxide for prostate cancer in vivo // *Phys. Med. Biol.* – 2020. – Vol. 65(16). – P. 1-14. doi:10.1088/1361-6560/ab9776.
20. Yang D.M., Cvetkovic D., Chen L., Charlie Ma C.M. Therapeutic effects of in-vivo radiodynamic therapy (RDT) for lung cancer treatment: a combination of 15MV photons and 5-aminolevulinic acid (5-ALA) // *Biomed. Phys. Eng. Express*. – 2022. – Vol. 8(6). – P. 1-15. doi: 10.1088/2057-1976/ac9b5c.
21. Matsuyama Y., Nakamura T., Yoshida K., Hagi T., Iino T., Asanuma K., Sudo A. Radiodynamic therapy with acridine orange local administration as a new treatment option for primary and secondary bone tumours // *Bone Joint Res.* – 2022. – Vol. 11(10). – P. 715-722. doi: 10.1302/2046-3758.1110.BJR-2022-0105.R2.
22. Dupin C., Sutter J., Amintas S., Derieppe M.A., Lalanne M., Coulibaly S., Guyon J., Daubon T., Boutin J., Blouin J.M., Richard E., Moreau-Gaudry F., Bedel A., Vendrely V., Dabernat S. An orthotopic model of glioblastoma is resistant to radiodynamic therapy with 5-aminolevulinic acid // *Cancers (Basel)*. – 2022. – Vol. 14(17). – P. 4244. doi:10.3390/cancers14174244.
23. ClinicalTrials.gov Identifier: NCT04381806.
24. ClinicalTrials.gov Identifier: NCT05590689.
25. Filonenko E.V., Ivanova-Radkevich V.I. Photodynamic therapy in the treatment of extramammary Paget disease // *Biomedical Photonics*. – 2022. – Vol. 11(3). – P. 24-34. doi: 10.24931/2413-9432-2022-11-3-24-34
26. Gilyadova A.V., Romanko Yu.S., Ishchenko A.A., Samoilova S.V., Shiryayev A.A., Alekseeva P.M., Efendiev K.T., Reshetov I.V. Photodynamic therapy for precancer diseases and cervical cancer (review of literature) // *Biomedical Photonics*. – 2021. – Vol. 10(4). – P. 59-67. doi: 10.24931/2413-9432-2021-10-4-59-67
27. Filonenko E.V., Ivanova-Radkevich V.I. Photodynamic therapy in the treatment of patients with mycosis fungoides // *Biomedical Photonics*. – 2022. – Vol. 11(1). – P. 27-36. doi: 10.24931/2413-9432-2022-11-1-27-37
10. He L., Yu X., Li W. Recent progress and trends in X-ray-induced photodynamic therapy with low radiation doses. *ACS Nano*, 2022, vol. 16(12), pp. 19691-19721. doi: 10.1021/acsnano.2c07286.
11. Guidelines for the experimental (preclinical) study of new pharmacological substances / under the general editorship of the corresponding member of the Russian Academy of Medical Sciences prof. R. U. Khabrieva. – 2nd ed., reprint. and additional – M.: JSC "Publishing House «Medicine», 2005, pp. 647-649.
12. Takahashi J., Nagasawa S., Doi M., Takahashi M., Narita Y., Yamamoto J., Ikemoto M.J., Iwahashi H. In vivo study of the efficacy and safety of 5-aminolevulinic radiodynamic therapy for glioblastoma fractionated radiotherapy. *Int. J. Mol. Sci.*, 2021, vol. 22, pp. 1-15. doi:10.3390/ijms22189762.
13. Kulka U., Schaffer M., Siefert A. Photofrin as a radiosensitizer in an in vitro cell survival assay. *Biochem. Biophys. Res. Commun*, 2003, vol. 311(1), pp. 98-103. doi: 10.1016/j.bbrc.2003.09.170.
14. Schaffer M., Kulka U., Ertl-Wagner B., Schaffer P.M., Friso E., Hell R., Jori G., Hofstetter A., Dühmke E. Effect of Photofrin II as a radiosensitizing agent in two different oesophageal carcinoma cell lines. *J. Porphyrins Phthalocyanines*, 2005, vol. 9, pp. 470-475. doi:10.1142/S1088424605000587.
15. Benayoun L., Schaffer M., Bril R., Gingis-Velitski S., Segal E., Nevelsky A., Satchi-Fainaro R., Shaked Y. Porfimer-sodium (Photofrin II) in combination with ionizing radiation inhibits tumor-initiating cell proliferation and improves glioblastoma treatment efficacy. *Cancer Biol. Ther.*, 2013, vol. 14(1), pp. 64-74. doi: 10.4161/cbt.22630.
16. Schaffer M., Schaffer P.M., Corti L., Gardiman M., Sotti G., Hofstetter A., Jori G., Dühmke E. Photofrin as a specific radiosensitizing agent for tumors: studies in comparison to other porphyrins, in an experimental in vivo model. *J. Photochem. Photobiol. B: Biol.*, 2002, vol. 66, pp. 157-164. doi: 10.1016/s1011-1344(02)00237-3.
17. Rutkovskienė L., Plėšnienė L., Sendiulienė D., Stančius A., Liutkevičiūtė-Navickienė J. Sensitization of rat C6 glioma cells to ionizing radiation by porphyrins. *Acta Medica Lituan.*, 2011, vol. 18(2), pp. 56-62. doi:10.6001/actamedica.v18i2.1816.
18. Yamamoto J., Ogura S.I., Tanaka T., Kitagawa T., Nakano Y., Saito T., Takahashi M., Akiba D., Nishizawa S. Radiosensitizing effect of 5-aminolevulinic acid-induced protoporphyrin IX in glioma cells in vitro. *Oncology Rep.*, 2012, vol. 27, pp. 1748-1752. doi: 10.3892/or.2012.1699.
19. Panetta J.V., Cvetkovic D., Chen X., Chen L., Charlie Ma C.M. Radiodynamic therapy using 15-MV radiation combined with 5-aminolevulinic acid and carbamide peroxide for prostate cancer in vivo. *Phys. Med. Biol.*, 2020, vol. 65(16), pp. 1-14. doi:10.1088/1361-6560/ab9776.
20. Yang D.M., Cvetkovic D., Chen L., Charlie Ma C.M. Therapeutic effects of in-vivo radiodynamic therapy (RDT) for lung cancer treatment: a combination of 15MV photons and 5-aminolevulinic acid (5-ALA). *Biomed. Phys. Eng. Express*, 2022, vol. 8(6), pp. 1-15. doi: 10.1088/2057-1976/ac9b5c.
21. Matsuyama Y., Nakamura T., Yoshida K., Hagi T., Iino T., Asanuma K., Sudo A. Radiodynamic therapy with acridine orange local administration as a new treatment option for primary and secondary bone tumours. *Bone Joint Res.*, 2022, vol. 11(10), pp. 715-722. doi: 10.1302/2046-3758.1110.BJR-2022-0105.R2.
22. Dupin C., Sutter J., Amintas S., Derieppe M.A., Lalanne M., Coulibaly S., Guyon J., Daubon T., Boutin J., Blouin J.M., Richard E., Moreau-Gaudry F., Bedel A., Vendrely V., Dabernat S. An orthotopic model of glioblastoma is resistant to radiodynamic therapy with 5-aminolevulinic acid. *Cancers (Basel)*, 2022, vol. 14(17), p. 4244. doi:10.3390/cancers14174244.
23. ClinicalTrials.gov Identifier: NCT04381806.
24. ClinicalTrials.gov Identifier: NCT05590689.
25. Filonenko E.V., Ivanova-Radkevich V.I. Photodynamic therapy in the treatment of extramammary Paget disease. *Biomedical Photonics*, 2022, vol. 11(3), pp. 24-34. doi: 10.24931/2413-9432-2022-11-3-24-34
26. Gilyadova A.V., Romanko Yu.S., Ishchenko A.A., Samoilova S.V., Shiryayev A.A., Alekseeva P.M., Efendiev K.T., Reshetov I.V. Photodynamic therapy for precancer diseases and cervical cancer (review of literature). *Biomedical Photonics*, 2021, vol. 10(4), pp. 59-67. doi: 10.24931/2413-9432-2021-10-4-59-67
27. Filonenko E.V., Ivanova-Radkevich V.I. Photodynamic therapy in the treatment of patients with mycosis fungoides. *Biomedical Photonics*, 2022, vol. 11(1), pp. 27-36. doi: 10.24931/2413-9432-2022-11-1-27-37

SPECTROSCOPIC STUDY OF METHYLENE BLUE PHOTOPHYSICAL PROPERTIES IN BIOLOGICAL MEDIA

Pominova D.V.^{1,2}, Ryabova A.V.^{1,2}, Romanishkin I.D.¹, Markova I.V.², Akhlustina E.V.²,
Skobeltsin A.S.^{1,2}

¹Prokhorov General Physics Institute of Russian Academy of Sciences, Moscow, Russia

²National Research Nuclear University MEPhI (Moscow Engineering Physics Institute),
Moscow, Russia

Abstract

A spectroscopic study of the photophysical properties of methylene blue (MB) in aqueous solutions was carried out. Absorption and fluorescence spectra as well as fluorescence lifetime were recorded. The concentration dependence of the intensity and shape of the spectra allowed establishing the ranges of MB concentrations for *in vitro* and *in vivo* studies at which aggregation is not observed (up to 0.01 mM, which corresponds to 3.2 mg/kg). Studies of photodegradation in biological media showed that photobleaching of more than 80% in plasma and culture media is observed already at a dose of 5 J/cm², while in water at this concentration and dose photobleaching is not yet observed, and at a dose of 50 J/cm² photobleaching of MB is about 30%. It was found that in media containing proteins and having an alkaline pH, photobleaching occurs significantly faster than in neutral aqueous media. The ionic strength of the solution has no effect on the photobleaching rate. Such photobleaching is caused by the photodegradation of MB rather than the transition to the leucoform.

The efficiency of singlet oxygen generation and photodynamic activity were evaluated *in vitro*. In the investigated range of MB concentrations, the efficiency of singlet oxygen generation is rather low, because positively charged MB binds to negatively charged cell membranes, which leads to a change in the type of photodynamic reaction. The emergence of other reactive oxygen species (ROS), different from singlet oxygen, in cells has been demonstrated. The generation of ROS and the low quantum yield of singlet oxygen generation indicate the tendency of MB to provide the type I photosensitization mechanism (electron transfer with the formation of semi-reduced and semi-oxidized MB⁺ radicals) rather than to the type II mechanism (energy transfer to oxygen with the formation of singlet oxygen) in biological media and *in vivo*.

Keywords: methylene blue, spectroscopy, absorption, fluorescence, photobleaching.

Contacts: Pominova D.V., e-mail: pominovadv@gmail.com

For citations: Pominova D.V., Ryabova A.V., Romanishkin I.D., Markova I.V., Akhlustina E. V., Skobeltsin A.S. Spectroscopic study of methylene blue photophysical properties in biological media, *Biomedical Photonics*, 2023, vol. 12, no. 2, pp. 34–47. doi: 10.24931/2413-9432-2023-12-2-34-47.

СПЕКТРОСКОПИЧЕСКОЕ ИССЛЕДОВАНИЕ ФОТОФИЗИЧЕСКИХ СВОЙСТВ МЕТИЛЕНОВОГО СИНЕГО В БИОЛОГИЧЕСКИХ СРЕДАХ

Д.В. Поминова^{1,2}, А.В. Рябова^{1,2}, И.Д. Романишкин¹, И.В. Маркова², Е.В. Ахлюстина²,
А.С. Скобельцин^{1,2}

¹Институт общей физики им. А. М. Прохорова Российской академии наук, Москва, Россия

²Национальный исследовательский ядерный университет «МИФИ», Москва, Россия

Резюме

Проведено спектроскопическое исследование фотофизических свойств метиленового синего (МС) в водных растворах и биологических жидкостях. Зарегистрированы спектры поглощения и флуоресценции, а также времена жизни флуоресценции. По зависимости интенсивности и формы спектров от концентрации удалось установить диапазоны концентраций МС для исследований *in vitro* и *in vivo* при которых не наблюдается агрегация (до 0,01 мМ, что соответствует 3,2 мг/кг).

Исследовано фотообесцвечивание МС под действием лазерного излучения. Исследования фотодеградации в биологических средах показали, что фотообесцвечивание более чем на 80% в плазме и культуральной среде наблюдается уже при дозе 5 Дж/см², в то время как в воде при такой концентрации при дозе 5 Дж/см² фотообесцвечивания еще не наблюдается, а при дозе 50 Дж/см² фотообесцвечивание МС составляет порядка 30%. Установлено, что в средах, содержащих белки и обладающих щелочным рН, фотообесцвечива-

ние происходит существенно быстрее, чем в нейтральных водных средах. Ионная сила раствора не оказывает влияния на скорость фотообесцвечивания. Такое фотообесцвечивание вызвано фотодеградацией МС, а не переходом в лейкоформу.

Проведена оценка эффективности генерации синглетного кислорода и фотодинамической активности *in vitro*. В исследуемом диапазоне концентраций МС эффективность генерации синглетного кислорода достаточно низкая, так как положительно заряженный МС связывается с негативно заряженными мембранами клеток, что приводит к изменению типа фотодинамической реакции. Продемонстрировано возникновение в клетках других активных форм кислорода (АФК), отличных от синглетного кислорода. Генерация АФК и невысокий квантовый выход генерации синглетного кислорода свидетельствуют о склонности МС к механизму фотосенсибилизации I типа (перенос электрона с образованием полувосстановленных и полуокисленных радикалов MB^+), а не к механизму II типа (перенос энергии к кислороду с образованием синглетного кислорода) в биологических средах и *in vivo*.

Ключевые слова: метиленовый синий, спектроскопия, флуоресценция, поглощение, фотообесцвечивание, АФК, синглетный кислород.

Контакты: Поминова Д.В., e-mail: pominovadv@gmail.com

Для цитирования: Поминова Д.В., Рябова А.В., Романишкин И.Д., Маркова И.В., Ахлюстина Е.В., Скобельцин А.С. Спектроскопическое исследование фотофизических свойств метиленового синего в биологических средах // Biomedical Photonics. – 2023. – Т. 12, № 2. – С. 34–47. doi: 10.24931/2413-9432-2023-12-2-34-47.

Introduction

Photodynamic therapy (PDT) is a very promising therapeutic method for treatment of tumors and non-malignant diseases. The method is based on use of photosensitizer (PS), which is selectively localized in target tissue, and irradiation with light. The PS absorbs the light and can then transfer the energy to molecular oxygen and create singlet oxygen (type II photochemical reaction), which is extremely phototoxic, causing photodamage and subsequent cell death. Another way is the participation of PS in electron-transfer reactions initiating formation of hydroxyl radicals and hydroperoxides and radical-induced damage in biomolecules (type I photochemical reaction) [1, 2]. For the vast majority of clinically approved PS, singlet oxygen is the main cytotoxic agent that determines the mechanism of photodynamic effect and causes cell death in PDT [3]. The type I photochemical reaction may be preferable for therapy of tumors which are hypoxic [1]. However *in vivo* it is difficult to establish without doubt which of these mechanisms is more prevalent, both processes can ultimately lead to cell death [4], but the knowledge how these processes are affected by biological environments is important [5].

Due to the popularity of fluorescence diagnostic methods and PDT [6–9], there is interest in the study of various dyes that can be used as PS. One of the actively studied PS is methylene blue (MB) – a heterocyclic aromatic phenothiazine dye discovered in 1876 by Heinrich Caro. In the dry state MB appears as odorless dark blue crystals, soluble in water, chloroform, and alcohol. Its molecular weight is 319.85 g/mol [10]. In its oxidized state, MB is blue in color because the phenothiazine molecule strongly absorbs in the 600–700 nm region. In aqueous solutions, the wavelength λ_{\max} of the absorption band maximum for monomer is given in various works as 668 nm, 664 nm [11], 660 nm [12, 13]; λ_{\max} for dimer is 614 nm [12, 13], 605 nm [11]; λ_{\max} for trimer is 580 nm [11]. In the UV region for the monomer $\lambda_{\max} = 292$ nm [13]. The oxidized form can be easily reduced to colorless

leucomethylene blue (LMB) in the absence of oxygen [14] or by interaction with NAD(P)H [15, 16] or reduced glutathione [17]. LMB predominantly absorbs in the UV region (256 nm).

MB redox properties are important because, depending on its form, it can be both an electron donor and an electron acceptor, changing rapidly from one state to another [18]. For example, MB interacts directly with the mitochondrial electronic circuit, donating electrons to complexes I and III and/or providing partial restoration of the Krebs cycle [19], whenever NADH is oxidized by MB or even resuscitation of the mitochondrial electronic circuit. The redox properties of MB are of great interest to researchers and make it possible to use it to treat various pathologies, for example, to treat methemoglobinemia by reducing iron to its divalent state [20–23], to relieve septic shock [24, 25], to treat lactoacidosis [26], and as an antidote for carbon monoxide poisoning [27] or cyanide [28, 29]. MB also increases oxygen consumption by tissues with aerobic glycolysis and tumors, while the effect of MB is approximately proportional to the enzymatic capacity of tissues [30], which is promising in terms of photodynamic therapy because the efficiency of singlet oxygen generation obviously depends on oxygen concentration.

The ability of MB to fluoresce is used to label tumors and other objects in order to visualize them [31]. For a long time, MB has been actively used for photodynamic therapy of neoplasms [32–36], photodynamic inactivation of pathogens [37–40], including antibiotic-resistant microflora [41–44].

The photophysical properties of MB in solutions are actively studied. Although its photochemical properties in isotropic solution are well established, its effect *in vivo* needs further study. Most of the results reported in the literature are obtained for MB in ethanol or water. Many papers report that efficient intersystem crossing is observed with quantum yields around 0.5 [2, 45], but it should be noted that this value was obtained in isotropic

ethanol solutions [46]. The quantum yield and generation of $^1\text{O}_2$ decreases to values close to zero if MB dimerizes due to a fast nonradiative decay (3–4 ps) of the excited dimer population [47, 48], favoring electron transfer reactions and consequent generation of radical species [45, 49, 50]. Dimerization could also lead to fluorescence quantum yield decrease [45, 50]. Another parameter which affects the singlet oxygen generation efficiency is the pH. According to literature data the production of singlet oxygen is approximately five times more efficient in alkaline than in acidic medium [51]. The ratio of monomer to dimer depends significantly on the solution composition as well as MB concentration [52, 53, 53–60]. According to literature data, in 20 μM aqueous solution only MB monomers are present, at higher concentration dimerization was observed, however at concentrations below ~ 20 ppm [61] or ~ 70 ppm [57] the existence of trimeric or tetrameric aggregates can be neglected.

The state of MB aggregation in aqueous solution is also sensitive to the ionic strength [52], it was shown that the increase of the inert salts concentration indicates the decreasing tendency of the MB molecules to undergo aggregation. The concentration of surfactant also influences the dimerization. The polarity of the solvent, concentration of surfactants [50], binding of molecules in membranes and interaction with surfaces [62] can cause the changes in ratio of monomer to dimer as well as the singlet oxygen production.

A large number of interrelated factors affecting the photophysical and photochemical properties of methylene blue make it difficult to study and implement in clinical practice, despite a number of unique properties that can be very useful for improving the effectiveness of photodynamic therapy. For clinical use, it is important to study the photophysical and photochemical properties of MB under conditions closest to real biological ones. In this regard, in this work, the absorption, fluorescence, photobleaching, and singlet oxygen generation efficiency of MB in biological media (serum and RPMI medium for cell cultivation) were studied using modern spectroscopic methods. The range of concentrations was chosen based on literature data on MB concentrations in blood after a typical daily dose: 19 μM after oral administration of 500 mg, 10 μM after intravenous administration of 100 mg [63, 64]. The data obtained for biological media were compared with aqueous solutions to determine the main mechanism of photodynamic activity.

Materials and methods

Materials

Methylene blue solution purchased in a pharmacy was used for the studies: Methylene blue, 1% aqueous solution, the active substance methylthioninium chloride (Samamedprom, Russia). Spectroscopic studies were performed for aqueous MB solutions with

concentrations in the range of 0.001–0.05 mM, which corresponds to 0.32–16 mg/kg.

Measurements were performed in distilled water (PanEco, Russia), blood serum (newborn calf blood serum, PanEco, Russia), cell culture medium RPMI (PanEco, Russia) with 10% calf blood serum added, and saline (0.9% sodium chloride, infusion solution, Grotex, Russia). pH of the solutions was controlled using indicator paper (Johnson universal indicator paper, pH 1–11). For water and saline, the pH was 7, for cell culture medium RPMI—8, for plasma—9. To analyze the effect of pH on the spectroscopic properties of MB we also used water with pH adjusted to 8 using 1M NaOH solution.

Absorption spectroscopy

Absorption spectra in the range 200–1000 nm were recorded using a Hitachi U3400 spectrophotometer (Hitachi, Japan) in quartz cuvettes with optical path lengths of 1 cm (for water and NaCl) and 2 mm (for plasma and RPMI medium). To compare the results obtained with each other, all optical density values were multiplied by the corresponding coefficients (0.1 and 0.5 for the centimeter and 2-mm cuvette, respectively) and scaled to the optical density value for a 1-mm cuvette. The analysis of absorption spectra allows studying the transition of the basic form of MB into its reduced form (LMB) under the influence of external factors, photodegradation, and aggregation of MB.

To analyze aggregation, the absorption spectrum shape was approximated in the 500–800 nm range by two Gaussian peaks with maximums at wavelengths corresponding to dimers and monomers, then the ratio of areas under these peaks was considered as a characteristic of dimerization. A linear approximation of the baseline was performed to account for scattering.

Fluorescence spectra and lifetime measurements

The fluorescence spectra of MB aqueous solutions were measured using a LESA-01-Biospec fiber spectrometer (Biospec, Russia) equipped with a longpass edge filter (LP640) in the wavelength range of 650–850 with HeNe laser excitation, 15 mW power output from the fiber.

To investigate the lifetime of aqueous MB fluorescence solutions, a system of Hamamatsu streak camera and streak scope (C9300 and C10627-13) was used to carry out measurements with picosecond resolution.

Study of photobleaching in biological media

To study the laser effect on the solutions, irradiation was performed in 1×1 cm optical cuvettes. The surface of the solution was uniformly irradiated with an LED source with a power density of 100 mW/cm² and a wavelength near the MB absorption maximum of 664 nm. The light source was controlled using a programmable timer, which enabled studying the dependence of the effect on the light dose in increments of 0.5 to 5 J/cm². The irradiation was performed in cyclic mode, the fluorescence intensity

was measured in pauses between irradiation windows when excited by a 632.8 nm laser. The MB photobleaching rate was estimated by the decrease in integral fluorescence intensity (area under the fluorescence peak in the wavelength range of 650–800 nm) as a function of light dose density. Fluorescence intensity was determined using a LESA-01-BIOSPEC fiber optic spectrometer (Biospec, Russia).

Assessment of photodynamic activity of MB in vitro

The photodynamic activity of MB was determined by measuring the oxygen content in erythrocyte solution with MB by the hemoglobin oxygenation level [65]. We measured the deoxygenation rate of PDT with MB on erythrocyte suspension with registration of MB fluorescence under 660 nm laser irradiation at a power density of 250 mW/cm² (10 min=150 J/cm²). As a result of the type II photosensitization mechanism, the formed ¹O₂ reacts irreversibly with biological molecules, resulting in a reduction of dissolved O₂ in the sample. We calculated the relative quantum yield of singlet oxygen generation for MB concentrations of 1–100 mg/kg by comparing with experimental data for aluminum phthalocyanine with the known quantum yield of singlet oxygen generation in aqueous medium from the literature ($\phi\Delta = 0.38$) [66].

Assessment of singlet oxygen generation efficiency in PDT with MB using the Singlet oxygen sensor green

Singlet oxygen sensor green (SOSG, Invitrogen, USA) reagent was dissolved in methanol to make a stock solution of 500 μ M. SOSG (with final concentration of 50 μ M) was added to 10 mg/l MB aqueous solution, irradiated with a 660 nm laser at a power density of 250 mW/cm². SOSG fluorescence was measured with a LESA-01-BIOSPEC fiber spectrometer in the range of 550–600 nm with 532 nm laser excitation. To quantify the generation of singlet oxygen, we compared it with the experimental data for the 1 mg/l of aluminum phthalocyanine.

Evaluating the efficiency of MB generation of reactive oxygen species in vitro

6-Carboxy-2',7'-dichlorodihydrofluorescein diacetate (Carboxy-H2-DCFDA, Lumiprobe RUS Ltd, Russia) was used as an indicator of reactive oxygen species (ROS is specific for hydrogen peroxide H₂O₂ and other ROS such as superoxide-anion O₂⁻, hydroxyl radical ·OH, hydroperoxides ROOH, and peroxy-nitrites ONOO-, but with much lower sensitivity compared to H₂O₂) in living cells after PDT with MB. HeLa cells were grown on RPMI-1640 medium (PanEco, Russia) supplemented with 10% fetal bovine serum (FBS, BioSera, Nuaille, France), 100 U/mL penicillin and 100 μ g/mL streptomycin (Life Technologies, Carlsbad, California, USA) in standard conditions (37°C, 5% CO₂). Cells were subcultured every third day. For confocal microscopy, cells were seeded in a POC-R2 glass-bottomed Petri dish (PeCon GmbH, Erbach,

Germany) at a density of 100 × 10³/cm² one day before the experiment. Twenty-four hours later, MB at a concentration of 20 mg/L was added to the cells 120 minutes before the microscopic examination. 30 minutes before the microscopic examination Carboxy-H2-DCFDA was added at a concentration of 25 μ M in FBS at 37°C, 5% CO₂. The cells were washed three times with prewarmed phosphate-buffered saline, replaced with fresh culture medium, and examined with a laser scanning fluorescence microscope. Sensor fluorescence was excited with a 514 nm laser and detected in the 530–600 nm range. MB fluorescence was excited with a 633 nm laser and detected in the 650–730 nm range.

Results and discussion

Concentration effects on absorption, fluorescence, and fluorescence lifetime of MB in various biological media

Absorption spectra of aqueous solutions of MB as a function of concentration are shown in Fig. 1.

Characteristic peaks are observed in the red (664 nm—monomer, shoulder at 615 nm—aggregates) and ultraviolet (250, 290, and 320 nm) parts of the spectra. Additional peaks in the absorption spectra of MB in plasma and medium are associated with their absorption (415 nm—plasma, 560 nm—phenol red in culture medium). There was also strong absorption in the UV region for plasma and culture medium, which makes it impossible to analyze the MB absorption peaks in this range.

To analyze the aggregation, the absorption spectra were normalized by their maximum, to observe how the spectrum shape changes with increase in concentration, Fig. 2.

The shape of the absorption spectrum changes at concentrations above 0.01 mM (3.2 mg/kg) for water and NaCl and at 0.03 mM (9.6 mg/kg) for serum and RPMI media, which appears as a dimer peak of MB in the spectral region of 600–630 nm.

To quantify and compare aggregation in different solutions, the spectrum was decomposed and the relationship between the areas under the peaks corresponding to monomers and dimers was determined depending on the concentration, Fig. 3.

In water, the most rapid increase in aggregation with increasing concentration is observed. At the same time, at low MB concentrations, the degree of aggregation is higher in serum solutions.

Fluorescence spectra of MB in water as a function of concentration are shown in Fig. 4.

To analyze aggregation and reabsorption, the fluorescence spectra in water and biological media were normalized to the fluorescence maximum (694 nm), Fig. 5.

The obtained spectra show that at a concentration of 0.01 mM (3.2 mg/kg) there is a shift of the maximum

to the long-wavelength region, which indicates the presence of aggregation as well as reabsorption at higher concentrations. The shape of the spectrum does not change in this case. More rapid shift of the fluorescence maximum to the long-wavelength region in case of serum confirms higher aggregation at low concentration.

Comparison of the MB fluorescence spectra registered in various biological media shows that the

most intense fluorescence is observed in saline and in water, Fig. 6.

The decreased fluorescence intensity of MB in culture medium and in plasma may be due to both interaction with plasma proteins and more alkaline pH. At the same time, the fluorescence intensity in culture medium is higher (pH = 8) than in pure plasma (pH = 9). The shape of the fluorescence spectrum did not change in the studied media. Analysis of the integral fluorescence intensity

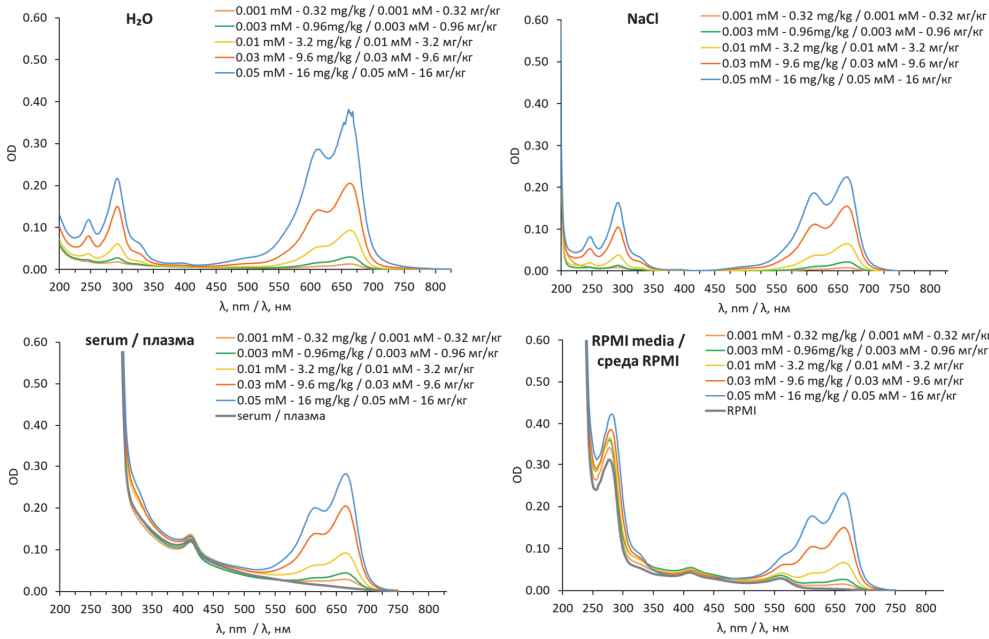


Рис. 1. Спектры поглощения МС в воде и биологических средах в зависимости от концентрации.
Fig. 1. Absorption spectra of MB in water and biological media depending on the concentration.

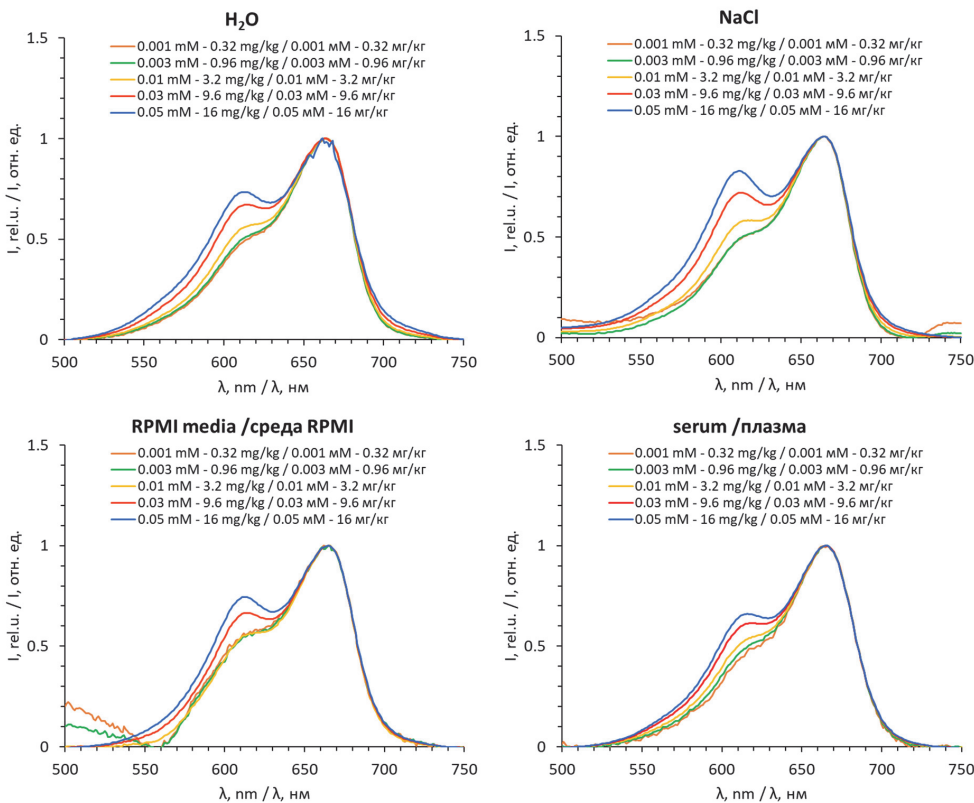


Рис. 2. Нормированные на максимум спектры поглощения МС в воде и биологических средах в зависимости от концентрации.
Fig. 2. Normalized by their maximum absorption spectra of MB in water and biological media as a function of concentration.

(estimated as the area under the fluorescence peak in the 650-800 nm range) shows that in all the studied media the dependence on concentration is nonlinear, a linear section is observed up to the concentration of 0.01 mM for all media, except for plasma, in which a deviation from the linear dependence is observed already at 0.003 mM, which presumably is associated with a large number of dimers in plasma at low concentrations. At concentrations of 0.01-0.03 mM, there is a sublinear section followed by

saturation, which could be associated with reabsorption of excitation in solution as well as with small penetration depth of laser irradiation in solution.

A study of the MB fluorescence lifetime depending on concentration was carried out. No significant differences in lifetime were observed for all investigated concentrations (Table 1), which may indicate that the aggregates formed at high concentrations of MB do not fluoresce.

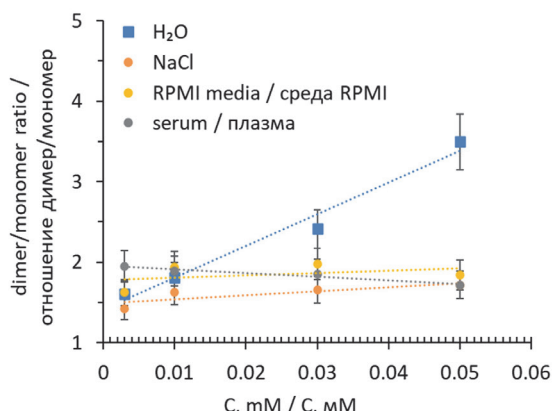


Рис. 3. Зависимость отношения площадей под пиками соответствующими димерам и мономерам (отношение димер/мономер) от концентрации.
Fig. 3. Dependence of the ratio of the areas under the peaks corresponding to dimers and monomers (dimer/monomer ratio) on concentration.

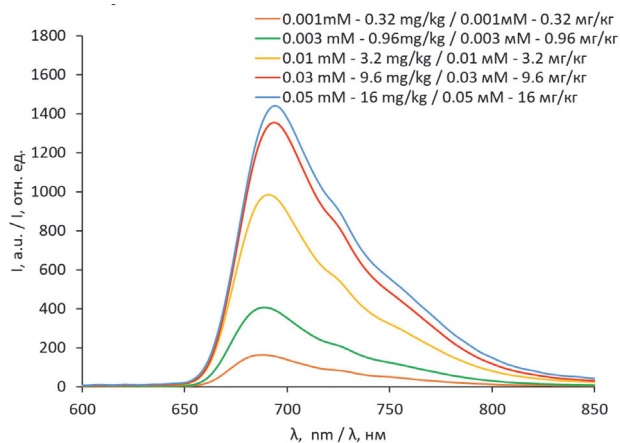


Рис. 4. Спектры флуоресценции МС в воде в зависимости от концентрации.
Fig. 4. Fluorescence spectra of MB in water as a function of concentration.

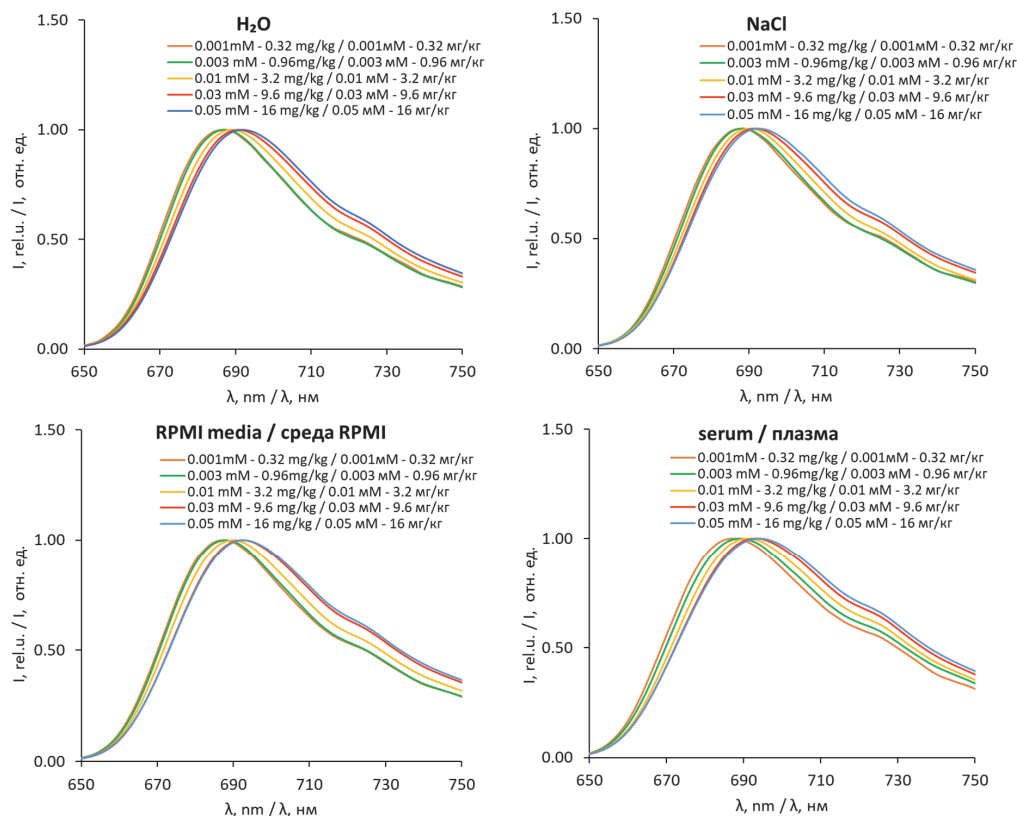


Рис. 5. Нормированные спектры флуоресценции МС в воде и биологических средах в зависимости от концентрации.
Fig. 5. Normalized spectra of MB fluorescence in water and biological media as a function of concentration.

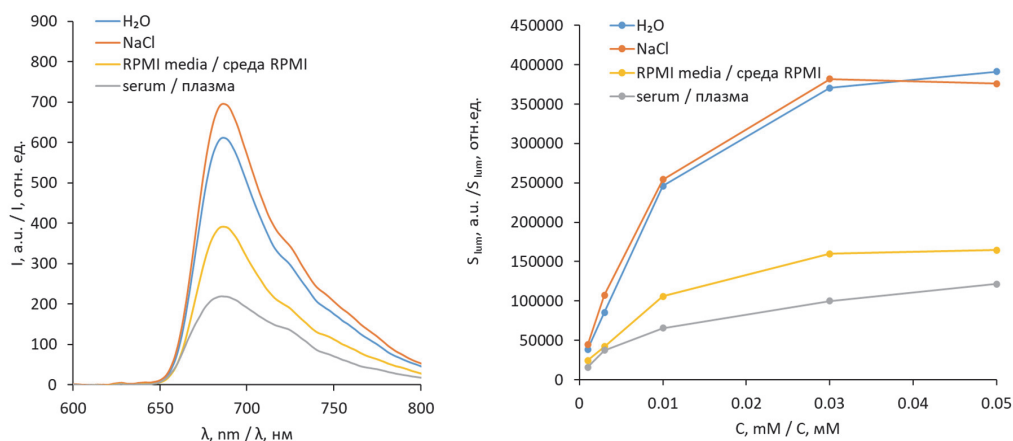


Рис. 6. Слева – спектры флуоресценции МС в различных биологических средах. Справа зависимость интегральной интенсивности флуоресценции (площади под пиком флуоресценции в диапазоне 650–800 нм) от концентрации МС. **Fig. 6.** Left – fluorescence spectra of MB in various biological media. Right – the integral fluorescence intensity (area under the fluorescence peak in the range of 650–800 nm) dependence on MB concentration.

Таблица 1

Времена жизни флуоресценции МС в водных растворах в зависимости от концентрации.

Table 1

Fluorescence lifetime of MB in aqueous solutions as a function of concentration.

C, mM / C, mM	τ , ns / τ , ns
0.001	0.3687
0.003	0.3700
0.01	0.3696
0.03	0.3696
0.1	0.3707

Influence of laser exposure on absorption and fluorescence

We studied the dependence of MB fluorescence intensity in biological media on the light dose density

for MB concentration of 10 μM (3.2 mg/kg). The studies of photodegradation in biological media showed that photobleaching by more than 80% in plasma and culture medium was already observed at the dose of 5 J/cm², while in water at such concentration there was no photobleaching yet at the dose of 5 J/cm², and at the dose of 50 J/cm² the photobleaching of MB was about 30%, Fig. 7.

The results of previous studies also show that MB is photostable in water, the photodegradation of molecules when irradiated with doses up to 50 J/cm² does not exceed 40% [43], while for lower concentrations of MB photobleaching occurs more rapidly, which is presumably due to the large volume of the irradiated area at low concentrations, at high concentrations of the drug is absorbed most of the radiation in a thin layer due to high optical density. Due to the small amount of oxygen in the thin layer, the photobleaching rate at high concentrations slows down because it is limited by the oxygen diffusion rate.

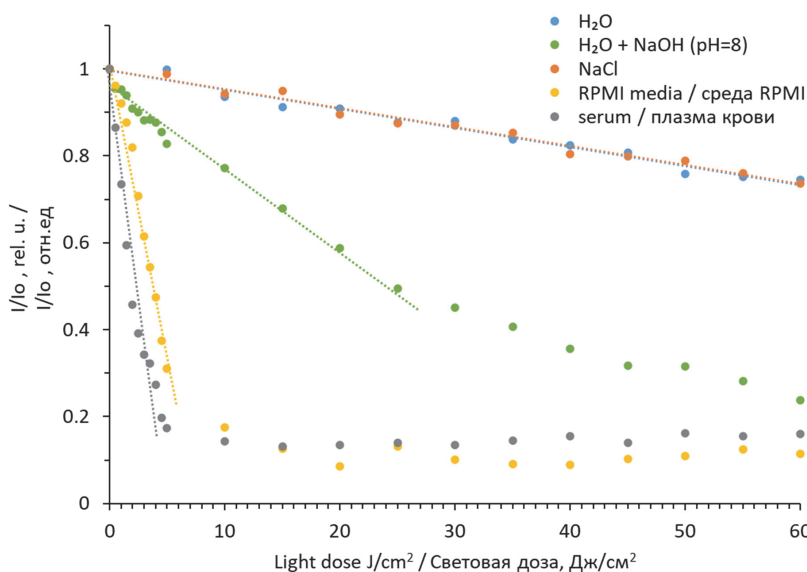


Рис. 7. Снижение интенсивности флуоресценции МС в зависимости от плотности дозы излучения за счет фотодеградации в различных средах. **Fig. 7.** Decrease of MB fluorescence intensity as a function of radiation dose density due to photodegradation in different media.

The photobleaching rate in physiological solution is the same as in water, and in the RPMI medium is the same as in serum, indicating that the ionic strength of the solution has no effect on the photobleaching rate.

The higher rate of photobleaching in plasma and culture media may be due to a more alkaline pH: according to the published data, the efficiency of MC singlet oxygen generation is 5 times higher at pH 9 than at pH 7 [51].

However, based on a comparison of the photobleaching rate of an aqueous solution with the addition of NaOH to pH 8, we can conclude that the change in pH is not the only reason for the increased photobleaching rate.

The photobleaching rate in plasma as well as in water [43] depends on concentration, and at high concentrations is slower, Fig. 8.

The obtained dependencies indirectly indicate that photobleaching in plasma occurs due to interaction with singlet oxygen; the rate of photobleaching is limited by the rate of oxygen diffusion in the medium.

To check the effect of interaction with plasma proteins on the spectroscopic properties of MB over time without laser exposure, the absorption spectrum of MB in plasma was recorded 30 minutes after preparation, and no change in the spectrum was observed. Absorption spectra recorded after photobleaching suggest that the photobleaching is caused by photodegradation of MB and is not related to the transition to the leucoform, Fig. 9.

Assessment of photodynamic activity and efficiency of singlet oxygen generation in vitro

The value of photodynamic activity determined by irreversible quenching of singlet oxygen which is

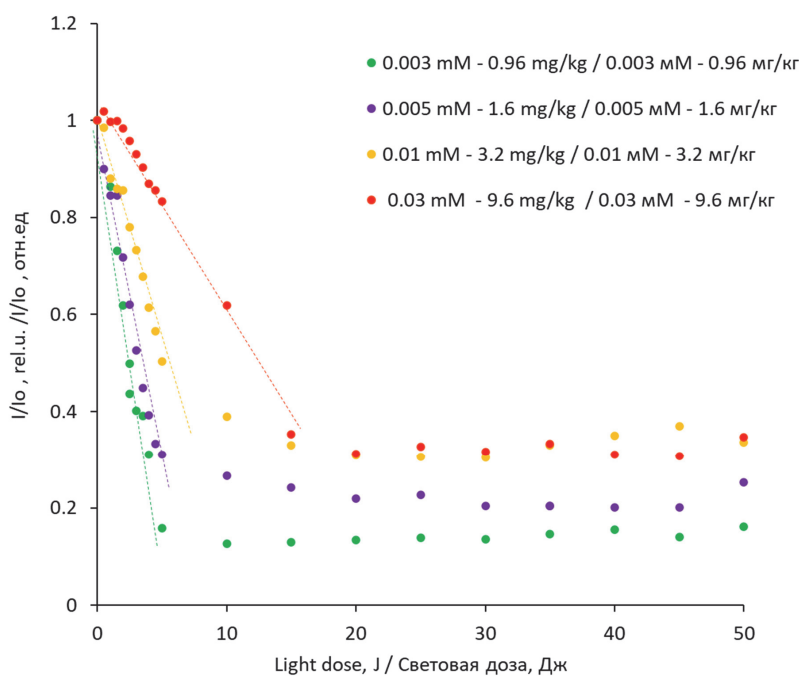


Рис. 8. Снижение интенсивности флуоресценции МС за счет фотодеградации в зависимости от плотности дозы излучения для различных концентраций МС в плазме.
Fig. 8. Decrease in MB fluorescence intensity due to photodegradation as a function of radiation dose density for different concentrations of MB in plasma.

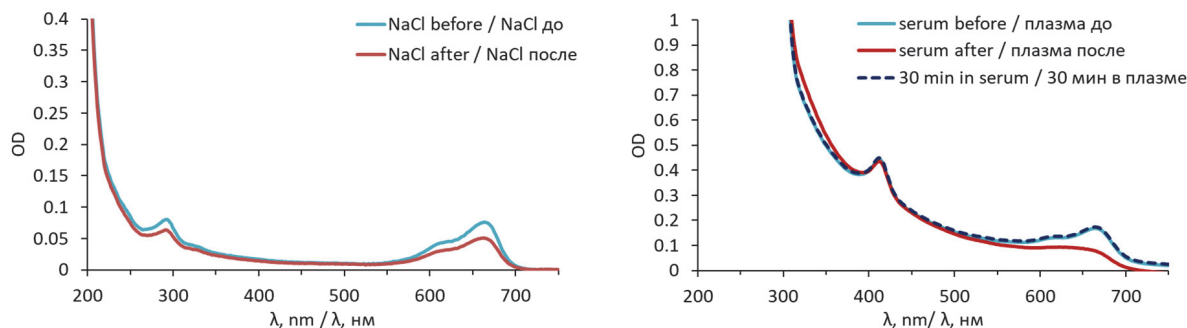


Рис. 9. Спектры поглощения МС до и после облучения в различных биологических средах.
Fig. 9. Absorption spectra of MB before and after irradiation in various biological media.

equivalent to the quantum yield of singlet oxygen generation for MB in the concentration range of 1-100 mg/kg relative to aluminum phthalocyanine ($\phi\Delta = 0.38$) was 0.0065 ± 0.0014 . In the investigated range of MB concentrations, the efficiency of singlet oxygen generation is rather low.

The measured quantum yield of singlet oxygen generation using the SOSG sensor in water demonstrated a similar value for the MB concentration of 10 mg/kg — $\phi\Delta$ 0.0028. Thus, it is shown that the photodynamic reaction *in vitro* in the presence of erythrocytes for MB proceeds according to type I, when not singlet oxygen but other reactive oxygen species are formed. We assume that this is caused by the positively charged MB binding

to negatively charged cell membranes, which leads to a change in the type of photodynamic reaction [36].

This is verified by the ROS generation test performed on the cell culture (Fig. 10).

After incubation with MB, cells show staining for ROS diffusely in the cytoplasm and brightly in some vesicles. After irradiation of cells with accumulated MB at 660 nm, 50 J/cm², the intensity of the ROS sensor in vesicles becomes brighter. In control cells without MB, the ROS sensor is not detected, even after irradiation.

The results on ROS generation and low quantum yield of singlet oxygen generation confirm the tendency of MB to shift from type II photosensitization mechanism (energy transfer to oxygen with formation of singlet

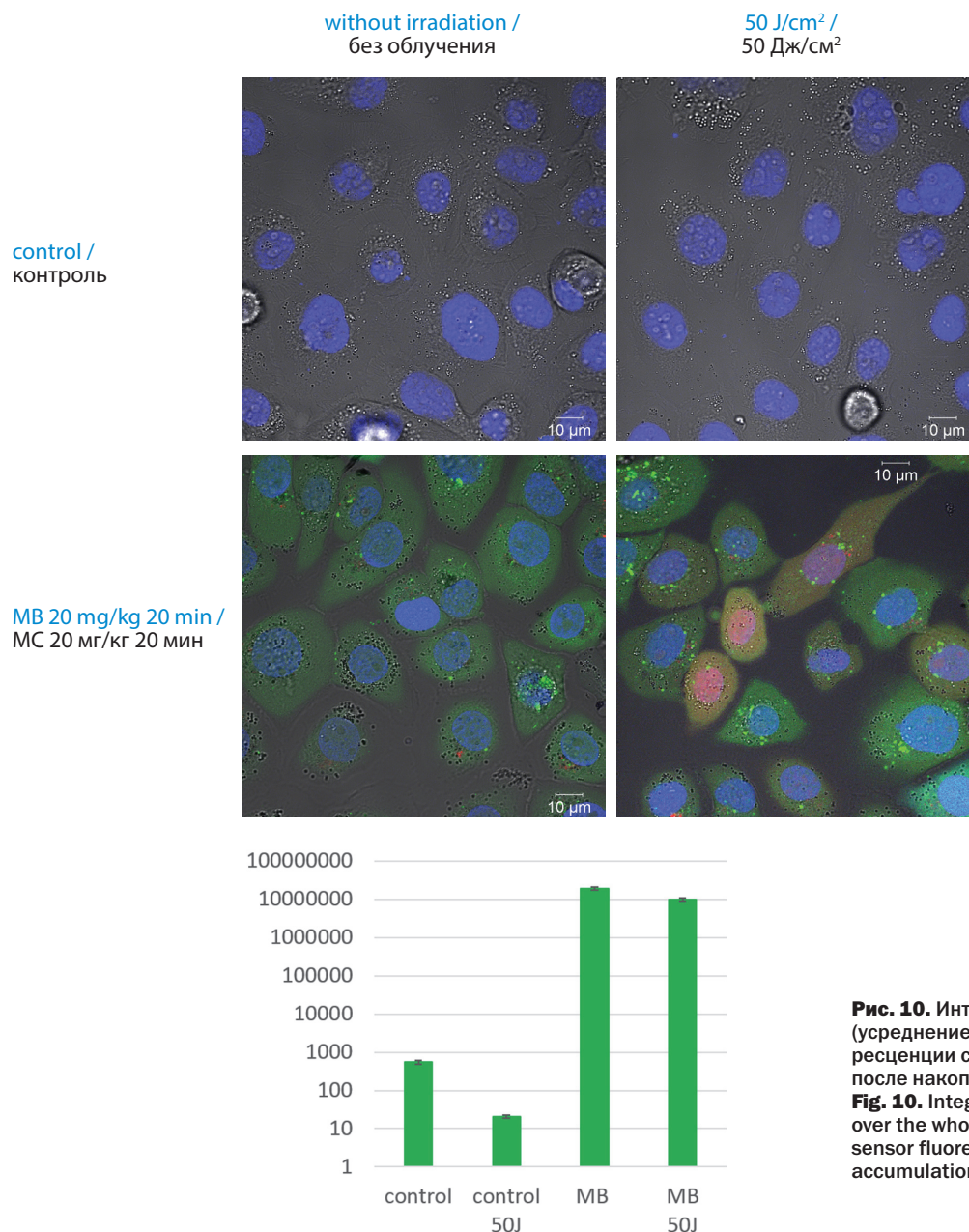


Рис. 10. Интегральная интенсивность (усреднение по всей картинке) флуоресценции сенсора на АФК в клетках после накопления МС и облучения.
Fig. 10. Integral intensity (averaging over the whole picture) of the ROS sensor fluorescence in cells after MB accumulation and irradiation.

oxygen) to type I mechanism (electron transfer with formation of MB⁺ semi-reduced and semi-oxidized radicals) [50].

Conclusion

Absorption and fluorescence spectra in water, saline, blood plasma and cell-culturing medium RPMI were measured for MB concentrations 0.001–0.05 mM, fluorescence lifetime was determined for different concentrations. The analysis of the spectrum shape indicates weak aggregation at concentrations above 0.01 mM (3.2 mg/kg), which manifests in the appearance of the MB dimer peak in the spectral region of 600–630 nm.

The obtained spectra of MB fluorescence in aqueous solutions show that at a concentration of 0.01 mM (3.2 mg/kg) there is a shift of the maximum to the long-wave region, indicating the presence of reabsorption and aggregation at higher concentrations. The shape of the spectrum in this case does not change. Comparison of MB fluorescence spectra recorded in various biological media shows that the most intense fluorescence is observed in saline and in water. The decrease of MB fluorescence intensity in the culture medium and in plasma may be due to both the interaction with plasma proteins and more alkaline pH. At the same time, the fluorescence intensity in culture medium is higher (pH 8) than in pure plasma (pH 9). The shape of the fluorescence spectrum does not change in the studied media. The analysis of integral fluorescence intensity dependence on MB concentration shows that in all the studied media it is non-linear, the linear section is observed up to the concentration of 0.01 mM for all the media, except for plasma, in which the deviation from linear dependence is observed up to 0.003 mM (presumably due to large number of dimers in plasma at low MB concentrations in comparison to water). At concentrations of 0.01–0.03 mM, the sublinear section of the dependence begins followed by saturation, which could be associated with reabsorption of excitation in solution as well as with small penetration depth of laser irradiation in solution.

A concentration-dependent MB fluorescence lifetime study was performed. No differences in the lifetime were observed for all studied concentrations, which may indicate that the aggregates formed at high concentrations of MB do not fluoresce.

Studies of photodegradation in biological media showed that more than 80% photobleaching in plasma and culture media is already observed at a dose of 5 J/cm², while in water at this concentration at a dose of 5 J/cm² there is no photobleaching yet, and at a dose of 50 J/cm² the photobleaching of MB is about 30%.

The photobleaching of MB under the effect of laser radiation was investigated. For lower concentrations of MB the photobleaching occurs more rapidly, which is presumably associated with a larger volume of irradiated area at low concentrations: at high concentrations of the drug most of the radiation is absorbed in a thin layer due to high optical density. The obtained relations indirectly indicate that photobleaching in plasma occurs due to interaction with singlet oxygen; the rate of photobleaching is limited by the diffusion rate of oxygen in the medium.

In media containing proteins with alkaline pH, photobleaching is significantly faster than in neutral aqueous media. The ionic strength of the solution has no effect on the photobleaching rate. The absorption spectra recorded after photobleaching suggest that the photobleaching is not due to the transition to the leucoform but is caused by the photodegradation of MB.

The efficiency of singlet oxygen generation and photodynamic activity were evaluated *in vitro*. In the investigated concentration range the efficiency of singlet oxygen generation is quite low. We assume that this is because the photodynamic reaction for MB proceeds according to type I, when not singlet oxygen is formed, but other reactive oxygen species. This is because the positively charged MB binds to negatively charged cell membranes, which leads to a change in the type of photodynamic reaction. It is demonstrated that in addition to the generation of singlet oxygen, the presence of other ROS in the cells is observed. After incubation with MB, cells show staining for ROS diffusely in the cytoplasm and brightly in some vesicles. After irradiation of cells with accumulated MB at 660 nm, 50 J/cm², the sensor intensity for ROS in vesicles becomes brighter. In control cells without MB the ROS sensor is not detected even after irradiation.

Acknowledgment

The study was funded by a grant from the Russian Science Foundation (project N 22-72-10117).

REFERENCES

1. Baptista M. S., Indig G. L. Effect of BSA Binding on Photophysical and Photochemical Properties of Triarylmethane Dyes. *The Journal of Physical Chemistry B*, 1998, Vol. 23 (102), pp. 4678-4688. doi: 10.1021/jp981185n.
2. Gabrielli D., Belisle E., Severino D., Kowaltowski A. J., Baptista M. S. Binding, Aggregation and Photochemical Properties of Methylene Blue in Mitochondrial Suspensions. *Photochemistry and Photobiology*, 2004, Vol. 3 (79), pp. 227. doi: 10.1562/BE-03-27.1.

ЛИТЕРАТУРА

1. Baptista M. S., Indig G. L. Effect of BSA Binding on Photophysical and Photochemical Properties of Triarylmethane Dyes // *The Journal of Physical Chemistry B*. – 1998. – Vol. 102(23). – P. 4678-4688. DOI: 10.1021/jp981185n.
2. Gabrielli D., Belisle E., Severino D., Kowaltowski A. J., Baptista M. S. Binding, Aggregation and Photochemical Properties of Methylene Blue in Mitochondrial Suspensions // *Photochemistry and Photobiology*. – 2004. – Vol. 79(3). – P. 227. DOI: 10.1562/BE-03-27.1.

3. Krasnovsky A. A. Photodynamic action and singlet oxygen. *Biophysics*, 2004, Vol. 2 (49). pp. 305-322.
4. Foote C. S. Mechanisms of Photosensitized Oxidation: There are several different types of photosensitized oxidation which may be important in biological systems. *Science*, 1968. Vol. 3857 (162), pp. 963-970. doi: 10.1126/science.162.3857.963.
5. Balzani V., Scandola F. Photochemical electron transfer reactions in homogeneous solution edited by J. S. Connolly. *New York: Academic Press*, 1983. pp. 97-130.
6. Crous A., Abrahamse H. Photodynamic therapy of lung cancer, where are we? *Frontiers in Pharmacology*, 2022, Vol.13. pp. 932098. doi: 10.3389/fphar.2022.932098.
7. Mfouo-Tynga I. S., Mouinga-Ondeme A. G. Photodynamic Therapy: A Prospective Therapeutic Approach for Viral Infections and Induced Neoplasia. *Pharmaceuticals*, 2022. Vol. 10 (15), pp. 1273. doi: 10.3390/ph15101273.
8. Reshetov I. V., Korenev S. V., Romanko Yu. S. Modern aspects of photodynamic therapy of basal cell skin cancer. *Biomedical Photonics*, 2022, Vol. 3 (11), pp. 35-39. doi: 10.24931/2413-9432-2022-11-3-35-39.
9. Panaseykin Y. A., Kapinus V. N., Filonenko E. V., Polkin V. V., Sevrukov F. E., Isaev P. A., Ivanov S. A., Kaprin A. D. Photodynamic therapy treatment of oral cavity cancer in patients with comorbidities. *Biomedical Photonics*, 2023, Vol. 4 (11), pp. 19-24. doi: 10.24931/2413-9432-2022-11-4-19-24.
10. Marr H. E., Stewart J. M., Chiu M. F. The crystal structure of methylene blue pentahydrate. *Acta Crystallographica Section B: Structural Crystallography and Crystal Chemistry*, 1973. Vol. 4 (29), pp. 847-853. doi: 10.1107/S0567740873003432.
11. Hamann C. H., Hamnett A., Vielstich W. *Electrochemistry / C. H. Hamann, A. Hamnett, W. Vielstich, 2nd ed. Weinheim: Wiley-VCH*, 2007, p. 531.
12. Lewis G. N., Goldschmid O., Magel T. T., Bigeleisen J. Dimeric and Other Forms of Methylene Blue: Absorption and Fluorescence of the Pure Monomer. *Journal of the American Chemical Society*, 1943, Vol. 6 (65), pp. 1150-1154. doi: 10.1021/ja01246a037.
13. Tacconi N. R. de, Carmona J., Rajeshwar K. Reversibility of Photoelectrochromism at the TiO₂/Methylene Blue Interface. *Journal of The Electrochemical Society*, 1997, Vol. 7 (144). pp. 2486. doi: 10.1149/1.1837841.
14. Wales D. J., Parker R. M., Gates J. C., Gressel M. C., Smith P. G. R. An integrated bragg grating oxygen sensor using a hydrophobic sol-gel layer doped with an organic dye Munich. *Germany: IEEE*, 2011, p. 1-1. doi: 10.1109/CLEOE.2011.5943057.
15. Sevcik P., Dunford H. B. Kinetics of the oxidation of NADH by methylene blue in a closed system. *The Journal of Physical Chemistry*, 1991, Vol. 6 (95), pp. 2411-2415. doi: 10.1021/j100159a054.
16. Engbersen J. F. J., Koudijs A., Van Der Plas H. C. Reaction of NADH models with methylene blue. *Recueil des Travaux Chimiques des Pays-Bas*, 2010, Vol. 5 (104), pp. 131-138. doi: 10.1002/recl.19851040503.
17. Schirmer R. H., Adler H., Pickhardt M., Mandelkow E. "Lest we forget you — methylene blue ...". *Neurobiology of Aging*, 2011, Vol. 12 (32), pp. 2325.e7-2325.e16. doi: 10.1016/j.neurobiolaging.2010.12.012.
18. Brooks M. M. The Mechanism of Methylene Blue Action on Blood. *Science*, 1934. Vol. 2062 (80), pp. 15-16. doi: 10.1126/science.80.2062.15.b.
19. Komlódi T., Tretter L. Methylene blue stimulates substrate-level phosphorylation catalysed by succinyl-CoA ligase in the citric acid cycle. *Neuropharmacology*, 2017, Vol. 123, pp. 287-298. doi: 10.1016/j.neuropharm.2017.05.009.
20. Herman M. I., Chyka P. A., Butler A. Y., Rieger S. E. Methylene blue by intraosseous infusion for methemoglobinemia. *Annals of Emergency Medicine*, 1999, Vol. 1 (33), pp. 111-113. doi: 10.1016/s0196-0644(99)70427-0.
21. Boylston M., Beer D. Methemoglobinemia: A Case Study. *Critical Care Nurse*, 2002, Vol. 4 (22), pp. 50-55. doi: 10.4037/ccn2002.22.4.50.
22. Wendel W. B. The Control of Methemoglobinemia with Methylene Blue. *Journal of Clinical Investigation*, 1939, Vol. 2 (18). pp. 179-185. doi: 10.1172/JCI101033.
3. Красновский А. А. Фотодинамическое действие и синглетный кислород // *Биофизика*. – 2004. – Т. 49, №2. – P. 305-322.
4. Foote C. S. Mechanisms of Photosensitized Oxidation: There are several different types of photosensitized oxidation which may be important in biological systems // *Science*. – 1968. – Vol. 162(3857). – P. 963-970. DOI: 10.1126/science.162.3857.963.
5. Balzani V., Scandola F. Photochemical electron transfer reactions in homogeneous solution под ред. J. S. Connolly // *New York: Academic Press*. – 1983. – P. 97-130.
6. Crous A., Abrahamse H. Photodynamic therapy of lung cancer, where are we? // *Frontiers in Pharmacology*. – 2022. – Vol. 13. – P. 932098. DOI: 10.3389/fphar.2022.932098.
7. Mfouo-Tynga I. S., Mouinga-Ondeme A. G. Photodynamic Therapy: A Prospective Therapeutic Approach for Viral Infections and Induced Neoplasia. // *Pharmaceuticals*. – 2022. – Vol. 15 (№10). – P. 1273. DOI: 10.3390/ph15101273.
8. Reshetov I. V., Korenev S. V., Romanko Yu. S. Modern aspects of photodynamic therapy of basal cell skin cancer. // *Biomedical Photonics*. – 2022. – Vol. 11 (№3). – P. 35-39. DOI: 10.24931/2413-9432-2022-11-3-35-39.
9. Panaseykin Y. A., Kapinus V. N., Filonenko E. V., Polkin V. V., Sevrukov F. E., Isaev P. A., Ivanov S. A., Kaprin A. D. Photodynamic therapy treatment of oral cavity cancer in patients with comorbidities // *Biomedical Photonics*. – 2023. – Vol. 11(4). – P. 19-24. DOI: 10.24931/2413-9432-2022-11-4-19-24.
10. Marr H. E., Stewart J. M., Chiu M. F. The crystal structure of methylene blue pentahydrate // *Acta Crystallographica Section B: Structural Crystallography and Crystal Chemistry*. – 1973. – Vol. 29(4). – P. 847-853. DOI: 10.1107/S0567740873003432.
11. Hamann C. H., Hamnett A., Vielstich W. *Electrochemistry / C. H. Hamann, A. Hamnett, W. Vielstich, 2-е изд., Weinheim: Wiley-VCH*, 2007. – P.531.
12. Lewis G. N., Goldschmid O., Magel T. T., Bigeleisen J. Dimeric and Other Forms of Methylene Blue: Absorption and Fluorescence of the Pure Monomer // *Journal of the American Chemical Society*. – 1943. – Vol. 65(6). – P. 1150-1154. DOI: 10.1021/ja01246a037.
13. Tacconi N. R. de, Carmona J., Rajeshwar K. Reversibility of Photoelectrochromism at the TiO₂/Methylene Blue Interface // *Journal of The Electrochemical Society*. – 1997. – Vol. 144(7). – P. 2486. DOI: 10.1149/1.1837841.
14. Wales D. J., Parker R. M., Gates J. C., Gressel M. C., Smith P. G. R. An integrated bragg grating oxygen sensor using a hydrophobic sol-gel layer doped with an organic dye Munich, Germany: *IEEE*. – 2011. – P. 1-1. DOI: 10.1109/CLEOE.2011.5943057.
15. Sevcik P., Dunford H. B. Kinetics of the oxidation of NADH by methylene blue in a closed system // *The Journal of Physical Chemistry*. – 1991. – Vol. 95(6). – P. 2411-2415. DOI: 10.1021/j100159a054.
16. Engbersen J. F. J., Koudijs A., Van Der Plas H. C. Reaction of NADH models with methylene blue // *Recueil des Travaux Chimiques des Pays-Bas*. – 2010. – Vol. 104(5). – P. 131-138. DOI: 10.1002/recl.19851040503.
17. Schirmer R. H., Adler H., Pickhardt M., Mandelkow E. "Lest we forget you — methylene blue ...". // *Neurobiology of Aging*. – 2011. – Vol. 32(12). – P. 2325.e7-2325.e16. DOI: 10.1016/j.neurobiolaging.2010.12.012.
18. Brooks M. M. The Mechanism of Methylene Blue Action on Blood. // *Science*. – 1934. – Vol. 80(2062). – P. 15-16. DOI: 10.1126/science.80.2062.15.b.
19. Komlódi T., Tretter L. Methylene blue stimulates substrate-level phosphorylation catalysed by succinyl-CoA ligase in the citric acid cycle // *Neuropharmacology*. – 2017. – Vol. 123. – P. 287-298. DOI: 10.1016/j.neuropharm.2017.05.009.
20. Herman M. I., Chyka P. A., Butler A. Y., Rieger S. E. Methylene blue by intraosseous infusion for methemoglobinemia // *Annals of Emergency Medicine*. – 1999. – Vol. 33(1). – P. 111-113. DOI: 10.1016/s0196-0644(99)70427-0.
21. Boylston M., Beer D. Methemoglobinemia: A Case Study. // *Critical Care Nurse*. – 2002. – Vol. 22(4). – P. 50-55. DOI: 10.4037/ccn2002.22.4.50.
22. Wendel W. B. The Control of Methemoglobinemia with Methylene Blue // *Journal of Clinical Investigation*. – 1939. – Vol. 18(2). – P. 179-185. DOI: 10.1172/JCI101033.

23. Tepaev R. F., Vishnevskiy V. A., Kuzin S. A., Sergey I. V., Gordeeva O. B., Pytal A. V., Murashkin N. N. Benzocaine-Induced Methemoglobinemia. A Clinical Case. *Pediatric pharmacology*, 2018, Vol. 5 (15), pp. 396-401. doi: 10.15690/pf.v15i5.1962.
24. Preiser J.-C., Lejeune P., Roman A., Carlier E., De Backer D., Leeman M., Kahn R. J., Vincent J.-L. Methylene blue administration in septic shock: A clinical trial. *Critical Care Medicine*, 1995, Vol. 2 (23), pp. 259-264. doi: 10.1097/00003246-199502000-00010.
25. Zhang H., Rogiers P., Preiser J.-C., Spapen H., Manikis P., Metz G., Vincent J.-L. Effects of methylene blue on oxygen availability and regional blood flow during endotoxic shock. *Critical Care Medicine*, 1995, Vol. 10 (23), pp. 1711-1721. doi: 10.1097/00003246-199510000-00016.
26. Tranquada R. E., Bernstein S., Grant W. J. Intravenous Methylene Blue in The Therapy of Lactic Acidosis. *Archives of Internal Medicine*, 1964, Vol. 1 (114), pp. 13-25. doi: 10.1001/archinte.1964.03860070059003.
27. Bell M. A. Methylene Blue in Carbon Monoxide Poisoning. *JAMA: The Journal of the American Medical Association*, 1933, Vol. 18 (100), pp. 1402. doi: 10.1001/jama.1933.27420180002007b.
28. Wendel W. B. The Mechanism of the Antidotal Action of Methylene Blue in Cyanide Poisoning. *Science*, 1934, Vol. 2078 (80), pp. 381-382. doi: 10.1126/science.80.2078.381.
29. Chen K. K. Nitrite and Thiosulfate Therapy in Cyanide Poisoning. *Journal of the American Medical Association*, 1952, Vol. 2 (149), pp. 113. doi: 10.1001/jama.1952.02930190015004.
30. Barron E. S. G. The Catalytic Effect of Methylene Blue on the Oxygen Consumption of Tumors and Normal Tissues. *Journal of Experimental Medicine*, 1930, Vol. 3 (52), pp. 447-456. doi: 10.1084/jem.52.3.447.
31. Park J., Mroz P., Hamblin M. R., Yaroslavsky A. N. Dye-enhanced multimodal confocal microscopy for noninvasive detection of skin cancers in mouse models. *Journal of Biomedical Optics*, 2010, Vol. 2 (15), pp. 026023. doi: 10.1117/1.3394301.
32. Wainwright M., Crossley K. B. Methylene Blue – a Therapeutic Dye for All Seasons? *Journal of Chemotherapy*, 2002, Vol. 5 (14), pp. 431-443. doi: 10.1179/joc.2002.14.5.431.
33. Orth K., Russ D., Beck G., Rück A., Beger H. G. Photochemotherapy of experimental colonic tumours with intra-tumorally applied methylene blue. *Langenbeck's Archives of Surgery*, 1998, Vol. 34 (383), pp. 276-281. doi: 10.1007/s004230050132.
34. König K., Bockhorn V., Dietel W., Schubert H. Photochemotherapy of animal tumors with the photosensitizer Methylene Blue using a krypton laser. *Journal of Cancer Research and Clinical Oncology*, 1987, Vol. 3 (113), pp. 301-303. doi: 10.1007/BF00396390.
35. Tardivo J. P., Del Giglio A., Paschoal L. H. C., Ito A. S., Baptista M. S. Treatment of melanoma lesions using methylene blue and RL50 light source. *Photodiagnosis and Photodynamic Therapy*, 2004, Vol. 4 (1), pp. 345-346. doi: 10.1016/S1572-1000(05)00005-0.
36. Tardivo J. P., Del Giglio A., De Oliveira C. S., Gabrielli D. S., Junqueira H. C., Tada D. B., Severino D., De Fátima Turchiello R., Baptista M. S. Methylene blue in photodynamic therapy: From basic mechanisms to clinical applications. *Photodiagnosis and Photodynamic Therapy*, 2005, Vol. 3 (2), pp. 175-191. doi: 10.1016/S1572-1000(05)00097-9.
37. Wainwright M. Methylene blue derivatives – suitable photoantimicrobials for blood product disinfection? *International Journal of Antimicrobial Agents*, 2000, Vol. 4 (16), pp. 381-394. doi: 10.1016/S0924-8579(00)00207-7.
38. Wagner S. J. Virus inactivation in blood components by photoactive phenothiazine dyes. *Transfusion Medicine Reviews*, 2002, Vol. 1 (16), pp. 61-66. doi: 10.1053/tmrv.2002.29405.
39. Calderón M., Weitzel T., Rodriguez M. F., Ciapponi A. Methylene blue for treating malaria. *Cochrane Database of Systematic Reviews*, 2017, Vol. 6 (2022). doi: 10.1002/14651858.CD012837.
40. Dewitt L. M. Preliminary Report of Experiments in the Vital Staining of Tubercles: Studies on the Biochemistry and Chemotherapy of Tuberculosis. IV. *Journal of Infectious Diseases*, 1913, Vol. 1 (12), pp. 68-92. doi: 10.1093/infdis/12.1.68.
41. Wainwright M., Phoenix D. A., Laycock S. L., Wareing D. R. A., Wright P. A. Photobactericidal activity of phenothiazinium dyes against methicillin-resistant strains of *Staphylococcus aureus*. *FEMS Microbiology Letters*, 1998, Vol. 2 (160), pp. 177-181. doi: 10.1111/j.1574-6968.1998.tb12908.x.
23. Tepaev R. F., Vishnevskiy V. A., Kuzin S. A., Sergey I. V., Gordeeva O. B., Pytal A. V., Murashkin N. N. Benzocaine-Induced Methemoglobinemia. A Clinical Case // *Pediatric pharmacology*. – 2018. – Vol. 5(5). – P. 396-401. DOI: 10.15690/pf.v15i5.1962.
24. Preiser J.-C., Lejeune P., Roman A., Carlier E., De Backer D., Leeman M., Kahn R. J., Vincent J.-L. Methylene blue administration in septic shock: A clinical trial // *Critical Care Medicine*. – 1995. – Vol. 23(2). – P. 259-264. DOI: 10.1097/00003246-199502000-00010.
25. Zhang H., Rogiers P., Preiser J.-C., Spapen H., Manikis P., Metz G., Vincent J.-L. Effects of methylene blue on oxygen availability and regional blood flow during endotoxic shock: // *Critical Care Medicine*. – 1995. – Vol. 23(10). – P. 1711-1721. DOI: 10.1097/00003246-199510000-00016.
26. Tranquada R. E., Bernstein S., Grant W. J. Intravenous Methylene Blue in The Therapy of Lactic Acidosis. // *Archives of Internal Medicine*. – 1964. – Vol. 114(1). – P. 13-25. DOI: 10.1001/archinte.1964.03860070059003.
27. Bell M. A. Methylene Blue in Carbon Monoxide Poisoning. // *JAMA: The Journal of the American Medical Association*. – 1933. – Vol. 100(18). – P. 1402. DOI: 10.1001/jama.1933.27420180002007b.
28. Wendel W. B. The Mechanism of the Antidotal Action of Methylene Blue in Cyanide Poisoning. // *Science*. – 1934. – Vol. 80(2078). – P. 381-382. DOI: 10.1126/science.80.2078.381.
29. Chen K. K. Nitrite and Thiosulfate Therapy in Cyanide Poisoning. // *Journal of the American Medical Association*. – 1952. – Vol. 149(2). – P. 113. DOI: 10.1001/jama.1952.02930190015004.
30. Barron E. S. G. The Catalytic Effect of Methylene Blue on the Oxygen Consumption of Tumors and Normal Tissues. // *Journal of Experimental Medicine*. – 1930. – Vol. 52(3). – P. 447-456. DOI: 10.1084/jem.52.3.447.
31. Park J., Mroz P., Hamblin M. R., Yaroslavsky A. N. Dye-enhanced multimodal confocal microscopy for noninvasive detection of skin cancers in mouse models // *Journal of Biomedical Optics*. – 2010. – Vol. 15(2). – P. 026023. DOI: 10.1117/1.3394301.
32. Wainwright M., Crossley K. B. Methylene Blue – a Therapeutic Dye for All Seasons? // *Journal of Chemotherapy*. – 2002. – Vol. 14(5). – P. 431-443. DOI: 10.1179/joc.2002.14.5.431.
33. Orth K., Russ D., Beck G., Rück A., Beger H. G. Photochemotherapy of experimental colonic tumours with intra-tumorally applied methylene blue. // *Langenbeck's Archives of Surgery*. – 1998. – Vol. 383(3-4). – P. 276-281. DOI: 10.1007/s004230050132.
34. König K., Bockhorn V., Dietel W., Schubert H. Photochemotherapy of animal tumors with the photosensitizer Methylene Blue using a krypton laser. // *Journal of Cancer Research and Clinical Oncology*. – 1987. – Vol. 113(3). – P. 301-303. DOI: 10.1007/BF00396390.
35. Tardivo J. P., Del Giglio A., Paschoal L. H. C., Ito A. S., Baptista M. S. Treatment of melanoma lesions using methylene blue and RL50 light source. // *Photodiagnosis and Photodynamic Therapy*. – 2004. – Vol. 1(4). – P. 345-346. DOI: 10.1016/S1572-1000(05)00005-0.
36. Tardivo J. P., Del Giglio A., De Oliveira C. S., Gabrielli D. S., Junqueira H. C., Tada D. B., Severino D., De Fátima Turchiello R., Baptista M. S. Methylene blue in photodynamic therapy: From basic mechanisms to clinical applications // *Photodiagnosis and Photodynamic Therapy*. – 2005. – Vol. 2(3). – P. 175-191. DOI: 10.1016/S1572-1000(05)00097-9.
37. Wainwright M. Methylene blue derivatives – suitable photoantimicrobials for blood product disinfection? // *International Journal of Antimicrobial Agents*. – 2000. – Vol. 16(4). – P. 381-394. DOI: 10.1016/S0924-8579(00)00207-7.
38. Wagner S. J. Virus inactivation in blood components by photoactive phenothiazine dyes // *Transfusion Medicine Reviews*. – 2002. – Vol. 16(1). – P. 61-66. DOI: 10.1053/tmrv.2002.29405.
39. Calderón M., Weitzel T., Rodriguez M. F., Ciapponi A. Methylene blue for treating malaria // *Cochrane Database of Systematic Reviews*. – 2017. – Vol. 2022(6). DOI: 10.1002/14651858.CD012837.
40. Dewitt L. M. Preliminary Report of Experiments in the Vital Staining of Tubercles: Studies on the Biochemistry and Chemotherapy of Tuberculosis. IV // *Journal of Infectious Diseases*. – 1913. – Vol. 12(1). – P. 68-92. DOI: 10.1093/infdis/12.1.68.
41. Wainwright M., Phoenix D. A., Laycock S. L., Wareing D. R. A., Wright P. A. Photobactericidal activity of phenothiazinium dyes against methicillin-resistant strains of *Staphylococcus aureus* // *FEMS Microbiology Letters*. – 1998. – Vol. 160(2). – P. 177-181. DOI: 10.1111/j.1574-6968.1998.tb12908.x.

42. Pascual A., Henry M., Briolant S., Charras S., Baret E., Amalvict R., Huyghues Des Etages E., Feraud M., Rogier C., Pradines B. *In Vitro* Activity of Proeveblue (Methylene Blue) on Plasmodium falciparum Strains Resistant to Standard Antimalarial Drugs. *Antimicrobial Agents and Chemotherapy*, 2011, Vol. 5 (55), pp. 2472-2474. doi: 10.1128/AAC.01466-10.
43. Tiganova I. G., Meerovich G. A., Zulufova I. D., Akhlyustina E. V., Ovchinnikov R. S., Solovyev A. I., Romanishkin I. D., Kozlikina E. I., Nekhoroshev A. V., Glechik D. A., Parshin A. V., Parshin V. D., Romanova Y. M., Loschenov V. B. On the possibility of photodynamic inactivation of tracheobronchial tree pathogenic microbiota using methylene blue (in vitro study). *Photodiagnosis and Photodynamic Therapy*, 2022, Vol. 38, pp. 102753. doi: 10.1016/j.pdpdt.2022.102753.
44. Shen X., Dong L., He X., Zhao C., Zhang W., Li X., Lu Y. Treatment of infected wounds with methylene blue photodynamic therapy: An effective and safe treatment method. *Photodiagnosis and Photodynamic Therapy*, 2020, Vol. 32, pp. 102051. doi: 10.1016/j.pdpdt.2020.102051.
45. Severino D., Junqueira H. C., Gugliotti M., Gabrielli D. S., Baptista M. S. Influence of Negatively Charged Interfaces on the Ground and Excited State Properties of Methylene Blue. *Photochemistry and Photobiology*, 2003, Vol. 5 (77), pp. 459-468. doi: 10.1562/0031-8655(2003)0770459IONCIO2.0.CO2.
46. Murov S. L., Hug G. L., Carmichael I. Handbook of photochemistry / S. L. Murov, G. L. Hug, I. Carmichael, 2 ed. New York: M. Dekker, 1993, p. 420.
47. Wang W., Zhang W., Sun H., Du Q., Bai J., Ge X., Li C. Enhanced photodynamic efficiency of methylene blue with controlled aggregation state in silica-methylene blue-acetate@tannic acid-iron(III) ions complexes. *Dyes and Pigments*, 2019, Vol. 160, pp. 663-670. doi: 10.1016/j.dyepig.2018.08.068.
48. Dean J. C., Oblinsky D. G., Rafiq S., Scholes G. D. Methylene Blue Exciton States Steer Nonradiative Relaxation: Ultrafast Spectroscopy of Methylene Blue Dimer. *The Journal of Physical Chemistry B*, 2016, Vol. 3 (120), pp. 440-454. doi: 10.1021/acs.jpcc.5b11847.
49. Coronel A., Catalán-Toledo J., Fernández-Jaramillo H., Godoy-Martínez P., Flores M. E., Moreno-Villoslada I. Photodynamic action of methylene blue subjected to aromatic-aromatic interactions with poly(sodium 4-styrenesulfonate) in solution and supported in solid, highly porous alginate sponges. *Dyes and Pigments*, 2017, Vol. 147, pp. 455-464. doi: 10.1016/j.dyepig.2017.08.042.
50. Junqueira H. C., Severino D., Dias L. G., Gugliotti M. S., Baptista M. S. Modulation of methylene blue photochemical properties based on adsorption at aqueous micelle interfaces. *Physical Chemistry Chemical Physics*, 2002, Vol. 11 (4), pp. 2320-2328. doi: 10.1039/b109753a.
51. Bonneau R., Pottier R., Bagno O., Jousset-Dubien J. pH Dependence of Singlet Oxygen Production in Aqueous Solutions Using Thiazine Dyes as Photosensitizers. *Photochemistry and Photobiology*, 1975, Vol. 3 (21), pp. 159-163. doi: 10.1111/j.1751-1097.1975.tb06646.x.
52. Patil K., Pawar R., Talap P. Self-aggregation of Methylene Blue in aqueous medium and aqueous solutions of Bu4NBr and urea. *Physical Chemistry Chemical Physics*, 2000, Vol. 19 (2), pp. 4313-4317. doi: 10.1039/b005370h.
53. Zhao Z., Malinowski E. R. Determination of the Hydration of Methylene Blue Aggregates and Their Dissociation Constants Using Visible Spectroscopy. *Applied Spectroscopy*, 1999, Vol. 12 (53), pp. 1567-1574. doi: 10.1366/0003702991946028.
54. Moreno-Villoslada I., Torres C., González F., Shibue T., Nishide H. Binding of Methylene Blue to Polyelectrolytes Containing Sulfonate Groups: Binding of Methylene Blue to Polyelectrolytes Containing ... *Macromolecular Chemistry and Physics*, 2009, Vol. 13-14 (210), pp. 1167-1175. doi: 10.1002/macp.200900042.
55. Moreno-Villoslada I., Torres-Gallegos C., Araya-Hermosilla R., Nishide H. Influence of the Linear Aromatic Density on Methylene Blue Aggregation around Polyanions Containing Sulfonate Groups. *The Journal of Physical Chemistry B*, 2010, Vol. 12 (114), pp. 4151-4158. doi: 10.1021/jp909105r.
56. Aznar A. J., Casal B., Ruiz-Hitzky E., Lopez-Arbeloa I., Lopez-Arbeloa F., Santaren J., Alvarez A. Adsorption of methylene blue on sepiolite gels: spectroscopic and rheological studies.
42. Pascual A., Henry M., Briolant S., Charras S., Baret E., Amalvict R., Huyghues Des Etages E., Feraud M., Rogier C., Pradines B. *In Vitro* Activity of Proeveblue (Methylene Blue) on Plasmodium falciparum Strains Resistant to Standard Antimalarial Drugs // *Antimicrobial Agents and Chemotherapy*. – 2011. – Vol. 55(5). – P. 2472-2474. DOI: 10.1128/AAC.01466-10.
43. Tiganova I. G., Meerovich G. A., Zulufova I. D., Akhlyustina E. V., Ovchinnikov R. S., Solovyev A. I., Romanishkin I. D., Kozlikina E. I., Nekhoroshev A. V., Glechik D. A., Parshin A. V., Parshin V. D., Romanova Y. M., Loschenov V. B. On the possibility of photodynamic inactivation of tracheobronchial tree pathogenic microbiota using methylene blue (in vitro study) // *Photodiagnosis and Photodynamic Therapy*. – 2022. – Vol. 38. – P. 102753. DOI: 10.1016/j.pdpdt.2022.102753.
44. Shen X., Dong L., He X., Zhao C., Zhang W., Li X., Lu Y. Treatment of infected wounds with methylene blue photodynamic therapy: An effective and safe treatment method // *Photodiagnosis and Photodynamic Therapy*. – 2020. – Vol. 32. – P. 102051. DOI: 10.1016/j.pdpdt.2020.102051.
45. Severino D., Junqueira H. C., Gugliotti M., Gabrielli D. S., Baptista M. S. Influence of Negatively Charged Interfaces on the Ground and Excited State Properties of Methylene Blue. // *Photochemistry and Photobiology*. – 2003. – Vol. 77(5). – P. 459-468. DOI: 10.1562/0031-8655(2003)0770459IONCIO2.0.CO2.
46. Murov S. L., Hug G. L., Carmichael I. Handbook of photochemistry / S. L. Murov, G. L. Hug, I. Carmichael, 2-e изд., New York: M. Dekker. – 1993. – P. 420.
47. Wang W., Zhang W., Sun H., Du Q., Bai J., Ge X., Li C. Enhanced photodynamic efficiency of methylene blue with controlled aggregation state in silica-methylene blue-acetate@tannic acid-iron(III) ions complexes // *Dyes and Pigments*. – 2019. – Vol. 160. – P. 663-670. DOI: 10.1016/j.dyepig.2018.08.068.
48. Dean J. C., Oblinsky D. G., Rafiq S., Scholes G. D. Methylene Blue Exciton States Steer Nonradiative Relaxation: Ultrafast Spectroscopy of Methylene Blue Dimer. // *The Journal of Physical Chemistry B*. – 2016. – Vol. 120(3). – P. 440-454. DOI: 10.1021/acs.jpcc.5b11847.
49. Coronel A., Catalán-Toledo J., Fernández-Jaramillo H., Godoy-Martínez P., Flores M. E., Moreno-Villoslada I. Photodynamic action of methylene blue subjected to aromatic-aromatic interactions with poly(sodium 4-styrenesulfonate) in solution and supported in solid, highly porous alginate sponges. // *Dyes and Pigments*. – 2017. – Vol. 147. – P. 455-464. DOI: 10.1016/j.dyepig.2017.08.042.
50. Junqueira H. C., Severino D., Dias L. G., Gugliotti M. S., Baptista M. S. Modulation of methylene blue photochemical properties based on adsorption at aqueous micelle interfaces. // *Physical Chemistry Chemical Physics*. – 2002. – Vol. 4(11). – P. 2320-2328. DOI: 10.1039/b109753a.
51. Bonneau R., Pottier R., Bagno O., Jousset-Dubien J. pH Dependence of Singlet Oxygen Production in Aqueous Solutions Using Thiazine Dyes as Photosensitizers. // *Photochemistry and Photobiology*. – 1975. – Vol. 21(3). – P. 159-163. DOI: 10.1111/j.1751-1097.1975.tb06646.x.
52. Patil K., Pawar R., Talap P. Self-aggregation of Methylene Blue in aqueous medium and aqueous solutions of Bu4NBr and urea. // *Physical Chemistry Chemical Physics*. – 2000. – Vol. 2(19). – P. 4313-4317. DOI: 10.1039/b005370h.
53. Zhao Z., Malinowski E. R. Determination of the Hydration of Methylene Blue Aggregates and Their Dissociation Constants Using Visible Spectroscopy. // *Applied Spectroscopy*. – 1999. – Vol. 53(12). – P. 1567-1574. DOI: 10.1366/0003702991946028.
54. Moreno-Villoslada I., Torres C., González F., Shibue T., Nishide H. Binding of Methylene Blue to Polyelectrolytes Containing Sulfonate Groups: Binding of Methylene Blue to Polyelectrolytes Containing // *Macromolecular Chemistry and Physics*. – 2009. – Vol. 210(13-14). – P. 1167-1175. DOI: 10.1002/macp.200900042.
55. Moreno-Villoslada I., Torres-Gallegos C., Araya-Hermosilla R., Nishide H. Influence of the Linear Aromatic Density on Methylene Blue Aggregation around Polyanions Containing Sulfonate Groups. // *The Journal of Physical Chemistry B*. – 2010. – Vol. 114(12). – P. 4151-4158. DOI: 10.1021/jp909105r.
56. Aznar A. J., Casal B., Ruiz-Hitzky E., Lopez-Arbeloa I., Lopez-Arbeloa F., Santaren J., Alvarez A. Adsorption of methylene blue on sepiolite gels: spectroscopic and rheological studies.

- Clay Minerals*, 1992, Vol. 1 (27), pp. 101-108. doi: 10.1180/claymin.1992.027.1.10.
57. Bergmann K., O'Konski C. T. A Spectroscopic Study of Methylene Blue Monomer, Dimer, and Complexes with Montmorillonite. *The Journal of Physical Chemistry*, 1963, Vol. 10 (67), pp. 2169-2177. doi: 10.1021/j100804a048.
58. Lemin D. R., Vickerstaff T. The aggregation of direct dyes and of Methylene Blue 2B in aqueous solution. *Transactions of the Faraday Society*, 1947, Vol. 0 (43), pp. 491-502. doi: 10.1039/TF9474300491.
59. Heger D., Jirkovský J., Klán P. Aggregation of Methylene Blue in Frozen Aqueous Solutions Studied by Absorption Spectroscopy. *The Journal of Physical Chemistry A*, 2005, Vol. 30 (109), pp. 6702-6709. doi: 10.1021/jp050439j.
60. Braswell E. Evidence for trimerization in aqueous solutions of methylene blue. *The Journal of Physical Chemistry*, 1968, Vol. 7 (72), pp. 2477-2483. doi: 10.1021/j100853a035.
61. Klika Z., Čapková P., Horáková P., Valášková M., Malý P., Macháň R., Pospíšil M. Composition, structure, and luminescence of montmorillonites saturated with different aggregates of methylene blue. *Journal of Colloid and Interface Science*, 2007, Vol. 1 (311), pp. 14-23. doi: 10.1016/j.jcis.2007.02.034.
62. Zhikhoreva A. A., Belashov A. V., Serebryakov E. B., Semenova I. V., Vasyutinskii O. S. Photophysical properties of methylene blue in aqueous solution sprayed onto biological surfaces. *Dyes and Pigments*, 2022, Vol. 208, pp. 110789. doi: 10.1016/j.dyepig.2022.110789.
63. Walter-Sack I., Rengelshausen J., Oberwittler H., Burhenne J., Mueller O., Meissner P., Mikus G. High absolute bioavailability of methylene blue given as an aqueous oral formulation. *European Journal of Clinical Pharmacology*, 2009, Vol. 2 (65), pp. 179-189. doi: 10.1007/s00228-008-0563-x.
64. Peter C., Hongwan D., Küpfer A., Lauterburg B. H. Pharmacokinetics and organ distribution of intravenous and oral methylene blue. *European Journal of Clinical Pharmacology*, 2000, Vol. 3 (56), pp. 247-250. doi: 10.1007/s002280000124.
65. Ryabova A. V., Stratonnikov A. A., Loshchenov V. B. Laser spectroscopy technique for estimating the efficiency of photosensitisers in biological media. *Quantum Electronics*, 2006, Vol. 6 (36), pp. 562-568. doi: 10.1070/QE2006v036n06ABEH013291.
66. Redmond R. W., Gamlin J. N. A Compilation of Singlet Oxygen Yields from Biologically Relevant Molecules. *Photochemistry and Photobiology*, 1999, Vol. 4 (70), pp. 391-475. doi: 10.1111/j.1751-1097.1999.tb08240.x.
- // *Clay Minerals*. – 1992. – Vol. 27(1). – P. 101-108. DOI: 10.1180/claymin.1992.027.1.10.
57. Bergmann K., O'Konski C. T. A Spectroscopic Study of Methylene Blue Monomer, Dimer, and Complexes with Montmorillonite. // *The Journal of Physical Chemistry*. – 1963. – Vol. 67(10). – P. 2169-2177. DOI: 10.1021/j100804a048.
58. Lemin D. R., Vickerstaff T. The aggregation of direct dyes and of Methylene Blue 2B in aqueous solution. // *Transactions of the Faraday Society*. – 1947. – Vol. 43. – №0. – P. 491-502. DOI: 10.1039/TF9474300491.
59. Heger D., Jirkovský J., Klán P. Aggregation of Methylene Blue in Frozen Aqueous Solutions Studied by Absorption Spectroscopy. // *The Journal of Physical Chemistry A*. – 2005. – Vol. 109(30). – P. 6702-6709. DOI: 10.1021/jp050439j.
60. Braswell E. Evidence for trimerization in aqueous solutions of methylene blue. // *The Journal of Physical Chemistry*. – 1968. – Vol. 72(7). – P. 2477-2483. DOI: 10.1021/j100853a035.
61. Klika Z., Čapková P., Horáková P., Valášková M., Malý P., Macháň R., Pospíšil M. Composition, structure, and luminescence of montmorillonites saturated with different aggregates of methylene blue. // *Journal of Colloid and Interface Science*. – 2007. – Vol. 311(1). – P. 14-23. DOI: 10.1016/j.jcis.2007.02.034.
62. Zhikhoreva A. A., Belashov A. V., Serebryakov E. B., Semenova I. V., Vasyutinskii O. S. Photophysical properties of methylene blue in aqueous solution sprayed onto biological surfaces. // *Dyes and Pigments*. – 2022. – Vol. 208. – P. 110789. DOI: 10.1016/j.dyepig.2022.110789.
63. Walter-Sack I., Rengelshausen J., Oberwittler H., Burhenne J., Mueller O., Meissner P., Mikus G. High absolute bioavailability of methylene blue given as an aqueous oral formulation. // *European Journal of Clinical Pharmacology*. – 2009. – Vol. 65(2). – P. 179-189. DOI: 10.1007/s00228-008-0563-x.
64. Peter C., Hongwan D., Küpfer A., Lauterburg B. H. Pharmacokinetics and organ distribution of intravenous and oral methylene blue. // *European Journal of Clinical Pharmacology*. – 2000. – Vol. 56(3). – P. 247-250. DOI: 10.1007/s002280000124.
65. Ryabova A. V., Stratonnikov A. A., Loshchenov V. B. Laser spectroscopy technique for estimating the efficiency of photosensitisers in biological media. // *Quantum Electronics*. – 2006. – Vol. 36(6). – P. 562-568. DOI: 10.1070/QE2006v036n06ABEH013291.
66. Redmond R. W., Gamlin J. N. A Compilation of Singlet Oxygen Yields from Biologically Relevant Molecules. // *Photochemistry and Photobiology*. – 1999. – Vol. 70(4). – P. 391-475. DOI: 10.1111/j.1751-1097.1999.tb08240.x.

PHOTODYNAMIC THERAPY OF ACNE

Filonenko E.V.¹, Ivanova-Radkevich V.^{1,2}

¹P.A. Herzen Moscow Oncology Research Center – branch of FSBI NMRRC of the Ministry of Health of the Russian Federation, Moscow, Russia

²RUDN University, Moscow, Russia

Abstract

Acne is one of the most common skin conditions in the world. A number of studies have shown that photodynamic therapy (PDT) is safe and effective for both inflammatory and non-inflammatory acne and can significantly improve skin conditions in this disease. The effectiveness of PDT against acne is mainly due to a decrease in the amount of sebum produced by the sebaceous glands due to a decrease in their activity as a result of direct photodynamic damage to the sebaceous glands, eradication of *Cutibacterium acnes*, and a decrease in the level of hyperkeratosis. Compared with systemic drug therapy, PDT treatment of severe acne has the following advantages: fast results, high efficiency, high selectivity, no systemic adverse reactions and drug resistance, and low recurrence rate. Most often for PDT in patients with acne, drugs based on 5-aminolevulinic acid (5-ALA) and its methyl ester (ME-ALA) are used. At the moment, there are no unified recommendations on PDT regimens for the treatment of this skin pathology. Various studies demonstrate the high efficiency of PDT with a wide range of doses of 5-ALA (3-20%) and ME-ALA (4-16%), light doses (15-120 J/cm²), and exposure time (30-90 min). The general trend in studies by different authors is that gentle low-intensity PDT regimens for acne demonstrate the same high efficiency with a significant reduction in pain during irradiation and local skin reactions (erythema, edema, and hyperpigmentation).

Key words: photodynamic therapy, acne, 5-aminolevulinic acid, 5-aminolevulinic acid methyl ester.

Contacts: Filonenko E.V., e-mail: elena.filonenko@list.ru

For citations: Filonenko E.V., Ivanova-Radkevich V.I. Photodynamic therapy of acne, *Biomedical Photonics*, 2023, vol. 12, no. 2, pp. 48–56. doi: 10.24931/2413–9432–2023–12-2-48–56.

ФОТОДИНАМИЧЕСКАЯ ТЕРАПИЯ ПРИ АКНЕ

Е.В. Филоненко¹, В.И. Иванова-Радкевич²

¹«Московский научно-исследовательский онкологический институт им. П.А. Герцена – филиал ФГБУ «Национальный медицинский исследовательский центр радиологии» Министерства здравоохранения Российской Федерации, Москва, Россия

²Российский Университет дружбы народов, Москва, Россия

Резюме

Акне – одна из самых распространенных в мире кожных патологий. Ряд исследований показал, что фотодинамическая терапия (ФДТ) безопасна и эффективна при воспалительной и невоспалительной форме акне и может значительно улучшить состояние кожи при этом заболевании. Эффективность ФДТ против акне в основном обусловлена уменьшением количества кожного сала, вырабатываемого сальными железами, за счет снижения их активности в результате прямого фотодинамического повреждения сальных желез, эрадикацией *Cutibacterium acnes* и снижением уровня гиперкератоза. По сравнению с системной медикаментозной терапией лечение тяжелой формы акне методом ФДТ имеет следующие преимущества: быстрый результат, высокая эффективность, высокая селективность, отсутствие системных побочных реакций и лекарственной устойчивости, низкая частота рецидивов. Наиболее часто для ФДТ у больных акне применяют препараты на основе 5-аминолевулиновой кислоты (5-АЛК) и ее метилового эфира (МЭ-АЛК). На данный момент не существует единых рекомендаций по режимам ФДТ для лечения данной кожной патологии. Различные исследования демонстрируют высокую эффективность ФДТ с широким диапазоном доз 5-АЛК (3-20%) и МЭ-АЛК (4-16%), световых доз (15-120 Дж/см²) и времени облучения (30-90 мин). Общая тенденция в исследованиях разных авторов сводится к тому, что щадящие низкоинтенсивные режимы ФДТ при акне демонстрируют такую же высокую эффективность при значительном снижении болевых ощущений в процессе облучения и местных кожных реакций (эритема, отек, гиперпигментация).

Ключевые слова: фотодинамическая терапия, акне, 5-аминолевулиновая кислота, метиловый эфир 5-аминолевулиновой кислоты.

Контакты: Филоненко Е.В., e-mail: elena.filonenko@list.ru

Для цитирования: Филоненко Е.В., Иванова-Радкевич В.И. Фотодинамическая терапия при акне // *Biomedical Photonics*. – 2023. – Т. 12, № 2. – С. 48–56. doi: 10.24931/2413–9432–2023–12-2-48–56.

Acne (acne vulgaris) is a chronic inflammatory skin disease characterized by overgrowth of the microorganism *Cutibacterium acnes*, formerly known as *Propionibacterium acnes*, in the sebaceous glands [1].

Epidemiology

Acne affects approximately 600 million people worldwide every year, making it the eighth most common skin disease in the world [1]. Acne occurs in 70-75% of prepubertal children up to 12 years of age (usually at 9-11 years of age). Up to 80-85% of teenagers and young adults suffer from acne. In older age groups, the percentage decreases, but still, almost one in ten adults over 25 suffers from acne [2]. Although acne is not a life-threatening disease, serious psychological consequences have been reported in various studies in patients, which can affect sociability, cause phobias, and lead to depressive symptoms [1].

Etiology and pathogenesis

Acne can occur against the background of seborrhea, which is characterized by a change in the chemical composition of sebum and increased secretion of sebum by the sebaceous glands. As a result, acne occurs in areas of the skin that are richest in sebaceous glands [2]. Acne pathogenesis involves four main mechanisms: follicular hyperkeratosis (epithelial proliferation with thickening of the stratum corneum of the sebaceous gland channels), increased secretion of sebum, *C. acnes* colonization, and localized inflammation [3]. It is believed that it is the colonization of *C. acnes* that plays a key role in the development of acne [3]. *C. acnes* is a Gram-positive, anaerobic, slow growing bacterium that metabolizes triglycerides and produces cytokines that induce inflammatory responses [3,4].

Classification

According to the ICD-10 classification, the following types of acne are distinguished: L.70.0 Acne vulgaris; L.70.1 Acne globose; L.70.2 Smallpox acne; L.70.3 Tropical eels; L.70.4 Children acne; L.70.5 Excoriated acne; L.70.8 Other acne and L.70.9 Acne unspecified. There is also a classification of acne vulgaris according to the type of lesions: 1. Non-inflammatory acne: closed and open comedones; 2. Inflammatory acne (superficial: papulopustular; deep: indurative, conglobate; complicated: nodular cystic, abscessing, phlegmonous, keloid, scarring, complicated by sinus tracts) [2].

The Leeds acne severity score takes into account acne lesions on the face, back, and chest and classifies them as inflammatory or non-inflammatory. Leeds scores range from 0 (least severe) to 10 (most severe). There are modified Leeds scales, the maximum score for which is 12 [5,6]. The Pillsbury Acne Rating Scale ranks acne severity from 1 (least severe) to 4 (most severe) [7,8].

Acne therapy

Traditional acne therapy includes topical and systemic antibiotics, such as tetracyclines and isotretinoin, as well as retinoids [1]. The use of antibiotics is significantly limited by the growth of antibiotic resistance in *C. acnes*, and the use of retinoids is limited by their serious side effects associated with teratogenicity, spontaneous abortion, skin irritation, cheilitis, photosensitivity, arthralgia, hypertriglyceridemia, inflammatory bowel disease, pancreatitis, and depression [3,9]. Acne therapy is very long. Thus, according to Cunliffe *et al.*, for complete resolution of mild to moderate acne, 3-4 years of treatment are required, and in the case of severe acne, 8-12 years may be required. According to Cunliffe, in 7% of patients with disease manifestation in adolescence, the manifestations of the disease can last up to 45-50 years [10]. Long-term use of antibiotics can cause a variety of side effects, including dysbiosis and an increased chance of infection with opportunistic pathogens. Long-term use of isotretinoin can cause dry skin and mucous membranes, increase blood lipid levels, and lead to impaired liver function, depression, and suicidal tendencies. In addition, this drug has a teratogenic effect and cannot be recommended in women of childbearing age [11]. The topical application of these drugs may cause skin irritation. It is also important that their use requires adherence to a clear regimen of administration, and in real clinical practice there is often a violation of the rules of admission by the patient.

Low efficacy, side effects, and duration of treatment with antibiotics and retinoids are prerequisites for finding new, safe, and effective ways to treat acne. In this context, various safe and effective physiotherapy procedures are becoming a new trend in the treatment of acne. One of the possible alternative methods of treatment can be photodynamic therapy (PDT) [1,11].

PDT in the treatment of acne

PDT is used for various tumor and precancerous skin pathologies [12,13,14]. A number of studies have shown that PDT is safe and effective in both inflammatory and non-inflammatory acne and can significantly improve skin conditions in this disease. Moreover, since the reactive oxygen species produced by PDT do not have any specific molecular target, PDT makes it possible to easily bypass drug resistance in microorganisms, which gives this therapy an advantage over antibiotic treatment. The effectiveness of PDT against acne is mainly due to a decrease in the amount of sebum produced by the sebaceous glands due to a decrease in their activity as a result of direct photodynamic damage to the sebaceous glands, eradication of *C. acnes* and a decrease in the level of hyperkeratosis [1,15].

The first edition of the 2002 European Clinical Guidelines for Local PDT contained information on the

Таблица

Сводные данные результативности применения фотодинамической терапии у больных акне

Table

Summary of the effectiveness of photodynamic therapy of acne

Авторы <i>Authors</i>	Число пациентов / <i>No. of patients</i>	Фотосенси- билизатор <i>Photosen- sitizer</i>	Режим облучения <i>Exposure mode</i>	Количество курсов ФДТ <i>Number of PDT courses</i>	Эффективность ФДТ <i>PDT efficiency</i>	Нежелательные реакции <i>Adverse reactions</i>
Asayama- Kosaka et al., 2014 [20]	11	5% 5-АЛК, ап- пликация 2 ч 5% 5-ALA, application 2 h	Широкополос- ное облучение (600-1100 нм), 15 Дж/см ² , 60 мВт/см ² Broadband irradiation (600- 1100 nm), 15 J/cm ² , 60 mW/cm ²	Однократно <i>Once</i>	Средний балл GAGS снизился с 22,1±3,8 в начале исследования до 19,4 через 1 мес и до 16,3 через 3 мес после ФДТ. The mean GAGS score decreased from 22.1±3.8 at baseline to 19.4 at 1 month and to 16.3 at 3 months after PDT.	У 10 из 11 пациентов наблюдались местные побочные эффекты, такие как эритема (от минимальной до легкой степени тяжести). Все нежелательные явления прошли в течение нескольких дней без поствоспалительной гиперпигментации. Ten out of 11 patients experienced local side effects such as erythema (from minimal to mild severity). All adverse events resolved within a few days without post-inflammatory hyperpigmentation.
Chen et al., 2015 [21]	Группа ФДТ – 25 пациентов (1 группа сравне- ния: только об- лучение) PDT group – 25 patients (1 comparison group: only irradiation)	5% 5-АЛК, ап- пликация 1,5 ч 5% 5-ALA, application 1,5 h	633±10 нм, 120 Дж/см ² , 10 мВт/см ² , 633±10 нм, 120 J/cm ² , 10 mW/cm ²	1 раз в неделю, 3 недели 1 time per week, 3 weeks	Общий показатель эффективности в группе ФДТ составил 54,2% против 21,6% в контрольной группе через 2 нед после лечения, 75,0% против 43,5% через 4 нед и 83,3% против 56,5% через 6 нед, соответственно. The overall success rate in the PDT group was 54.2% vs. 21.6% in the control group 2 weeks after treatment, 75.0% vs. 43.5% after 4 weeks, and 83.3% vs. 56.5% after 6 weeks, respectively.	В группе ФДТ 7 пациентов испыты- вали жжение, боль, эритему и отек в течение 1-4 дней после ФДТ. У 3 пациентов наблюдалась временная гиперпигментация. У 2 пациентов появились высыпания на коже. В контрольной группе у 2 пациентов наблюдалось покраснение и сухость лица. In the PDT group, 7 patients experienced burning, pain, erythema, and edema within 1-4 days after PDT. Three patients had transient hyperpigmentation. 2 patients developed skin rashes. In the control group, redness and dryness of the face were observed in 2 patients.

Calzavara-Pinton et al., 2013 [22]	92	16% МЭ-АЛК, аппликация 3-4 ч 16% MAL, application 3-4 h	635±18 нм, 37 Дж/см ² , 10 мВт/см ² 635±18 нм, 37 Дж/см ² , 10 мВт/см ²	От 2 до 4 курсов с интервалом 2-4 недели From 2 to 4 courses with an interval of 2-4 weeks	Общее улучшение течения акне было оценено как выраженное у 71 (77,2%) пациента, умеренное у 12 (13,0%) пациентов и слабое у 9 (9,8%) пациентов. У 67 (72,8%) пациентов косметический результат, был оценен как отличный. The overall improvement in the course of acne was assessed as pronounced in 71 (77.2%) patients, moderate in 12 (13.0%) patients, and weak in 9 (9.8%) patients. In 67 (72.8%) patients, the cosmetic result was rated as excellent.	У 4 пациентов с типом кожи IV на месте лечения образовались участки гиперпигментации. In 4 patients with skin type IV, areas of hyperpigmentation formed at the treatment site.
Liu et al., 2014 [3]	Группа ФДТ – 50 пациентов (2 группы сравнения: импульсное облучение и только облучение LED) PDT group – 50 patients (2 comparison groups: pulsed irradiation and LED irradiation only)	5% 5-АЛК, аппликация 1 ч 5% 5-ALA, application 1 h	633±6 нм, 127 Дж/см ² , 105 мВт/см ² 633±6 нм, 127 Дж/см ² , 105 мВт/см ²	1 раз в неделю, до очищения очагов на 90% и более (в среднем количество курсов 3±1,5) 1 time per week, until the foci are cleared by 90% or more (on average, the number of courses is 3 ± 1.5)	Через 1 мес после начала лечения у 60% пациентов – полное очищение кожи, у 32% – умеренное улучшение, у 8% – небольшое улучшение. 1 month after the start of treatment, 60% of patients have complete skin cleansing, 32% have a moderate improvement, and 8% have a slight improvement.	У 46 (92%) пациентов после каждого курса ФДТ были отмечены легкая или умеренная боль, эритема и отек, которые проходили в течение 5-7 дней. У 2 (4%) пациентов наблюдалась гиперпигментация, которая прошла через 1 мес. In 46 (92%) patients after each course of PDT, mild or moderate pain, erythema and edema were noted, which disappeared within 5-7 days. In 2 (4%) patients, hyperpigmentation was observed, which disappeared after 1 month.
Tao et al., 2016 [23]	125	3,6% 5-АЛК, аппликация 1,5 ч 3,6% 5-ALA, application 1,5 h	633 нм, 126 Дж/см ² , 66 мВт/см ² 633 нм, 126 Дж/см ² , 66 мВт/см ²	1 раз в 2 недели, 3 курса 1 time in 2 weeks, 3 courses	Общие показатели эффективности составили 1,6%, 24,8%, 68,8%, 89,6% и 88,8% через 2, 4, 6, 8 и 12 нед после начала лечения, соответственно. The overall success rates were 1.6%, 24.8%, 68.8%, 89.6% and 88.8% at 2, 4, 6, 8 and 12 weeks after the start of treatment, respectively.	У 40 (32%) пациентов наблюдалось обострение угревой сыпи до 2 и 3 курса лечения, которое проходило после 3 курса лечения. Побочные явления были умеренными и обратимыми. In 40 (32%) patients, an exacerbation of acne was observed before the 2nd and 3rd courses of treatment, which disappeared after the 3rd course of treatment. Side effects were moderate and reversible.

Dessinioti et al., 2016 [24]	12	4% МЭ-АЛК, аппликация 1 ч 4% MAL, application 1 h	635 нм, 37 Дж/см ² 635 нм, 37 J/cm ²	1 раз в неделю, 2 курса 1 time per week, 2 courses	Количество очагов угревой сыпи снизилось в среднем на 35% от исходного уровня на 1-й неделе после двух процедур и в среднем на 30% при 4-недельном наблюдении. The number of acne lesions decreased by an average of 35% from baseline at week 1 after two treatments and by an average of 30% at a 4-week follow-up.	Пациенты хорошо переносили ФДТ. Побочные эффекты ограничивались легкой преходящей эритемой в местах лечения и продолжались несколько часов. Отеков, пустул, образования корок или стойкой эритемы не наблюдалось. Пациенты не сообщали о болевых ощущениях. The patients tolerated PDT well. Side effects were limited to mild transient erythema at the treatment sites and lasted several hours. Edema, pustules, crusting, or persistent erythema were not observed. Patients did not report pain.
Hong et al., 2013 [25]	20 20 Each patient has 2 treatment regimens (right and left side of the face)	16% МЭ-АЛК, аппликация 3 ч 16% MAL, application 3 h	1 режим: красный свет (длина волны не указана), 22 Дж/см ² , 34 мВт/см ² 2 режим: импульсное облучение, 530-750 нм, 2,5 мс, длительность с задержкой 10 мс, 8-10 Дж/см ² 1 mode: red light (wavelength not specified), 22 J/cm ² , 34 mW/cm ² 2 mode: pulsed irradiation, 530-750 nm, 2.5 ms, duration with a delay of 10 ms, 8-10 J/cm ²	1 раз в 2 недели, 3 курса 1 time in 2 weeks, 3 courses	В результате воздействия обоих режимов количество очагов угревой сыпи уменьшилось. Результаты были чуть лучше при воздействии режима 1. As a result of exposure to both regimens, the number of acne foci decreased. The results were slightly better when exposed to mode 1.	Побочные явления были умеренными и обратимыми. Side effects were moderate and reversible.
Yew et al., 2016 [26]	15	5% 5-АЛК, аппликация 3 ч 5% 5-ALA, application 3 h	630 нм, 37 Дж/см ² , 38 мВт/см ² 630 нм, 37 J/cm ² , 38 mW/cm ²	Однократно Once	В целом, к концу 12-недельного наблюдения количество воспалительных поражений сократилось на 64,2%, количество невоспалительных поражений – на 24,3%. In general, by the end of the 12-week follow-up, the number of inflammatory lesions decreased by 64.2%, the number of non-inflammatory lesions by 24.3%.	Незначительные болевые ощущения. Minor pain.
Guo et al., 2023 [11]	18	5% 5-АЛК, аппликация 1-1,5 ч 5% 5-ALA, application 1-1.5 h	630 нм, 60 Дж/см ² 630 нм, 60 J/cm ²	1 раз в неделю, 2 курса 1 time in 2 weeks, 2 courses	Показатель эффективности с 1 по 3 недели наблюдения увеличился с 27,78% до 55,56%, а затем до 83,33%. The success rate from 1 to 3 weeks of observation increased from 27.78% to 55.56%, and then to 83.33%.	Побочные явления были умеренными и обратимыми. Side effects were moderate and reversible.

possibility of using PDT for the treatment of warts and acne, with 5-aminolevulinic acid (5-ALA) being listed as the most widely used PDT drug. The recommendations also contained an indication of the possibility of using both coherent and incoherent light sources for PDT [16]. By 2008 [17], PDT for the treatment of acne, warts, and cutaneous leishmaniasis was rated clinical recommendation level IB (strength of recommendation B, quality of evidence I). In the latest edition of the European Clinical Guidelines for Local PDT, severe acne remains indicated as an indication for PDT with an IB level [11].

Guo et al., based on almost 20 years of experience in the clinical use of PDT for the treatment of severe acne, conclude that, compared with systemic drug therapy, the treatment of severe acne with PDT has the following advantages: fast results, high efficiency, high selectivity, no systemic adverse reactions, drug resistance, and low recurrence rate [1]. Picone et al. [18] also indicate that the undoubted advantage of PDT for the treatment of acne is the absence of scars after treatment.

Interestingly, low concentrations of the photosensitizer, short incubation time, and low light doses (about 13 J/cm²) under blue light irradiation provide short-term antimicrobial and immunomodulatory effects, while higher light doses (up to 150 J/cm²) of red light additionally cause destruction of the sebaceous glands. An additional effect of all PDT modes, leading to a decrease in follicle obstruction and a decrease in sebum secretion, is an increase in epidermal renewal [4].

In recent years, several large clinical studies have been conducted on the efficacy and safety of PDT in the treatment of acne using 5-ALA and 5-ALA methyl ester (ME-ALA) (Table). Even though there were no reports on the use of chlorin derivatives for PDT in patients with acne in clinical practice, *in vitro* and *in vivo* studies using chlorins also showed satisfactory results [19]. Phthalocyanines, to the best of our knowledge, have not yet been investigated for the treatment of this skin pathology.

We searched for published results of studies on the clinical efficacy of PDT in acne patients over the past 10 years using the Pubmed database. We included in the analysis only studies conducted with the participation of 10 or more patients, in which PDT was performed in mono mode using standard sources and irradiation modes. Selected clinical cases of interest are further described below. The analysis made it possible to identify 9 studies that present data obtained in total in the treatment of 368 patients with acne (Table). Most studies have used 5% of 5-ALA as an application for 1-4 hours for PDT. In one study, the concentration of 5-ALA was lower – 3.6%. Three studies used ME-ALA for PDT at a standard concentration of 16% or a lower concentration of 4%. For irradiation, red light was most often used. Light doses ranged from 15 to 120 J/cm². All studies have shown an overall improvement in acne after PDT.

The main task in the development of the PDT method in the field of acne treatment at the moment is the search for regimens that reduce pain and the development of local reactions in the area of irradiation while maintaining the high treatment efficiency achieved in previous studies.

A number of studies demonstrate a significant reduction in the intensity of pain during an irradiation session and other adverse events while maintaining high treatment efficiency during low-intensity PDT. For example, in a study by Chen *et al.*, [21] PDT with a light dose of 120 J/cm² and a power density of 10 mW/cm² caused significant pain, burning, erythema, and edema that persisted up to 4 days after PDT in 28% of patients and temporary pigmentation in 12% of patients. Liu *et al.* [3] reported the development of adverse events (moderate pain, erythema, and edema lasting up to 5 days) in 92% of patients after PDT with a light dose of 127 J/cm² and a power density of 105 mW/cm². In a study by Calzavara-Pinton *et al.* [22], the light dose was reduced to 37 J/cm² at a power density of 10 mW/cm². The authors of the study did not report significant pain sensations or other adverse events. Only 4% of patients with skin type IV developed areas of hyperpigmentation at the treatment site.

Pain sensations are also reduced with the use of 5-ALA and ME-ALA at lower concentrations than usual. For example, in a study by Dessinioti *et al.* [24] ME-ALA cream was used for PDT with a concentration 4 times lower than the standard (4%). Side effects were limited to mild transient erythema at the treatment sites and lasted several hours. Edema, pustules, crusting, or persistent erythema were not observed. Patients did not report pain. At the same time, the effectiveness of treatment was quite high – immediately after 2 courses of PDT, the number of acne foci decreased by an average of 35% from the initial level.

Many researchers note that the use of high concentrations of 5-ALA for acne PDT causes significant side effects. For example, Pollock *et al.* [27] reported on the use of 5-ALA in 10 patients with acne at a concentration of 20% with application for 3 hours. Despite the rather sparing irradiation regimen (15 J/cm², 25 mW/cm²), patients experienced significant pain during the irradiation session and erythema. The effectiveness of the treatment was even lower than when using lower concentrations of 5-ALA: after the second course of treatment, a statistically significant decrease in the number of inflammatory foci of acne was observed in the treatment area compared to the baseline, but not in comparison with the control areas. As a result of the treatment, no statistically significant amount of *C. acnes* or the level of sebum secretion was obtained.

Some researchers recommend shortening the application time of 5-ALA as a way to reduce the intensity of

pain during irradiation. Thus, the results of one recent small-scale study in which 5% 5-ALA cream was used in patients with acne showed that a reduction in the application time from 90 to 30 minutes led to an almost complete absence of pain during irradiation in patients with the same effectiveness of treatment [28]. Chinese dermatologists also give the results of studies demonstrating that PDT with a 5-ALA concentration of 3–5% and a shorter application time (30 min) can effectively improve the condition of moderate to severe acne vulgaris with minimal pain and other adverse reactions [29].

The use of a ventilator, air cooling, and possible short breaks in irradiation may also be used to reduce treatment-related pain during PDT. Local anesthesia can usually be used before and after PDT [30].

A separate promising area of application of PDT in patients with acne is PDT after ineffective acne treatment by other methods, in particular, after an exacerbation of the disease during isotretinone treatment. Despite the fact that no large-scale studies of the effectiveness of PDT in this group of patients have been conducted, several interesting clinical cases have been described in the literature. Thus, Liu J. et al. [31] report the successful treatment of a patient with acne flare-ups after treatment with isotretinoin. Acne *exacerbation* develops in a small proportion of patients at the start of oral isotretinoin. Clinically, it usually manifests as painful, ulcerated, and hemorrhagic lesions. Traditional therapy in this case is the ingestion of corticosteroids. However, in some patients, such therapy can also be accompanied by side effects, such as metabolic disorders, suppression of immune function, and other effects. The authors report a young man with acne exacerbation after taking isotreti-

noin, who was treated with PDT (2-hour application of 5% 5-ALA, irradiation 633 ± 6 mm, 42 mW/cm^2 , 75.6 J/cm^2 , 7 cycles). The result of the treatment was rated as a complete cleansing of the skin with an excellent cosmetic result). Picone et al. [18] report another case of successful treatment of acne exacerbation while taking isotretinone. PDT was performed in a patient with ulcerative and hemorrhagic lesions from acne on the face and trunk with an exacerbation of the disease after the start of treatment with isotretinoin, which did not respond to systemic prednisolone in combination with topical application of clindamycin and disinfectants. The patient underwent 6 courses of PDT with ME-ALA (application of 16% ointment) with red light irradiation (630 nm , light dose 39 J/cm^2). At a 6-month follow-up, the patient showed no active lesions, only scarring, and no side effects were reported during and after each treatment session.

Conclusion

In recent years, the method of acne treatment, PDT, has been actively developed, demonstrating high efficiency and a satisfactory safety profile. For acne PDT, 5-ALA and ME-ALA are used. Both drugs show high efficacy in both inflammatory and non-inflammatory lesions, in mild, moderate, and severe forms of acne, as well as after ineffective acne treatment by other methods, in particular after an exacerbation of the disease during treatment with isotretinone. The main direction in the development of PDT in acne patients is the search and development of low-intensity PDT schemes to minimize pain and local reactions to radiation.

REFERENCES

1. De Annunzio S.R., Costa N.C.S., Mezzina R.D., Graminha M.A.S., Fontana C.R. Chlorin, Phthalocyanine, and Porphyrin Types Derivatives in Phototreatment of Cutaneous Manifestations: A Review. *Int J Mol Sci*, 2019, vol. 20(16), p. 3861. doi:10.3390/ijms20163861.
2. Barinova A.N. Etiology, pathogenesis, classification and clinical picture of vulgar acne. Modern view of the problem. *Russian Family Doctor*, 2018, vol. 22(3), pp. 14-22. doi 10.17816/RFD2018314-223.
3. Liu L.H., Fan X., An Y.X., Zhang J., Wang C.M. & Yang, R.Y. Randomized trial of three phototherapy methods for the treatment of acne vulgaris in Chinese patients. *Photodermatology, photoimmunology & photomedicine*, 2014, vol. 30(5), pp. 246-253. https://doi.org/10.1111/phpp.12098
4. Mackay A.M. The evolution of clinical guidelines for antimicrobial photodynamic therapy of skin. *Photochem Photobiol Sci*, 2022, vol. 21(3), pp. 385-395. doi:10.1007/s43630-021-00169
5. Chiang A., Hafeez F., Maibach H.I. Skin lesion metrics: role of photography in acne. *Journal of dermatological treatment*, 2014, vol. 25(2), pp. 100-105.
6. O'Brien S.C., Lewis J.B., Cunliffe W.J. The Leeds revised acne grading system. *Journal of dermatological treatment*, 1998, vol. 9(4), pp. 215-220.
7. Tan J. K. L. et al. Evaluation of essential clinical components and features of current acne global grading scales. *Journal of the American Academy of Dermatology*, 2013, vol. 69(5), pp. 754-761.

ЛИТЕРАТУРА

1. De Annunzio S.R., Costa N.C.S., Mezzina R.D., Graminha M.A.S., Fontana C.R. Chlorin, Phthalocyanine, and Porphyrin Types Derivatives in Phototreatment of Cutaneous Manifestations: A Review // *Int J Mol Sci*. – 2019. – Vol. 20(16). – P. 3861. doi:10.3390/ijms20163861.
2. Баринова А.Н. Этиология, патогенез, классификация и клиническая картина вульгарных угрей. Современный взгляд на проблему // *Российский семейный врач*. – 2018. – Т. 22, № 3. – С. 14-22. doi 10.17816/RFD2018314-223
3. Liu L.H., Fan X., An Y.X., Zhang J., Wang C.M. & Yang, R.Y. Randomized trial of three phototherapy methods for the treatment of acne vulgaris in Chinese patients // *Photodermatology, photoimmunology & photomedicine*. – 2014. – Vol. 30(5). – P. 246-253. https://doi.org/10.1111/phpp.12098
4. Mackay A.M. The evolution of clinical guidelines for antimicrobial photodynamic therapy of skin // *Photochem Photobiol Sci*. – P. 2022. – Vol. 21(3). – P. 385-395. doi:10.1007/s43630-021-00169-w
5. Chiang A., Hafeez F., Maibach H.I. Skin lesion metrics: role of photography in acne // *Journal of dermatological treatment*. – 2014. – Vol. 25(2). – P. 100-105.
6. O'Brien S.C., Lewis J.B., Cunliffe W.J. The Leeds revised acne grading system // *Journal of dermatological treatment*. – 1998. – Vol. 9(4). – P. 215-220.
7. Tan J. K. L. et al. Evaluation of essential clinical components and features of current acne global grading scales // *Journal of the American Academy of Dermatology*. – 2013. – Vol. 69(5). – P. 754-761.

8. Purdy, S. & Deberker D. Acne vulgaris. *BMJ clinical evidence*, 2008, p. 1714.
9. Yilmaz S. Toxicity Genotoxicity, and Carcinogenicity of tretinoin. *Current molecular pharmacology*, 2023, vol. 16(1), pp. 83-90. <https://doi.org/10.2174/187446721566-6220520143124>
10. Goldsmith LA, Katz SI, Gilchrist BA, et al. Dermatologiya Fitzpatricka v klinicheskoy praktike. *Moscow: Izdatel'stvo Panfilova*, 2015. (In Russ.)
11. Guo, Y., Zeng, M., Yuan, Y., Yuan, M., Chen, Y., Yu, H., Liu, R., Ruan, Z., Xie, Q., Jiao, X. & Lu, T. Photodynamic therapy treats acne by altering the composition of the skin microbiota. *Skin research and technology: official journal of International Society for Bioengineering and the Skin (ISBS) and International Society for Digital Imaging of Skin (ISDIS)*. *International Society for Skin Imaging*, 2023, vol. 29(1), p. e13269. <https://doi.org/10.1111/srt.13269>
12. Filonenko E.V., Ivanova-Radkevich V.I. Photodynamic therapy of psoriasis. *Biomedical Photonics*, 2023, vol. 12(1), pp. 28-36. doi: 10.24931/2413-9432-2023-12-1-28-36.
13. Filonenko E.V., Ivanova-Radkevich V.I. Photodynamic therapy in the treatment of extramammary Paget disease. *Biomedical Photonics*, 2022, vol. 3, pp. 24-34. doi: 10.24931/2413-9432-2022-11-3-24-34.
14. Filonenko E.V., Ivanova-Radkevich V.I. Photodynamic therapy in the treatment of mycosis fungoides. *Biomedical Photonics*, 2022, vol. 11(1), pp. 27-37. doi: 10.24931/2413-9432-2022-11-1-27-37.
15. Wen, X., Li, Y. & Hamblin M. R. Photodynamic therapy in dermatology beyond non-melanoma cancer: An update. *Photodiagnosis and photodynamic therapy*, 2017, vol. 19, pp. 140-152. <https://doi.org/10.1016/j.pdpdt.2017.06.010>
16. Morton C.A., Brown S.B., Collins S., Ibbotson S., Jenkinson H., Kurwa H., Langmack K., McKenna K., Moseley H., Pearse A.D., Stringer M., Taylor D.K., Wong G., Rhodes L.E. Guidelines for topical photodynamic therapy: Report of a workshop of the British Photodermatology Group. *The British Journal of Dermatology*, 2002, vol. 146(4), pp. 552-567. doi: 10.1046/j.1365-2133.2002.04719.x.
17. Morton, C.A., McKenna, K.E., Rhodes, L.E. & British. Association of Dermatologists Therapy Guidelines and Audit Subcommittee and the British Photodermatology Group Guidelines for topical photodynamic therapy: Update. *The British Journal of Dermatology*, 2008, vol. 159(6), pp. 1245-1266. doi: 10.1111/j.1365-2133.2008.08882.x.
18. Picone V., Potestio L., Fabbrocini G., Monfrecola G. & Marasca C. A case of acne fulminans successfully treated with photodynamic therapy. *Photodermatology, photoimmunology & photomedicine*, 2022, vol. 38(4), pp. 401-403. <https://doi.org/10.1111/phpp.12761>
19. Wang Y.Y., Ryu A.R., Jin S., Jeon Y.M., Lee M.Y. Chlorin e6-Mediated Photodynamic Therapy Suppresses P. acnes-Induced Inflammatory Response via NFκB and MAPKs Signaling Pathway. *PLoS ONE*, 2017, vol. 12, p. e0170599. doi: 10.1371/journal.pone.0170599.
20. Asayama-Kosaka S, Akilov OE, Kawana S. Photodynamic Therapy with 5% delta-Aminolevulinic Acid is Safe and Effective Treatment of Acne Vulgaris in Japanese Patients. *Laser Ther*, 2014, vol. 23, pp. 115-120.
21. Chen X., Song H., Chen S., Zhang J., Niu G., Liu X. Clinical efficacy of 5-aminolevulinic acid photodynamic therapy in the treatment of moderate to severe facial acne vulgaris. *Exp Ther Med*, 2015, vol. 10(3), pp. 1194-1198. doi:10.3892/etm.2015.2638
22. Calzavara-Pinton P.G., Rossi M.T., Aronson E., Sala R. & Italian Group For Photodynamic Therapy. A retrospective analysis of real-life practice of off-label photodynamic therapy using methyl aminolevulinate (MAL-PDT) in 20 Italian dermatology departments. Part 1: inflammatory and aesthetic indications. *Photochemical & photobiological sciences: Official journal of the European Photochemistry Association and the European Society for Photobiology*, 2013, vol. 12(1), pp. 148-157. <https://doi.org/10.1039/c2pp25124h>
23. Tao S.Q., Xia R.S., Li F., Cao L., Fan H., Fan Y. & Yang, L.J. Efficacy of 3.6% topical ALA-PDT for the treatment of severe acne vulgaris. *European review for medical and pharmacological sciences*, 2016, vol. 20(2), pp. 225-231.
24. Dessinioti C., Masouri S., Drakaki E., Katsambas A. & Antoniou, C. Short-contact, low-dose methyl aminolevulinate photodynamic
8. Purdy, S. & Deberker D. Acne vulgaris // *BMJ clinical evidence*. – 2008. – P. 1714.
9. Yilmaz S. Toxicity Genotoxicity, and Carcinogenicity of tretinoin // *Current molecular pharmacology*. – 2023. – Vol. 16(1). – P. 83–90. <https://doi.org/10.2174/187446721566-6220520143124>
10. Goldsmith LA, Katz SI, Gilchrist BA, et al. *Dermatologiya Fitzpatricka v klinicheskoy praktike* // *Moscow: Izdatel'stvo Panfilova*. – 2015. (In Russ.)
11. Guo, Y., Zeng, M., Yuan, Y., Yuan, M., Chen, Y., Yu, H., Liu, R., Ruan, Z., Xie, Q., Jiao, X., & Lu, T. Photodynamic therapy treats acne by altering the composition of the skin microbiota. *Skin research and technology: official journal of International Society for Bioengineering and the Skin (ISBS) and International Society for Digital Imaging of Skin (ISDIS)* // *International Society for Skin Imaging*. – 2023. – Vol. 29(1). – P. e13269. <https://doi.org/10.1111/srt.13269>
12. Filonenko E.V., Ivanova-Radkevich V.I. Photodynamic therapy of psoriasis // *Biomedical Photonics*. – 2023. – Vol. 12(1). – P. 28-36. doi: 10.24931/2413-9432-2023-12-1-28-36.
13. Filonenko E.V., Ivanova-Radkevich V.I. Photodynamic therapy in the treatment of extramammary Paget disease // *Biomedical Photonics*, 2022. – Vol.3. – P. 24-34. doi: 10.24931/2413-9432-2022-11-3-24-34.
14. Filonenko E.V., Ivanova-Radkevich V.I. Photodynamic therapy in the treatment of mycosis fungoides // *Biomedical Photonics*. – 2022. – Vol. 11(1). – P. 27-37 (in Russian). doi: 10.24931/2413-9432-2022-11-1-27-37.
15. Wen, X., Li, Y., & Hamblin, M. R. Photodynamic therapy in dermatology beyond non-melanoma cancer: An update // *Photodiagnosis and photodynamic therapy*. – 2017. – Vol. 19. – P. 140-152. <https://doi.org/10.1016/j.pdpdt.2017.06.010>
16. Morton C.A., Brown S.B., Collins S., Ibbotson S., Jenkinson H., Kurwa H., Langmack K., McKenna K., Moseley H., Pearse A.D., Stringer M., Taylor D.K., Wong G., Rhodes L.E. Guidelines for topical photodynamic therapy: Report of a workshop of the British Photodermatology Group // *The British Journal of Dermatology*. – 2002. – Vol. 146(4). – P. 552-567. doi: 10.1046/j.1365-2133.2002.04719.x.
17. Morton, C.A., McKenna, K.E., Rhodes, L.E. & British. Association of Dermatologists Therapy Guidelines and Audit Subcommittee and the British Photodermatology Group Guidelines for topical photodynamic therapy: Update // *The British Journal of Dermatology*. – 2008. – Vol. 159(6). – P. 1245-1266. doi: 10.1111/j.1365-2133.2008.08882.x.
18. Picone V., Potestio L., Fabbrocini G., Monfrecola G. & Marasca C. A case of acne fulminans successfully treated with photodynamic therapy // *Photodermatology, photoimmunology & photomedicine*. – 2022. – Vol. 38(4). – P. 401-403. <https://doi.org/10.1111/phpp.12761>
19. Wang Y.Y., Ryu A.R., Jin S., Jeon Y.M., Lee M.Y. Chlorin e6-Mediated Photodynamic Therapy Suppresses P. acnes-Induced Inflammatory Response via NFκB and MAPKs Signaling Pathway // *PLoS ONE*. – 2017. – Vol. 12. – P. e0170599. doi: 10.1371/journal.pone.0170599.
20. Asayama-Kosaka S, Akilov OE, Kawana S. Photodynamic Therapy with 5% delta-Aminolevulinic Acid is Safe and Effective Treatment of Acne Vulgaris in Japanese Patients // *Laser Ther*. – 2014. – Vol. 23. – P. 115-120.
21. Chen X., Song H., Chen S., Zhang J., Niu G., Liu X. Clinical efficacy of 5-aminolevulinic acid photodynamic therapy in the treatment of moderate to severe facial acne vulgaris // *Exp Ther Med*. – 2015. – Vol. 10(3). – P. 1194-1198. doi:10.3892/etm.2015.2638
22. Calzavara-Pinton P.G., Rossi M.T., Aronson E., Sala R. & Italian Group For Photodynamic Therapy // A retrospective analysis of real-life practice of off-label photodynamic therapy using methyl aminolevulinate (MAL-PDT) in 20 Italian dermatology departments. Part 1: inflammatory and aesthetic indications // *Photochemical & photobiological sciences: Official journal of the European Photochemistry Association and the European Society for Photobiology*. – 2013. – Vol. 12(1). – P. 148-157. <https://doi.org/10.1039/c2pp25124h>
23. Tao S.Q., Xia R.S., Li F., Cao L., Fan H., Fan Y. & Yang, L.J. Efficacy of 3.6% topical ALA-PDT for the treatment of severe acne vulgaris // *European review for medical and pharmacological sciences*. – 2016. – Vol. 20(2). – P. 225-231.
24. Dessinioti C., Masouri S., Drakaki E., Katsambas A. & Antoniou, C. Short-contact, low-dose methyl aminolevulinate photodynamic

- therapy for acne vulgaris. *The British journal of dermatology*, 2016, vol. 175(1), pp. 215. <https://doi.org/10.1111/bjd.14460>
26. Hong J.S., Jung J.Y., Yoon J.Y. & Suh D.H. Acne treatment by methyl aminolevulinate photodynamic therapy with red light vs. intense pulsed light. *International journal of dermatology*, 2013, vol. 52(5), pp. 614-619. <https://doi.org/10.1111/j.1365-4632.2012.05673.x>
 27. Yew Y.W., Lai Y.C., Lim Y.L., Chong W.S. & Theng C. Photodynamic Therapy With Topical 5% 5-Aminolevulinic Acid for the Treatment of Truncal Acne in Asian Patients. *Journal of drugs in dermatology : JDD*, 2016, vol. 15(6), pp. 727-732.
 28. Pollock B., Turner D., Stringer M.R., Bojar R.A., Goulden V., Stables G.I. & Cunliffe, W.J. Topical aminolevulinic acid-photodynamic therapy for the treatment of acne vulgaris: a study of clinical efficacy and mechanism of action. *The British journal of dermatology*, 2004, vol. 151(3), pp. 616-622. <https://doi.org/10.1111/j.1365-2133.2004.06110.x>
 29. Zhang J., Zhang X., He Y. et al. Photodynamic therapy for severe facial acne vulgaris with 5% 5-aminolevulinic acid vs 10% 5-aminolevulinic acid: A split-face randomized controlled study. *J Cosmet Dermatol*, 2020, vol. 19(2), pp. 368-374.
 30. Wang P., Wang B., Zhang L., Liu X., Shi L., Kang X., Lei X., Chen K., Chen Z., Li C., Zhang C., Tu P., Pan M. Ju Q., Man X., Lu Y., Yu N., Li Y., Zhu H., Zhang R., Wang, X. Clinical practice Guidelines for 5-Aminolevulinic acid photodynamic therapy for acne vulgaris in China. *Photodiagnosis and photodynamic therapy*, 2023, vol. 41, p. 103261. <https://doi.org/10.1016/j.pdpdt.2022.103261>
 31. Zeitouni N.C., Bhatia N., Ceilley R.I., Cohen J.L., Del Rosso J.Q., Moore, A.Y., Munavalli G., Pariser D.M., Schlesinger T., Siegel D.M., Willey A. & Goldman, M.P. Photodynamic Therapy with 5-aminolevulinic Acid 10% Gel and Red Light for the Treatment of Actinic Keratosis, Non-melanoma Skin Cancers, and Acne: Current Evidence and Best Practices. *The Journal of clinical and aesthetic dermatology*, 2021, vol. 14(10), pp. E53-E65.
 32. Liu J., Shi L., Zhang L., Liu X., Zhang H., Zhang Y., Wang P., Zhang G., Zhou Z. & Wang X. Acute acne flare following isotretinoin administration successfully treated by 5-aminolevulinic acid photodynamic therapy. *Photodiagnosis and photodynamic therapy*, 2022, vol. 39, p. 102893. <https://doi.org/10.1016/j.pdpdt.22.102893>
 - therapy for acne vulgaris // *The British journal of dermatology*. – 2016. – Vol. 175(1). – P. 215. <https://doi.org/10.1111/bjd.14460>
 26. Hong J.S., Jung J.Y., Yoon J.Y. & Suh D.H. Acne treatment by methyl aminolevulinate photodynamic therapy with red light vs. intense pulsed light // *International journal of dermatology*. – 2013. – Vol. 52(5). – P. 614-619. <https://doi.org/10.1111/j.1365-4632.2012.05673.x>
 27. Yew Y.W., Lai Y.C., Lim Y.L., Chong W.S. & Theng C. Photodynamic Therapy With Topical 5% 5-Aminolevulinic Acid for the Treatment of Truncal Acne in Asian Patients // *Journal of drugs in dermatology : JDD*. – 2016. – Vol. 15(6). – P. 727-732.
 28. Pollock B., Turner D., Stringer M.R., Bojar R.A., Goulden V., Stables G.I. & Cunliffe, W.J. Topical aminolevulinic acid-photodynamic therapy for the treatment of acne vulgaris: a study of clinical efficacy and mechanism of action // *The British journal of dermatology*. – 2004. – Vol. 151(3). – P. 616-622. <https://doi.org/10.1111/j.1365-2133.2004.06110.x>
 29. Zhang J., Zhang X., He Y. et al. Photodynamic therapy for severe facial acne vulgaris with 5% 5-aminolevulinic acid vs 10% 5-aminolevulinic acid: A split-face randomized controlled study // *J Cosmet Dermatol*. – 2020. – Vol. 19(2). – P. 368-374.
 30. Wang P., Wang B., Zhang L., Liu X., Shi L., Kang X., Lei X., Chen K., Chen Z., Li C., Zhang C., Tu P., Pan M. Ju Q., Man X., Lu Y., Yu N., Li Y., Zhu H., Zhang R., Wang, X. Clinical practice Guidelines for 5-Aminolevulinic acid photodynamic therapy for acne vulgaris in China // *Photodiagnosis and photodynamic therapy*. – 2023. – Vol. 41. – P. 103261. <https://doi.org/10.1016/j.pdpdt.2022.103261>
 31. Zeitouni N.C., Bhatia N., Ceilley R.I., Cohen J.L., Del Rosso J.Q., Moore, A.Y., Munavalli G., Pariser D.M., Schlesinger T., Siegel D.M., Willey A. & Goldman, M.P. Photodynamic Therapy with 5-aminolevulinic Acid 10% Gel and Red Light for the Treatment of Actinic Keratosis, Non-melanoma Skin Cancers, and Acne: Current Evidence and Best Practices // *The Journal of clinical and aesthetic dermatology*. – 2021. – Vol. 14(10). – P. E53-E65.
 32. Liu J., Shi L., Zhang L., Liu X., Zhang H., Zhang Y., Wang P., Zhang G., Zhou Z. & Wang X. Acute acne flare following isotretinoin administration successfully treated by 5-aminolevulinic acid photodynamic therapy // *Photodiagnosis and photodynamic therapy*. – 2022 – Vol. 39. – P. 102893. <https://doi.org/10.1016/j.pdpdt.22.102893>



ЖИВАЯ
ЭНЕРГИЯ
СВЕТА



Фоторан e₆[®]

НОВЫЙ РОССИЙСКИЙ ПРЕПАРАТ ДЛЯ ФОТОДИНАМИЧЕСКОЙ ТЕРАПИИ

- ✓ Действующее вещество природного происхождения
- ✓ Быстрое накопление в патологической ткани – 1,5-3 часа
- ✓ Отсутствие аллергических реакций
- ✓ Длительное хранение без потери активности вещества – 3 года
- ✓ Отсутствие гепато и нефротоксичности, низкая фототоксичность
- ✓ Низкая стоимость

ПАРТНЁРЫ:



Национальный медицинский
исследовательский центр онкологии

Адыгейский республиканский
онкологический диспансер

СККОД

ГБУЗ Челябинский областной клинический
центр онкологии и ядерной медицины

По вопросам
приобретения

+7 (495) 659-64-93
+7 (499) 726-26-98



ФОТОДИТАЗИН®

[fotoditazin]

ФОТОСЕНСИБИЛИЗАТОР ХЛОРИНОВОГО РЯДА



«ФОТОДИТАЗИН®» гель — РУ № ФСР 2012/13043 от 03.02.2012 г.

«ФОТОДИТАЗИН®» концентрат для приготовления раствора для инфузий — РУ № ЛС 001246 от 18.05.2012 г.

«ФОТОДИТАЗИН®» применяется для флуоресцентной диагностики и фотодинамической терапии онкологических заболеваний различных нозологических форм, а так же патологий не онкологического характера в следующих областях медицины:

- | | |
|------------------------|-----------------------------|
| ✓ дерматология | ✓ офтальмология |
| ✓ гинекология | ✓ травматология и ортопедия |
| ✓ урология | ✓ комбустиология |
| ✓ торакальная хирургия | ✓ гнойная хирургия |
| ✓ стоматология | ✓ ангиология |
| ✓ нейрохирургия | |

В соответствии с приказами МИНИСТЕРСТВА ЗДРАВООХРАНЕНИЯ РФ:

Приказ № 1629н от 29 декабря 2012 г. «Об утверждении перечня видов высокотехнологичной медицинской помощи»

Приказ № 915н от 15 ноября 2012 г. «Об утверждении порядка оказания медицинской помощи взрослому населению по профилю „онкология“»

 www.fotoditazin.com
www.фотодитазин.рф

ООО «ВЕТА-ГРАНД»

123056, г. Москва, ул. Красина, д. 27, стр. 2
Тел.: +7 (499) 253-61-81, +7 (499) 250-40-00
E-mail: fotoditazin@mail.ru

